Selection and population demography shape evolution of two long-lived ectotherms

by

Jessica Martin Judson

A dissertation submitted to the graduate faculty

in partial fulfillment of the requirements for the degree of

DOCTOR OF PHILOSOPHY

Major: Ecology and Evolutionary Biology

Program of Study Committee:
Fredric J. Janzen, Major Professor
Anne M. Bronikowski
John D. Nason
Kevin J. Roe
Amy L. Toth

The student author, whose presentation of the scholarship herein was approved by the program of study committee, is solely responsible for the content of this dissertation. The Graduate College will ensure this dissertation is globally accessible and will not permit alterations after a degree is conferred.

Iowa State University

Ames, Iowa

2021

DEDICATION

To Opa, who always believed in me.

TABLE OF CONTENTS

ACKNOWLEDGMENTS

I have many people to acknowledge for my path through my doctoral program. First and foremost, thank you to my husband and best friend, Matthew. You have given me your time, courage, strength, wisdom, and support for the last decade, along with so many laughs when I needed to see the bright side of this fantastic world we live in. This truly could not have been done without you. You are the first one of you I've ever met.

Thank you to my family for supporting me from a distance, as this journey has taken me far from my Texas home. To my parents, Thomas and Charlotte, I owe my love of science and my stubbornness to continue when I felt defeated. They have loved me unconditionally. For my continual inspiration to keep reaching higher and learning new things, I thank my brother Daniel. I also must acknowledge my dogs, Leila and Daphne, for their constant companionship and the needed motivation to go outside and enjoy the sunshine and inevitable Iowa wind.

Thank you to my grandparents, both here with me and gone before me. I have always been surrounded by love and the belief that I could do anything I put my mind to. I owe my stress coping mechanism of fiber arts to Oma, which has kept me sane these last six years. I would also like to thank my aunt Annette, who gave me National Geographic magazine subscriptions upon finding me reading as many as I could in her library when I was young.

My path to becoming the scientist I am was made possible by many brilliant scientists who have supported and encouraged me. I thank my advisor, Fred, for giving me the freedom and support (and money) to explore my interests and ask challenging questions, even when they were outside of both of our comfort zones. He reminded me of what I could do, even when I doubted myself. I also thank my committee member Anne, who has given me opportunities to expand my research in new directions and always gave her time when I needed it. For providing

support and feedback on my diverse projects, I thank my committee members John, Amy, and Kevin. Finally, I thank my Master's advisor, Mark Welch, for getting me through the beginning of my graduate school journey and showing me that chasing reptiles and genotyping them was something I could do for a living.

For the vast teaching experience I have gained during my time at Iowa State, I must thank Anne and Matt Hufford for giving me the opportunity to design my own teaching approach in Evolutionary Genetics. I also thank Jim Colbert, who has been an invaluable mentor as I have taught my first solo course in Introductory Biology. I treasure the lessons I have learned through teaching at Iowa State and will continue to seek innovative ways to inspire undergraduates with the beauty of biology.

I thank the many undergraduates, Grace Kline, Kelsi Hagerty, Alison Basel, Elena Thornhill, Jayla Pettway, and Elizabeth Hannan, who have been such an inspiration to me as I have worked alongside them in the lab. You all are so deserving of the success you have achieved, and I hope you continue to find joy in research.

To the members of the Janzen lab, thank you for the hard work, feedback on my rough drafts, and endless laughter that helped make these projects a possibility. Brooke Bodensteiner, you are one of the reasons I came to Iowa State; you welcomed me with open arms and helped me get on my feet. You have been a true friend since we met, and I am eternally grateful. To David, my competition and friend, thank you for making field seasons more tolerable and for motivating me to try to keep up with your inspiring research. I'd like to say it was a tie, in the end. Luke, you have always given me insightful questions and perspectives that have made me deeply consider why I do what I do, and you have helped me with all of my projects in some form or another. This work would not have been possible without you.

Finally, I must thank my friends. There are many difficult moments during a dissertation, but I look back and remember the moments of laughter and joy much more easily because of all of you. To Kaitlyn, I owe this degree. You will never let me leave without it. You remind me of what I have accomplished and a laugh when I need it. You have been my steadfast supporter and best friend. Indeed, we are together for the long haul. I also want to thank Justin Conover for answering my many bioinformatics questions, listening to me complain about minor slights of the world, and sharing my joy of discovery, Hannah Carroll for the multiple years of hosting our stitching meet-ups that kept me sane, Ashley Hedrick for the funny memes and field memories, and many others for their support and encouragement. Thank you to the graduate students and faculty of EEB for sharing their brilliant science and their invaluable time.

ABSTRACT

Selection and demography are powerful forces that shape the evolution of populations, and these forces can be investigated in greater detail with the advent of genomic technologies for non-model organisms. Further, long-term population monitoring of wild populations of long-lived organisms can offer insight into the evolution of phenotypes and how populations change over time, which is of importance for vulnerable species. The following research presented in this dissertation assesses the roles of mate choice, demography, and genetics on phenotypic evolution across multiple scales, using experimental, population and species-wide comparisons in two long-lived ectotherms, the painted turtle (*Chrysemys picta*) and the western terrestrial garter snake (*Thamnophis elegans*).

Certain phenotypes are the result of a complex interplay between natural selective pressures and sexual selection, such that phenotypes can both honestly signal health to potential mates and influence survivorship. In the first study, I assessed the role of adult painted color forelimb coloration as an honest signal of health status, measured through stress physiology and immune function, and found relationships between color and physiology were dependent upon sex and size in contrasting ways. In the second study, I assessed the relationships of various phenotypes, including color, stress levels, and sexually dimorphic traits, and reproductive success of adult male and female painted turtles in a semi-natural experiment with three adult sex-ratio treatments. Contrary to predictions, certain female phenotypes, including size and stress levels, were predictive of female reproductive success, but male phenotypes did not predict male reproductive success. These two studies represent some of the first tests of the function of color in adult painted turtles and suggest that female phenotypes may be the subject of male mate choice in painted turtles, contrary to former hypotheses of female mate choice in this species.

Phenotypes that vary across populations of widespread species are often attributed to local adaptation to the disparate environmental conditions experienced across the species' range. However, phenotypic plasticity can also contribute to phenotypic variation across populations, and genomic sampling can provide insight into the drivers of phenotypic variation. In the third study of my dissertation, I assessed population genomic variation across the western range of painted turtles to understand the contribution of local adaptation to the species' distribution. I found that population genomic structure was consistent with serial founder effects from the eastern to the western United States, but found little evidence for genomic regions under different selective pressures across populations. Thus, while I could not exclude local adaptation, phenotypic plasticity is likely an important mechanism allowing painted turtles to colonize such a wide geographic range.

Life-history traits can also be the result of local adaptation to disparate environments, even in the face of strong gene flow. With gene flow, local adaptation can be maintained through the combination of strong selection on individuals with traits mismatched to their environments and genomic architecture, including inversions, preventing recombination from breaking up favorable allelic combinations. In the fourth study of my dissertation, I investigated the genomics of life-history variation in populations of western terrestrial garter snakes in Lassen County, California. I found that despite recent gene flow among populations, there were regions of the genome that were strongly diverged between populations of the two life-history strategies, and many of these regions show patterns consistent with inversions. These regions contain genes related to many functions, including cellular senescence and the DNA damage-repair pathway, which support measured differences in these pathways between the two life-history strategies.

Thus, both strong selection and genomic architecture play a role in the maintenance of these life-history strategies in these populations of long-lived reptiles.

CHAPTER 1. INTRODUCTION

Abiotic environmental factors are strong drivers of phenotypic evolution through time and space, as supported by the increasing evidence that populations are often locally adapted to their environments (Hereford 2009). Reciprocal transplant and common-garden experiments have repeatedly demonstrated this link between locally adapted phenotypes and fitness (e.g., Niewiarowski and Roosenburg 1993; Thrall et al. 2002; Leimu and Fischer 2008; Refsnider and Janzen 2012). However, natural selection is not the only selective force shaping phenotypes across populations (Fig. 1). Sexual selection also can play a role in the evolution of phenotypes, as desirable phenotypes are chosen by a certain sex or certain phenotypes display increased ability to gain increased mating success and subsequent reproductive success (Andersson and Iwasa 1996). As originally proposed by Darwin (1871), these sexually selected phenotypes may even be at odds with natural selection, and can interact with local environment to promote local adaptation among populations and eventual speciation in some cases (Maan and Seehausen 2011).

The ability of populations to adapt to their local environments in response to selective pressures is conditional upon multiple aspects of population demography and structure. For populations to adapt to novel selective pressures in the absence of phenotypic plasticity, there must be genetic variation underlying phenotypic differences among individuals on which selection can act. In

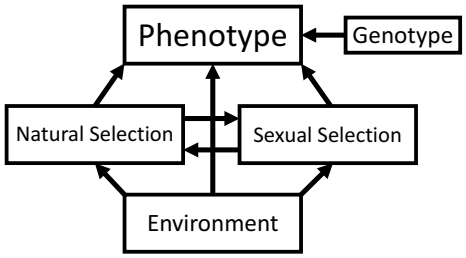

Fig. 1: Diagram of the forces shaping phenotypes, and the translation of changes in phenotype to potential changes in genotypes at the population level. Environmental contexts, including both abiotic factors and biotic factors (e.g., population demography), influence selective pressures, which in turn are the result of interactions between sexual selection and natural selection. These selective pressures shape phenotypes through evolutionary time.

isolated populations, the sources of this genetic variation within a population are standing genetic variation, which is critical for short-term adaptive responses (Hill 1982; reviewed in Barrett and Schluter 2008), or new mutations. The presence of standing genetic variation, and the number of new mutations, is shaped by a population's demographic history (e.g., Allendorf 1986). Populations that have experienced a bottleneck or decreased population sizes demonstrate a reduction in standing genetic variation across taxa (Frankham 1996), which can decrease the ability of populations to respond to novel environments (Lande and Shannon 1996) and increase the incidence of inbreeding among remaining individuals. The deleterious influence of inbreeding depression, coupled with reduced standing genetic variation and the decreased incidence of new mutations, can further decrease population fitness and reduce the ability of populations to survive future environmental changes (Frankham 2005).

In sexually reproducing species, genetic variation, and a population's ability to persist through time, is also shaped by the balance in ratio of males to females. Extreme shifts in sex ratio, particularly toward male-biased sex ratios, decrease the effective population size and genetic variation through a reduction in the number of reproducing females, which can threaten population persistence (Grayson et al. 2014). Sexual selection can also decrease survival in populations with skewed adult sex ratios. For example, in the common lizard, male-biased sex ratios result in increased aggression by males toward females for mating opportunities, which subsequently reduces female survival and fecundity (Le Galliard et al. 2005). In both monogamous and polygynous mating systems, sex-ratio bias can increase extinction risk with demographic stochasticity (Lee et al. 2011).

Population structuring, and the migration of individuals among populations, is yet another force hindering or promoting local adaptation. Gene flow among populations can

homogenize genetic composition and thereby limit adaptation to local environments (Kawecki and Ebert 2004). In more heterogeneous landscapes with barriers to gene flow, phenotypic and genetic divergence can proceed according to standing genetic variation through natural selection and genetic drift (e.g., Sánchez-Ramírez et al. 2018). However, when gene flow is present among populations from disparate environments, populations can share alleles maladapted to the local environments, resulting in the loss of local adaptation through time and a decrease in fitness across populations (Lenormand 2002). For populations to overcome the influence of maladaptive gene flow and locally adapt, selection must be exceedingly strong (Lenormand 2002), and thus the prevalence of local adaptation among organisms implies extreme selection across environments. Alternatively, populations can locally adapt despite high gene flow through genomic architecture, including chromosomal rearrangements, inversions, fusions, and positional changes of genes, which can decrease gene flow in regions important to fitness (Tigano and Friesen 2016). Although gene flow can hinder local adaptation, it can also spread locally adapted alleles and facilitate local adaptation. Hybridization among species can provide new genetic material on which selection can act, which can be adaptive in local environments (e.g., mimicry wing pattern genes in *Heliconius* butterflies); these new genes can accelerate the process of local adaptation to new environments (Hedrick 2013; Takuno et al. 2015).

In the era of genomics, we can now more deeply assess the genetic pathways of phenotypic change (e.g., Shaffer et al. 2013), confirm our past conclusions formed from limited genetic data (Bradbury et al. 2015), and address new questions relating to genomic patterns of adaptation across the tree of life (Stapley et al. 2010). Characterizing the underlying genomic basis of local adaptation across populations is an important step in understanding which environmental and demographic factors contribute to phenotypic change (Tiffin and Ross-

Ibarra 2014). To that end, my Ph.D. research assesses multiple aspects of the relationships among environment, selection, and phenotype using genomic data in two ectotherms, the painted turtle (*Chrysemys picta*) and the western terrestrial garter snake (*Thamnophis elegans*). Specifically, I address the following questions:

1) What are the relationships among phenotypes and fitness in adult painted turtles, and how does the environmental context of skewed adult sex ratio influence these relationships?

2) How do disparate abiotic environments across the western range of the painted turtle influence local adaptation, as assessed by genomic variation?

3) How do demography and selection interact to influence the evolution of distinct life-history strategies in the western terrestrial garter snake?

Study Organisms

The Painted Turtle (Chrysemys picta)

The painted turtle is a widespread temperate ectotherm, with a range extending across North America from the Atlantic to the Pacific Ocean (Ernst and Lovich 2009). The cold temperatures experienced by these temperate aquatic ectotherms require a host of physiological adaptations to survive, including the ability to tolerate freezing of extracellular body fluid as hatchlings (Paukstis et al. 1989) and the ability to survive extremely hypoxic conditions during winter months when water surfaces are frozen (Ultsch and Jackson 1982; Fanter et al. 2020). Painted turtles are long-lived, and sequence evolution rate is slow compared to other vertebrates (Shaffer et al. 2013). When assessing genetic variation at a mitochondrial DNA locus, for example, Starkey et al. (2003) found very little genetic divergence across much of the range of the species. Further, microsatellite DNA analyses detected low divergence among three sampled

sites from the western range of the painted turtle (Reid et al. 2019). Despite the low genetic divergence at measured loci, populations across the western range of the painted turtle display phenotypic variation that may be driven by local adaptation to the environmental conditions experienced in the northern and southern United States. For example, thermal reaction norms for hatchling body mass and incubation duration varied across the western range in a common-garden experiment (Bodensteiner et al. 2019). An additional common garden experiment found differences in nesting phenology and nest depth in these western populations (Refsnider and Janzen 2012)

Sexual selection may also play a role in phenotypic evolution of painted turtles. Adults display sexual dimorphism, as males are smaller and have elongated foreclaws and tails compared to females (Ernst and Lovich 2009; Hoekstra et al. 2018). Males also display courtship behavior by vibrating their elongated foreclaws against the sides of the female's head, potentially allowing female choice of male mates in this polygynandrous species. Further, painted turtles are named for the colorful stripes on the head, neck, limbs, and plastron, and yet the function of this coloration is unknown. The coloration may play an anti-predatory function in hatchlings (Britson and Gutzke 1993; but see Reinke et al. 2017). In adult pond turtles, it is hypothesized that coloration may also play a role in mate choice or communication among conspecifics (e.g., Polo-Cavia et al. 2013). In species with mate choice, adult sex ratio can be important for mate choice dynamics and resulting sexual selection (Lee et al. 2011). Painted turtles exhibit temperature-dependent sex determination (TSD), which can skew sex ratios and thereby influence patterns of mate choice and reproductive success among populations (e.g., Grayson et al. 2014). As climate rapidly shifts due to anthropogenic climate change, the future of species with TSD relies strongly on the ability of populations to either plastically respond or adapt to these changes (Refsnider

and Janzen 2016). Skewed sex ratios from temperature increases could accelerate population declines as mating dynamics change, and the resulting loss of standing genetic variation may further predispose populations to extinction (Mitchell and Janzen 2010).

The Western Terrestrial Garter Snake (Thamnophis elegans)

The western terrestrial garter snake is another widespread ectothermic vertebrate in western North America, with multiple described subspecies varying in color, scalation, and diet preferences (Arnold 1977; Stebbins 2003). Populations near Eagle Lake in the Sierra Nevada mountain range in northern California exhibit one of two ecotypes, which are characterized by distinct life-history strategies (Bronikowski and Arnold 1999). The first strategy represents a fast pace-of-life ecotype, with faster growth and maturation, larger adult body size, larger litters of offspring, and a shorter lifespan, whereas the other strategy (slow pace-of-life) displays opposing life-history traits (Bronikowski and Arnold 1999). These ecotypes are found in contrasting environments in the region, with fast pace-of-life animals inhabiting the rocky lakeshore of Eagle Lake and slow pace-of-life animals inhabiting the montane meadows. These environments differ in prey availability (Bronikowski and Arnold 1999), parasite pressure (Robert and Bronikowski 2010), predation pressure (Sparkman et al. 2013), and temperature (Bronikowski 2000). Despite these differences in life-history traits and selective pressures, microsatellite DNA analysis reveals abundant gene flow among populations (Manier and Arnold 2005). Thus, selective pressures must be exceedingly strong to maintain life-history divergence, or genomic architecture must differentiate populations in some way as to prevent gene flow at important adaptive loci. However, the genomic underpinnings of this divergence among ecotypes is as yet unknown.

These populations of garter snake have been studied for over 40 years, and thus represent a wealth of data on life-history evolution through time. Long-term field studies are invaluable to understanding population dynamics, particularly with anthropogenic factors contributing to population extirpations worldwide (Reinke et al. 2019). With the increasing incidence of extreme weather events, including droughts in California, multiple lakeshore populations have been extirpated during the past decade of monitoring. The samples collected from these extinct populations could provide insight into what genomic features, including genetic diversity, may have contributed to the fate of these populations. Thus, this long-term field dataset provides a unique opportunity to investigate genomic structure of populations through time, as well as among populations.

Dissertation Organization

With this research, I aim to increase our understanding of the relationships among phenotypes and reproductive success and clarify how local adaptation to disparate environments may be aided or hindered by population demography and gene flow. Understanding these factors and how they interact in ectotherms is increasingly important for ensuring species persistence. While populations have locally adapted to their current environments in many cases, the ability of populations to adapt to anthropogenic selective pressures is less certain (Lande and Shannon 1996; Jergenson et al. 2014; Radchuk et al. 2019). Anthropogenic climate change in particular presents a significant environmental challenge for already vulnerable ectotherms, many of which rely on aquatic resources that may limit dispersal capability to track a suitable environment across the landscape (Urban et al. 2013). Ectotherms with TSD face the additional challenge of sex-ratio bias with warming temperatures, which could further increase their risk of extinction (Mitchell and Janzen 2010). Reptile abundance is rapidly declining across the globe (Gibbons et

al. 2000; Sinervo et al. 2010; Böhm et al. 2016), and yet much remains unknown about their capacity to respond and survive into this anthropogenic era.

Chapter 2: Sex- and size-dependent relationships of physiology to forelimb stripe coloration in the painted turtle

Coloration is an honest signal of health to mates of many taxa, yet the role of coloration is unknown for many vertebrates, including the painted turtle. If coloration reflects physiological fitness, this coloration may be used to choose mates with increased fitness, and thus coloration can evolve beyond the influence of natural selection alone. In this study, my colleagues and I assessed relationships among multiple aspects of physiology, including stress physiology and innate and adaptive immune function, and coloration of the forelimb stripes of painted turtles. Some aspects of physiology were associated with coloration, and these associations were both sex- and size-dependent in contrasting ways. These results indicate the importance of measuring multiple aspects of physiology to assess physiological fitness, and suggest that there may indeed be trade-offs in signaling ability and organismal health in painted turtles, consistent with coloration being an honest signal of fitness in this aquatic ectotherm.

Chapter 3: Phenotypic and environmental predictors of reproductive success in painted turtles

The evolution of sexually dimorphic traits is often the result of sexual selection in vertebrates. Yet, the relationship between these phenotypes and reproductive success has not been explored in many ectotherms with sexually dimorphic traits. Further, in ectotherms with TSD, adult sex ratio can vary through time, but the relationship between adult sex ratio and reproductive success also remains largely unknown. In this study, I investigated the relationship between multiple phenotypes, including body size, claw length, forelimb stripe coloration, and

blood corticosterone concentrations, which reflect stress levels, and reproductive success in a semi-natural experiment with three adult sex-ratio treatments. I found that, contrary to predictions, male phenotypes did not predict male reproductive success. However, larger females and females with decreased corticosterone concentrations had increased reproductive success. Finally, there were weak effects of adult sex ratio on male reproductive success, with males in the male-biased adult sex-ratio treatment displaying decreased reproductive success compared to the equal and female-biased treatments. These results imply that female mate choice may not be driving the evolution of male phenotypes, but rather males may choose females based on their coloration, which is associated with stress levels in female painted turtles. In this species with TSD, skewed adult sex ratio does appear to at least weakly influence reproductive success, which could have negative consequences for population persistence for this and other species with environmental sex determination in the future.

Chapter 4: Demographic history shapes population genomic structure in a long-lived aquatic vertebrate

Phenotypic variation across populations of widespread species may be the result of phenotypic plasticity or adaptation to local environmental conditions. In long-lived organisms, the prevalence of local adaptation can be difficult to assess with classical methods, including common-garden experiments. Genomic variation can provide evidence of local adaptation across populations, particularly when divergence in allele frequencies is associated with environmental variables. I used reduced-representation sequencing to genotype adult painted turtles from seven locations in the species' western range. Population genetic divergence was consistent with east-west distribution of sampling sites, with Illinois individuals displaying much higher genetic diversity than all other sampled populations. The distribution of genetic variation and patterns of

homozygosity across the genome confirmed prior hypotheses of the range expansion of painted turtles from east to west following the glaciers receding during the Pleistocene; genetic variation declined and runs of homozygosity increased in the populations west of the Rocky Mountains (Idaho, Oregon, and New Mexico). There was no evidence of local adaptation among populations of painted turtles. Instead, loci with high F_{ST} among populations were characterized by heterozygosity in Illinois painted turtles and fixed homozygotes in Oregon, Idaho, and New Mexico, consistent with serial founder effects leading to the fixation of different alleles in northwestern versus southern populations. Thus, genetic drift, rather than local adaptation, was the most prominent driver of genetic variation among populations of painted turtles west of the Mississippi River.

Chapter 5: Genomic architecture underlies two distinct life-history strategies in the western terrestrial garter snake (*Thamnophis elegans*)

In metapopulations spanning multiple distinct habitat types, selection must be stronger than gene flow to result in the evolution of phenotypes adapted to these specific habitats, and reduced recombination offers a mechanism by which selection can reduce gene flow in regions important to producing adaptive phenotypes. To test the genomic patterns of selection with gene flow, I performed whole genome resequencing of 121 western terrestrial garter snakes from 11 populations in the vicinity of Eagle Lake in Lassen County, California. These populations display one of two distinct life-history strategies, and previous microsatellite work and mark-recapture efforts suggest gene flow is common among populations. Population genomic analyses supported a role of gene flow in homogenizing neutral variation across the genome and found multiple individuals that appeared to be the result of recent gene flow between populations of the two life-history strategies. However, multiple regions across the genome were highly diverged

between populations of the different life-history strategies. Further, these regions displayed genotypic patterns consistent with inversions which contained multiple genes associated with documented phenotypic differences between life-history strategies, including color, metabolism, and DNA damage repair mechanisms. Inversions would reduce recombination among these genes and allow suites of genes to be passed on to offspring even with gene flow. The presence of these inversions that are strongly diverged among life-history strategies also supports the hypothesis that genes or alleles of large effect on phenotype are more abundant in systems with gene flow, as they are more resistant to the effects of gene flow than genes of small effect.

References

Allendorf FW. 1986. Genetic drift and the loss of alleles versus heterozygosity. Zoo Biol. 5:181-190.

Andersson M, Iwasa Y. 1996. Sexual selection. Trends Ecol Evol. 11:53-58.

Arnold SJ. 1977. Polymorphism and geographic variation in the feeding behavior of the garter snake *Thamnophis elegans*. Science. 197:676-678.

Barrett RD, Schluter D. 2008. Adaptation from standing genetic variation. Trends Ecol Evol. 23:38-44.

Bodensteiner BL, Warner DA, Iverson JB, Milne-Zelman CL, Mitchell TS, Refsnider JM, Janzen FJ. 2019. Geographic variation in thermal sensitivity of early life traits in a widespread reptile. Ecology and Evolution. 9:2791-2802.

Böhm M, Cook D, Ma H, Davidson AD, García A, Tapley B, Pearce-Kelly P, Carr J. 2016. Hot and bothered: using trait-based approaches to assess climate change vulnerability in reptiles. Biol Conserv. 204:32-41.

Bradbury IR, Hamilton LC, Dempson B, Robertson MJ, Bourret V, Bernatchez L, Verspoor E. 2015. Transatlantic secondary contact in Atlantic Salmon, comparing microsatellites, a single nucleotide polymorphism array and restriction-site associated DNA sequencing for the resolution of complex spatial structure. Mol Ecol. 24:5130-5144.

Britson CA, Gutzke WH. 1993. Antipredator mechanisms of hatchling freshwater turtles. Copeia:435-440.

Bronikowski AM. 2000. Experimental evidence for the adaptive evolution of growth rate in the garter snake *Thamnophis elegans*. Evolution. 54:1760-1767.

Bronikowski AM, Arnold SJ. 1999. The evolutionary ecology of life history variation in the garter snake *Thamnophis elegans*. Ecology. 80:2314-2325.

Darwin C. 1871. The descent of man, and selection in relation to sex. London: John Murray.

Ernst CH, Lovich JE. 2009. Turtles of the United States and Canada. 2nd ed. Baltimore: Johns Hopkins University Press.

Fanter CE, Lin Z, Keenan SW, Janzen FJ, Mitchell TS, Warren DE. 2020. Development-specific transcriptomic profiling suggests new mechanisms for anoxic survival in the ventricle of overwintering turtles. J Exp Biol. 223:213918.

Frankham R. 1996. Relationship of Genetic Variation to Population Size in Wildlife. Conserv Biol. 10:1500-1508.

Frankham R. 2005. Genetics and extinction. Biol Conserv. 126:131-140.

Gibbons JW, Scott DE, Ryan TJ, Buhlmann KA, Tuberville TD, Metts BS, Greene JL, Mills T, Leiden Y, Poppy S, et al. 2000. The Global Decline of Reptiles, Déjà Vu Amphibians. Bioscience. 50

Grayson KL, Mitchell NJ, Monks JM, Keall SN, Wilson JN, Nelson NJ. 2014. Sex ratio bias and extinction risk in an isolated population of Tuatara (*Sphenodon punctatus*). PLoS One. 9:e94214.

Hedrick PW. 2013. Adaptive introgression in animals: examples and comparison to new mutation and standing variation as sources of adaptive variation. Mol Ecol. 22:4606-4618.

Hereford J. 2009. A quantitative survey of local adaptation and fitness trade-offs. Am Nat. 173:579-588.

Hill WG. 1982. Rates of change in quantitative traits from fixation of new mutations. Proceedings of the National Academy of Sciences. 79:142-145.

Hoekstra LA, Weber RC, Bronikowski AM, Janzen FJ. 2018. Sex-specific growth, shape, and their impacts on life history of a long-lived vertebrate. Evol Ecol Res. 19:639–657.

Jergenson AM, Miller DA, Neuman-Lee LA, Warner DA, Janzen FJ. 2014. Swimming against the tide: resilience of a riverine turtle to recurrent extreme environmental events. Biol Lett. 10:20130782.

Kawecki TJ, Ebert D. 2004. Conceptual issues in local adaptation. Ecol Lett. 7:1225-1241.

Lande R, Shannon S. 1996. The role of genetic variation in adaptation and population persistence in a changing environment. Evolution. 50:434-437.

Le Galliard JF, Fitze PS, Ferriere R, Clobert J. 2005. Sex ratio bias, male aggression, and population collapse in lizards. Proceedings of the National Academy of Sciences. 102:18231–18236.

Lee AM, Sæther B-E, Engen S. 2011. Demographic stochasticity, Allee effects, and extinction: the influence of mating system and sex ratio. The American Naturalist. 177:301-313.

Leimu R, Fischer M. 2008. A meta-analysis of local adaptation in plants. PLoS One. 3:e4010.

Lenormand T. 2002. Gene flow and the limits to natural selection. Trends Ecol Evol. 17:183-189.

Maan ME, Seehausen O. 2011. Ecology, sexual selection and speciation. Ecol Lett. 14:591-602.

Manier MK, Arnold SJ. 2005. Population genetic analysis identifies source-sink dynamics for two sympatric garter snake species (*Thamnophis elegans* and *Thamnophis sirtalis*). Mol Ecol. 14:3965-3976.

Mitchell NJ, Janzen FJ. 2010. Temperature-dependent sex determination and contemporary climate change. Sex Dev. 4:129-140.

Niewiarowski PH, Roosenburg W. 1993. Reciprocal transplant reveals sources of variation in growth rates of the lizard *Sceloporus undulatus*. Ecology. 74:1992-2002.

Paukstis GL, Shuman RD, Janzen FJ. 1989. Supercooling and freeze tolerance in hatchling painted turtles (*Chrysemys picta*). Can J Zool. 67:1082-1084.

Polo-Cavia N, López P, Martín J. 2013. Head coloration reflects health state in the red-eared slider *Trachemys scripta elegans*. Behav Ecol Sociobiol. 67:153-162.

Radchuk V, Reed T, Teplitsky C, Van De Pol M, Charmantier A, Hassall C, Adamík P, Adriaensen F, Ahola MP, Arcese P. 2019. Adaptive responses of animals to climate change are most likely insufficient. Nat Commun. 10:1-14.

Refsnider JM, Janzen FJ. 2012. Behavioural plasticity may compensate for climate change in a long-lived reptile with temperature-dependent sex determination. Biol Conserv. 152:90-95.

Refsnider JM, Janzen FJ. 2016. Temperature-dependent sex determination under rapid anthropogenic environmental change: Evolution at a turtle's pace? J Hered. 107:61-70.

Reid B, Kass J, Wollney S, Jensen E, Russello M, Viola E, Pantophlet J, Iverson J, Peery M, Raxworthy C. 2019. Disentangling the genetic effects of refugial isolation and range expansion in a trans-continentally distributed species. Heredity. 122:441-457.

Reinke BA, Calsbeek R, Stuart-Fox D. 2017. A test of an antipredatory function of conspicuous plastron coloration in hatchling turtles. Evol Ecol. 31:463-476.

Reinke BA, Miller DAW, Janzen FJ. 2019. What Have Long-Term Field Studies Taught Us About Population Dynamics? Annual Review of Ecology, Evolution, and Systematics. 50:261-278.

Robert KA, Bronikowski AM. 2010. Evolution of senescence in nature: physiological evolution in populations of garter snake with divergent life histories. Am Nat. 175:147-159.

Sánchez-Ramírez S, Rico Y, Berry KH, Edwards T, Karl AE, Henen BT, Murphy RW. 2018. Landscape limits gene flow and drives population structure in Agassiz's desert tortoise (*Gopherus agassizii*). Scientific reports. 8:1-17.

Shaffer HB, Minx P, Warren DE, Shedlock AM, Thomson RC, Valenzuela N, Abramyan J, Amemiya CT, Badenhorst D, Biggar KK, et al. 2013. The western painted turtle genome, a model for the evolution of extreme physiological adaptations in a slowly evolving lineage. Genome Biol. 14:R28.

Sinervo B, Mendez-de-la-Cruz F, Miles DB, Heulin B, Bastiaans E, Villagran-Santa Cruz M, Lara-Resendiz R, Martinez-Mendez N, Calderon-Espinosa ML, Meza-Lazaro RN, et al. 2010. Erosion of lizard diversity by climate change and altered thermal niches. Science. 328:894-899.

Sparkman A, Bronikowski A, Billings J, Von Borstel D, Arnold S. 2013. Avian predation and the evolution of life histories in the garter snake *Thamnophis elegans*. The American Midland Naturalist. 170:66-85.

Stapley J, Reger J, Feulner PG, Smadja C, Galindo J, Ekblom R, Bennison C, Ball AD, Beckerman AP, Slate J. 2010. Adaptation genomics: the next generation. Trends Ecol Evol. 25:705-712.

Starkey DE, Shaffer HB, Burke RL, Forstner MRJ, Iverson JB, Janzen FJ, Rhodin AGJ, Ultsch GR. 2003. Molecular Systematics, Phylogeography, and the Effects of Pleistocene Glaciation in the Painted Turtle (*Chrysemys Picta*) Complex. Evolution. 57

Stebbins R. 2003. A field guide to western reptiles and amphibians. 3rd editionHoughton Mifflin Company. Boston, MA. xvi. 533:377–380.

Takuno S, Ralph P, Swarts K, Elshire RJ, Glaubitz JC, Buckler ES, Hufford MB, Ross-Ibarra J. 2015. Independent Molecular Basis of Convergent Highland Adaptation in Maize. Genetics. 200:1297-1312.

Thrall PH, Burdon JJ, Bever JD. 2002. Local Adaptation in the Linum Marginale–Melampsora Lini Host-Pathogen Interaction. Evolution. 56

Tiffin P, Ross-Ibarra J. 2014. Advances and limits of using population genetics to understand local adaptation. Trends Ecol Evol. 29:673-680.

Tigano A, Friesen VL. 2016. Genomics of local adaptation with gene flow. Mol Ecol. 25:2144-2164.

Ultsch GR, Jackson D. 1982. Long-Term Submergence at 3°C of the Turtle, *Chrysemys Picta Bellii,* in Normoxic And Severely Hypoxic Water: I. Survival, Gas Exchange And Acid-Base Status. The Journal of Experimental Biology. 96:11-28.

Urban MC, Zarnetske PL, Skelly DK. 2013. Moving forward: dispersal and species interactions determine biotic responses to climate change. Ann N Y Acad Sci. 1297:44-60.

CHAPTER 2. SEX- AND SIZE-DEPENDENT RELATIONSHIPS OF PHYSIOLOGY TO FORELIMB STRIPE COLORATION IN THE PAINTED TURTLE

Jessica M. Judson, Luke A. Hoekstra, Kaitlyn G. Holden, Anne M. Bronikowski, and Fredric J. Janzen

Department of Ecology, Evolution, and Organismal Biology, Iowa State University, Ames, Iowa, USA

Modified from a manuscript in revision in *Behavioral Ecology and Sociobiology*

Abstract

Color reflects physiological fitness in many taxa. Painted turtles (*Chrysemys picta*) are brightly colored, but the function of this color, and its relation to stress levels and immune function, are unknown. We investigated the hypothesis that stress levels and immune function predict painted turtle forelimb stripe coloration using a suite of physiological traits, emphasizing measures of baseline stress and both innate and adaptive immune function. Additionally, we assessed the sex- and size-specific relationships of color and physiology. Some measures of physiology predicted coloration of the forelimb stripes, conditional upon the sex and body size of the turtle. i) Increased levels of baseline corticosterone predicted decreased brightness, with females displaying much steeper declines in brightness than males. ii) Increased glucose concentration and bactericidal competence predicted reddening of females' forelimb stripes and yellowing of males' stripes. iii) Increased body size predicted reddening of forelimb stripes for both males and females. iv) Larger turtles with high T-lymphocyte proliferative ability had redder forelimb stripes than smaller turtles with high T-lymphocyte proliferative ability. These results suggest that signals transmitted by color are conditional upon the bearer, which may have

important implications for the function of forelimb stripe coloration in this polygynandrous species. Finally, as not all physiological measures relate to color, we suggest both stress and immune physiology be assessed to understand the context-dependence of color signaling.

Introduction

Color is important for conspecific and heterospecific communication, thermoregulation, and camouflage in many vertebrates (Bybee et al. 2012; Smith et al. 2016). Some of the most dramatic instances are attributed to sexual selection driving the evolution and maintenance of brightly colored ornaments used to attract mates (e.g., Hill and McGraw 2006). One mechanism thought to elicit the evolution of mate choice in this way is when coloration is an honest signal of overall mate quality (Andersson 1986). If producing coloration is costly, as has been suggested for multiple pigment types (reviewed in Kemp et al. 2012), an individual's coloration should reflect its physiological state. Healthy individuals can afford to dedicate resources to coloration, while other individuals must dedicate those resources to other physiological functions (e.g., immune function) for survival (Faivre et al. 2003; but see Koch et al. 2018). Different aspects of physiological state likely interact to influence coloration, including stress levels and immune function. However, despite continued interest in the ecological role of animal color (Caro et al. 2017), relatively few studies have analyzed multiple aspects of physiology and their comprehensive relationships with color. In wild organisms for which direct tests of signal honesty (e.g., immune challenge) can be difficult, associations between existing variation in color and physiology can isolate the potential mechanisms by which color can honestly signal health.

Physiological stress is associated with changes in characteristics of color (e.g., brightness and hue) across animals, including birds (Mougeot et al. 2010), fish (Sefc et al. 2014),

amphibians (Desprat et al. 2017), and reptiles (Cote et al. 2010a). Brightness, or how light or dark a color appears (i.e., overall achromatic intensity) is generally hypothesized to be inversely related to stress, such that stressed organisms are duller (e.g., San-Jose and Fitze 2013). Additionally, the hue of these colors, or the wavelength at which energy is maximally reflected from an object (e.g., redness), might shift from the optimum for mate attraction during stress, such that stressed individuals receive fewer mating opportunities and experience decreased fitness (nutritional stress, Blount et al. 2003; parasites, Mougeot et al. 2010). For carotenoid-based pigmentation, the functional process for changes in color with stress is thought to involve reallocation of carotenoids from skin or feather pigmentation toward the stress response and immune function (reviewed in Svensson and Wong 2011; but see Koch et al. 2018). The most common stress response biomarker analyzed in relation to color is corticosterone (CORT), which is produced in response to a stressor through actions of the hypothalamo-pituitary-adrenocortical (HPA) axis in vertebrates (Balm 1999). The release of CORT induces increases in circulating glucose (Landys et al. 2006), increases in heterophils (neutrophils in mammals), and decreases in lymphocytes in the bloodstream to prepare the organism to appropriately respond to the stressor (reviewed in Goessling et al. 2015). Increased CORT concentrations are associated with decreased brightness in birds (Kennedy et al. 2013) and lizards (San-Jose and Fitze 2013), and increased CORT is often associated with increased red hue (lizards, Fitze et al. 2009; birds, McGraw et al. 2011).

Other studies have assessed the relationship between color and immune function. Increased immune function is predicted to be reflected positively in coloration of vertebrates due to the immunomodulatory effects of many pigment types (Griffith et al. 2006; Svensson and Wong 2011). For carotenoids, these immunomodulatory effects include increased lymphocyte

proliferative ability, increased tumor resistance, and protection of non-target tissues from reactive oxidative species during immune responses (reviewed in Chew and Park 2004; but see Koch et al. 2018). In tree swallows, brighter and bluer individuals had increased bactericidal competence of plasma (Beck et al. 2015), and immune-challenged male Schreiber's green lizards with bluer throats and yellower chests had greater immune responses (Martín and López 2009). Despite the independent support of associations between stress or immune function and color, few studies have incorporated measures of both functions to assess the overall physiological state of an organism when evaluating relationships between color and physiology.

Stress responses can influence immune function, both in the short and long term, which may have contrasting impacts on color. Chronic stress and resulting overstimulation of the HPA axis can cause immune dysregulation over time (Padgett and Glaser 2003). However, appropriate HPA response is also essential to maintain allostasis, as CORT and its effects are important for fight-or-flight responses, feeding, circadian rhythms, and reproduction (Landys et al. 2006). In male common lizards, experimentally elevated CORT increased the red hue of the belly, which is associated with increased copulations (Fitze et al. 2009). However, this higher CORT also induced increased oxidative damage, perhaps due to decreased antioxidants available for immune function (Cote et al. 2010a). Thus, to understand the relationships between physiology and color, it is critical to have measures not only of biomarkers of stress (CORT, glucose, and heterophil:lymphocyte ratios), but also of immune function (Johnstone et al. 2012). Moreover, the immune system of vertebrates can be described as multifaceted, with both innate (e.g., bactericidal competence) and adaptive (acquired, e.g., phytohemagglutinin response) branches. These separate arms of the immune system may be reflected differently in the coloration of an organism (Saks et al. 2003), particularly when sex or age are considered (Cote et al. 2010b;

Kelly et al. 2012). Thus, to understand the relationship between the immune system and color, the function of both immune branches should be assessed.

In this study, we tested an array of measures associated with function of the HPA axis and both the innate and adaptive immune system to assess the relationship between physiological state and coloration of a reptile in a comprehensive manner. The painted turtle (*Chrysemys picta*) has a widespread distribution in slow-moving freshwater systems across North America. This species is named for its colorful plastrons and red, orange, and yellow stripes on the limbs and head, which are produced by carotenoids (Steffen et al. 2015). Given the role of carotenoids in immune function in many vertebrates (Svensson and Wong 2011), carotenoids may be involved in signaling stress or immune function in painted turtles; carotenoid availability in the diet impacts color of painted turtle stripes, which may indicate a trade-off in carotenoid allocation (Steffen et al. 2019). Further, in a closely related turtle species, the red-eared slider, brightness decreased markedly with a direct immune challenge (Ibáñez et al. 2014). In painted turtles, the role of stripe coloration is unknown, but it may be used as a signal to conspecifics. Painted turtles have tetrachromatic vision, and thus should be able to see the reds and yellows present on their stripes and plastron, as well as ultraviolet light (Zana et al. 2001). Male painted turtles perform an underwater courtship display to females before mating, called titillation, during which a male strokes the sides of a female's head with his foreclaws (Ernst and Lovich 2009). This process allows females to assess forelimb coloration, and perhaps quality, of a male. Conversely, males may assess female quality by female coloration. Using adult painted turtles, we test the hypothesis that stress levels and immune function predict forelimb stripe coloration. We measured stress response (CORT, glucose, and H:L ratios), innate immune function (natural antibodies, lysis ability, and bactericidal competence), and adaptive immune function

(lymphocyte proliferative ability to three mitogens) to understand the effects of multiple axes of physiology on coloration in a reptile. We predicted that individuals with decreased stress and increased immune function would display increased brightness and distinct hues when compared to individuals with greater stress levels and decreased immune function. Further, we predicted that sex and size, which is a proxy for age in painted turtles (Hoekstra et al. 2018), are associated with color, and that the relationships between physiological state and color may be conditional on the bearer's sex or size (e.g., Cote et al. 2010b; Kelly et al. 2012; Ibáñez et al. 2013).

Methods

Husbandry and Physiology Sampling

We captured painted turtles for this study using hoop nets in July 2014 from the Thomson Causeway Recreation Area (TCRA) in Thomson, IL in the United States. We transported these turtles ~300 km directly west to Iowa State University (ISU), where we housed turtles for hibernation (Supplementary Material). We followed all applicable ISU guidelines for the care and use of animals in this study. In April 2016, we seeded three semi-natural experimental ponds at the ISU Horticulture Research Farm with 57 painted turtles (36 males, 21 females). Turtles lived in the ponds during the summer months, consuming aquatic plants, anurans, and invertebrates that colonized the ponds along with supplementary Mazuri® Aquatic Turtle Diet.

In July 2016, we drained all experimental ponds and removed the turtles. We obtained a blood sample from the caudal vein of each turtle with a heparin-rinsed syringe within 10 minutes of capture to assess baseline measures of circulating CORT and glucose (Polich 2016). We aliquoted whole blood (50µL) into tubes with 50µL of AIM V serum-free lymphocyte cell medium for lymphocyte proliferation assays (Palacios et al. 2013) and made a blood smear stained with Wright Giemsa for differential cell counts. We centrifuged the remaining whole

blood (from 30-150µL) and separated the plasma into two aliquots for CORT and immune assays before flash freezing in liquid nitrogen and storing at -80ºC. To assess age and its potential effects on color and physiology, we measured plastron length, which can be used as a proxy for age in these turtles (Hoekstra et al. 2018).

Color Analysis

We took RAW-formatted photographs (tripod-mounted Canon EOS Digital Rebel XSi camera and EF-S18-55mm lens) of each turtle's cranial region under controlled incandescent lighting and included a grey standard (18% reflectance; Insignia NS-DWB3M) in every photograph. We took two photographs of each turtle to assess repeatability and checked photographs for overexposure before analysis of reflectance using the Image Calibration and Analysis Toolbox v. 1.22 (Troscianko and Stevens 2015) in ImageJ v. 1.52a (Schneider et al. 2012). Reflectance is the measure of electromagnetic energy reflected off an object and is measured for each of the camera's color channels (blue, green, red). These color channels each correspond to a range of wavelengths (short wavelengths, SW; medium wavelengths, MW; long wavelengths, LW; Troscianko and Stevens 2015). For this study, we chose two regions of interest (ROIs) to measure in each photograph: the middle point of the colored stripe of the right forelimb and of the left forelimb, respectively (Fig. S1). We chose the forelimb stripes on each side because we did not measure reflectance in the ultraviolet (UV) spectrum; the limb stripes demonstrate low levels of reflectance in the UV spectrum in painted turtles and are visible to conspecifics during mating behaviors (Steffen et al. 2015). If the stripe did not extend unbroken down the forelimb, we measured the nearest point to the middle of the stripe (Fig. S1).

We $\log_{10}$-transformed reflectance measures for the three color channels for normality before assessing repeatability (intraclass correlation coefficient, Lessells and Boag 1987) across

the measures for each ROI (left or right forelimb stripe) in each color channel in R v. 3.6.1 (R Core Team 2019). Measures of stripe reflectance were highly repeatable across photographs of the same individual and between forelimbs within a photograph (Supplemental Material). Thus, we used reflectance measures from only the right forelimb ROI to calculate brightness and hue. We calculated brightness with non-transformed reflectance measures across color channels using the equation $\frac{(LW+MW+SW)/3}{655.35}$, which results in a brightness percentage (Stevens et al. 2014; Troscianko and Stevens 2015); high values indicate increased brightness and thus lighter color. We then $\log_{10}$-transformed these percentages to achieve normality for statistical analyses.

We calculated hue using multiple approaches that aim to assess hues visible to painted turtles through knowledge of color-opponent channels (Supplemental Material). Our first measure of hue was based on one of the color-opponent channels, Red/Green, that has been established in turtle Red/Green C-type horizontal cells (Twig et al. 2003; Twig and Perlman 2004). Thus, we calculated hue using the equation LW/MW. This measure of hue should not be sensitive to UV wavelengths (Zana et al. 2001), and includes the wavelengths for which painted turtles can discriminate and show maximal spectral sensitivity during behavioral trials (625nm to 685nm; Graf 1967). The second method of measuring hue was based on a principal components analysis (PCA) to assess the axes of color variation in the forelimb stripes (Supplementary Material; Stevens et al. 2014). The resulting equation to calculate hue, LW/(MW+SW), was strongly positively correlated with the first measure based on the known turtle color-opponent channel, LW/MW (Pearson's $r > 0.99$). Thus, we only use the ratio LW/MW to characterize hue, which represents the ratio of long wavelengths (reds) to medium wavelengths (yellows and greens); a higher ratio represents a more reddish hue. Our final dependent variables of color are

log_{10}-transformed brightness and hue (LW/MW). Brightness and hue of the forelimb stripes of turtles in this study varied considerably (Fig. S1).

Finally, as these turtles were held in controlled ponds with supplemented diet, we compared our results for brightness and hue to a dataset collected from the painted turtle source population at the TCRA (Judson, unpublished data). Variance in brightness and hue displayed by painted turtles at the TCRA and captive turtles used in this study were not different (two-sample F-test $P > 0.22$; Supplementary Material), and thus the variation in our captive study was representative of color variation in the wild. Additionally, the captive turtles did not appear to be more stressed than those at the TCRA, as baseline CORT values were similar to those reported across multiple studies at the TCRA (mean CORT this study=11.95 ng/mL; Refsnider et al. 2015 back-transformed least-square means=7 ng/mL; Polich 2016=27.45 ng/mL).

Physiological Measures

Stress Response: Corticosterone, Glucose, and Heterophil:Lymphocyte Ratios

Glucocorticoids, such as CORT, are common biomarkers used to assess individual health, as they mediate multiple physiological functions including an animal's stress response (Landys et al. 2006). Our double-antibody radioimmunoassay (N=57) follows previously described protocols validated in painted turtles (Supplemental Material; Refsnider et al. 2015; Polich 2016).

Circulating glucose concentrations are produced by antagonism between glucocorticoids and insulin (Strack et al. 1995); appropriate concentrations of glucose are essential to both homeostatic functions and stress responses. We measured the baseline concentration of circulating glucose (Mg/dL) using 1.5μL blood plasma with a FreeStyle Lite® glucometer

(Abbott Diabetes Care, Alameda, CA) and FreeStyle Lite® test strips (N=55; Gangloff et al. 2017).

Leukocyte profiles such as heterophil:lymphocyte (H:L) ratios measure physiological response to stressors (Davis et al. 2008). Here, we analyzed H:L ratios via stained blood smears by identifying 100 leukocytes at 1000x magnification and counting the number of heterophils and lymphocytes within those leukocytes (N=54; Gangloff et al. 2017). Under chronic stress conditions, a large H:L ratio is produced by glucocorticoids mobilizing lymphocytes into tissues and out of the bloodstream, while heterophils are increased in the bloodstream (Davis et al. 2008).

Innate Immune Function: Bactericidal Competence of Plasma, Natural Antibodies, and Lysis

The bactericidal competence (BC) of plasma measures constitutive innate immune function. Turtles with increased innate immune function are characterized by a high bacterial killing capacity, or competence, while individuals with depressed immune function may exhibit lower bactericidal competence (Matson et al. 2006). We assessed BC of plasma (N=54) according to Refsnider et al. (2015) with a few modifications (Supplementary Material). We detected a batch effect due to decreased survivorship of the *E. coli* working stock over time, and thus z-transformed BC for each batch (3 batches over 3 days).

Natural antibodies (NAbs) and complement-mediated lysis (CL) are two additional measures of constitutive innate immunity; high levels of NAbs and CL activity indicate a higher level of innate immune defense (Matson et al. 2005). We assessed these immune measures using a haemolysis-haemagglutination assay (N=52) modified from Matson et al. (2005) for use in painted turtles (Supplementary Material; Schwanz et al. 2011; Refsnider et al. 2015).

Adaptive Immune Function: Lymphocyte proliferative ability

Lymphocyte proliferation assays measure an organism's adaptive immune function by assessing the activation and proliferation of B- and T-lymphocytes in response to a mitogen; increased proliferation indicates a stronger immune response (Palacios et al. 2013). We gauged lymphocyte proliferation ability with a whole-blood mitogenic stimulation assay (Palacios et al. 2013) performed within 24 hours of blood collection (N=54). We used two T-cell mitogens, concanavalin A (ConA) and phytohemagglutinin (PHA), and one B-cell mitogen, lipopolysaccharide (LPS). Detailed methods for mitogens and concentrations can be found in Palacios et al. (2013; Supplementary Material). The proliferative ability of lymphocytes is expressed as a stimulation index (SI; Palacios et al. 2013), which is a ratio that compares mean counts per minute of mitogen-stimulated samples and non-stimulated controls. To control for differences in the initial number of lymphocytes in each sample, we estimated total leukocyte counts using the indirect Phloxin B method (Campbell and Ellis 2007) with 0.1% phloxin stain (Vetlab Supply, Palmetto Bay, FL) and hemocytometer (Palacios et al. 2013). To correct the SI for starting number of lymphocytes, as greater numbers of lymphocytes should increase SI, we performed a linear regression of starting number of lymphocytes versus SI for each mitogen. We use the residuals from those models as values for SI of the three mitogens.

Statistics

We used SAS v. 9.4 (SAS Institute, Cary, NC) for all statistical analyses described here. We assessed the influence of independent variables on $\log_{10}$-transformed brightness and hue with general linear models in PROC GLM. First, we removed outliers that were less than or greater than three standard deviations from the mean (N=1 for BC, H:L, CORT, SI_{ConA}; N=2 for SI_{PHA},SI_{LPS}). We calculated correlations among all physiological variables to assess our

prediction that stress measures and immune function measures are associated with one another and to avoid multicollinearity in the models. To more effectively test the influence of separate immune and stress responses, we ran two sets of models including either the stress-response measures or the immune-system measures with brightness or hue as the dependent variable. For all models, we included sex and the pond in which each turtle was kept as fixed effects. We also included plastron length standardized by sex (zPL) using a sex-specific z-transformation, as female painted turtles attain larger body sizes than males (Hoekstra et al. 2018). The original models for stress response included pond, sex, zPL, CORT, glucose, and H:L ratio. We also included interactions among sex, zPL, and the stress measures, as interactions among these factors may differentially influence color depending upon the sex or size of the individual. There were no strong correlations among stress variables (Supplemental Table 1), and we found no multicollinearity in the models. We removed non-significant interactions ($P > 0.1$) and kept all main effects in the models. The final models for stress response are summarized in Table 1.

The original models for immune function included pond, sex, zPL, standardized BC, NAbs, CL, SI_{ConA}, SI_{PHA}, and all two-way interactions among sex, zPL, and these immune measures. We excluded SI_{LPS} from the models, as it was strongly positively correlated with SI_{PHA} (Pearson's $r = 0.69$; Supplemental Table 1) and model results were the same when including either SI_{PHA} or SI_{LPS}. We removed non-significant interactions ($P > 0.1$) and kept all main effects. The final models for immune function are summarized in Table 2. We graphed significant relationships using ggplot2 (Wickham 2016) in R version 3.6.1 (R Core Team 2019).

Results

Effect of Stress Physiology on Brightness and Hue

Though we expected that baseline stress levels and immune responses would be correlated within individuals, there was only one strong (Pearson's $r > 0.6$) positive correlation between lymphocyte proliferative responses to PHA and LPS (Supplementary Table 1). There were moderate (Pearson's $r > 0.4$) positive correlations between NAbs and CORT and between standardized BC and CL, but there were no substantive overall relationships among stress levels or immune function.

We predicted that less stressed painted turtles would display increased brightness and distinct hue compared to their more stressed counterparts, and this prediction was partially supported (Table 1). CORT predicted brightness of the forelimb stripe ($P < 0.01$), such that higher CORT was associated with lower brightness (Fig. 1). Additionally, CORT predicted brightness in a sex-specific manner: brightness declined more drastically with higher CORT in females than in males ($P < 0.05$; Fig. 1). In the model for how stress measures predict hue (Table 1), size (zPL) was significant such that color was redder in larger turtles (Fig. 2). In addition, sex and glucose interacted to predict hue: as glucose concentrations increased, female hue increased in redness, while male hue decreased in redness (i.e., increased in yellow hue; Fig. 3A).

Effect of Immune Physiology on Brightness and Hue

Brightness was not explained by any immune variables (Table 2). Variation in hue was significantly explained by two interactions (Table 2). For sex and BC, female redness increased with increasing BC, while males showed an opposing relationship (Fig. 3B). Hue increased with increasing T-lymphocyte proliferative ability (PHA) in a size-dependent manner, but the overall trend was that animals with greater proliferative ability were redder (Fig. 3C; Table 2).

Discussion

Our hypothesis that stress levels and immune function predict painted turtle forelimb stripe coloration was supported indirectly. Specifically, stress and immune variables interacted with sex and size to predict brightness and hue of the forelimb stripe. Furthermore, we found a direct relationship between size and hue, such that larger turtles had redder forelimb stripes than smaller turtles. This study offers a comprehensive view of relationships among multiple axes of physiology and coloration in a reptile and emphasizes the importance of measuring many variables in both sexes in species with little human-visible sexual dimorphism in color. Based on these results, we explore the potential roles of forelimb stripe coloration in signaling physiological fitness in painted turtles and discuss the future questions that should be addressed to ascertain the function(s) of coloration in this brightly colored reptile.

Color and physiology

Color signals physiological state across taxa, particularly in males (e.g., birds, Hill and McGraw 2006; lizards, Plasman et al. 2015; frogs, Desprat et al. 2017). In turtles, multiple studies support a role for color in signaling health. When red-eared slider turtles received an immune challenge, brightness of the yellow chin stripes decreased compared to control individuals (Ibáñez et al. 2014). This result is supported by an earlier study that detected a relationship between H:L ratio, an immune challenge, and coloration in red-eared slider turtles (Polo-Cavia et al. 2013). In this study, we find relationships between both stress and immune measures of physiology and coloration of the forelimb stripes, consistent with a link between turtle health and color. However, these relationships are sex- or size-specific, such that the

physiological states of males and females, or of differently sized turtles, are reflected in coloration in contrasting ways.

Sex-specific correlations – despite an absence of sex chromosomes – between stress levels, immune function, and color have important implications for painted turtle color evolution. Forelimb stripes become duller as baseline CORT concentrations increase for both sexes, but females experience much greater declines in brightness than males (Fig. 1). Reduced brightness might be expected for individuals with high CORT levels (e.g., San-Jose and Fitze 2013), as greater concentrations generally indicate increased stress, which can adversely affect immune function if experienced over long periods (Padgett and Glaser 2003). The mechanism for this change in brightness with increasing CORT in turtles is unknown, but one hypothesis is that stressed animals allocate carotenoids, which produce the limb stripe colors of painted turtles (Steffen et al. 2015), toward immune function and away from skin deposition (reviewed in Svensson and Wong 2011). The steeper decline in brightness with increasing CORT for females suggests that females may shift carotenoid allocation in response to stress, whereas males apparently exhibit an attenuated response to stress. However, CORT not only mediates stress responses, but also plays a role in maintenance of homeostasis during daily or seasonal activities (e.g., reproduction, Landys et al. 2006). Energetic demands of reproductive activity vary between sexes in the summer months; females lay nests in the months of May and June, while spermatogenesis and mating activities for males peak in the fall (Ernst and Lovich 2009). Male turtles may prioritize maintaining brightness during late summer if brightness is important for mate choice. The results for forelimb stripe hue revealed additional interactions between sex and physiology, including differences in responses to glucose and BC (Fig. 3). Female hue was positively associated with glucose concentrations and the ability of plasma to kill or prevent

growth of bacteria (i.e., BC), such that females with redder forelimb stripes are likely healthier than those with yellower forelimb stripes. Males, however, had a negative association between these physiological variables and hue. These results imply that painted turtles may signal their physiological state to conspecifics conditional upon the sex of the bearer.

Most studies regarding coloration as a signal to conspecifics have focused on males; in systems where female choice drives male ornamentation, male coloration should reflect male health. Female ornamentation, and species with no human-visible sexual dimorphism in ornamentation, are relatively understudied, particularly in reptiles (e.g., López et al. 2009; Plasman et al. 2015). However, the transmitted message does depend on the sex of the signaler in birds. In American goldfinches, female bill color was positively associated with immunoglobulin Y and plumage color was positively associated with NAbs levels, but color and immune function were not associated in males (Kelly et al. 2012). López et al. (2008) detected similar sex-specific relationships between color, parasite infection, and leukocyte counts in European goldfinches, and Maney et al. (2008) found a relationship between female color and increased white blood cell counts in northern cardinals. In reptiles, Spanish terrapin limb stripe brightness positively relates to immune health of females, but males lack this relationship (Ibáñez et al. 2013).

Relationships between female color and health state are typically hypothesized to signal increased competitive ability (e.g., Maney et al. 2008). Although intraspecific competition may be a factor in painted turtle coloration, we propose instead that this may be a signal of female health to males. Painted turtles perform courtship displays before mating, and if the female is receptive, mating occurs (Ernst and Lovich 2009). This behavior would imply that only female choice occurs in this species, yet males have been documented performing coercive behaviors such as biting and nudging to achieve copulation (Moldowan et al. 2015; Hawkshaw et al. 2019).

Such courtship behavior could permit both male and female mate choice, with the color signals displayed in the forelimb stripes allowing females to distinguish males by their CORT, glucose, and BC, while males simultaneously assess brightness and redness of the female's forelimb stripes to ascertain health state.

Little is known regarding male mate choice in painted turtles. However, male mate choice based on female size should be important, as larger females lay larger eggs (e.g., Hoekstra et al. 2018) and may have more frequent second clutches (Congdon et al. 2003). Choosing healthy females should additionally increase a male's evolutionary fitness if those females allocate more resources to reproduction than self-maintenance. One mechanism by which carotenoid coloration in females may indicate their reproductive health is transmission of carotenoids to egg yolk. In striped plateau lizards, the size of a female's ornament patch is positively related to the amount of antioxidants deposited in egg yolk, which presumably produces healthier offspring (Weiss et al. 2011). While the ornament patch in these lizards is produced by pterins, carotenoids also play an antioxidant role (reviewed in Krinsky 2001). In zebra finches, increased deposition of carotenoids into eggs increases survivorship of embryos and hatchlings (McGraw et al. 2005). Painted turtles in northern populations display extreme anoxia tolerance and cold tolerance (e.g., Fanter et al. 2020), and additional carotenoids could buffer hatchlings and adults from oxidative damage that occurs during winter (Reinke et al. 2017). Healthier females should be able to allocate additional carotenoids both to skin pigmentation and to offspring, rather than their own immune demands, and thus brightness and hue of the forelimb stripes may honestly advertise quality.

In addition to interactions between sex and physiology, we found an interaction of size and lymphocyte proliferative responses to a T-cell mitogen, phytohemagglutinin (PHA), on hue

(Fig. 3). In turtles, size positively predicts age due to the growth exhibited throughout their lives (Hoekstra et al. 2018; Reinke et al. 2019). Immune health can change with age in reptiles (reviewed in Hoekstra et al. 2020), including innate immunity in painted turtles from the same source population (TCRA, Judson et al. 2020). Increased lymphocyte proliferative responses to PHA predicted increased hue, but the pattern was more pronounced in larger, older turtles. This pattern may indicate increased investment of carotenoids toward signaling and away from self-maintenance or survival as future reproductive potential decreases, and thus increasing signal honesty with age (Proulx et al. 2002). Healthy older turtles invest more resources in reproductive activities (e.g., older females lay larger eggs; Hoekstra et al. 2018), and attracting healthy mates may be prioritized.

Not all physiological measures predicted color in this study, and few physiological measures correlated with each other. This result emphasizes the importance of quantifying multiple physiological axes, as most studies focus on only one or two measures of physiology to represent overall individual health (e.g., in reptiles: Ibáñez et al. 2013; Lindsay et al. 2016). The lack of correlation among measures may be explained by the often condition-dependent nature of stress measures and their influence on immune function (reviewed in Johnstone et al. 2012). We provide evidence that immune health and stress predict color in an experiment where no turtles received a direct immune challenge, which may be more reflective of color variation and health state in the wild. Still, direct infection of individuals with an immune challenge may strengthen the relationship between health and color, as was found in red-eared slider turtles (Ibáñez et al. 2014), and may validate that forelimb stripe coloration is an honest signal when color expression is costly.

Hue and size

In addition to relationships among physiology and coloration, larger turtles displayed redder stripes than smaller turtles independent of sex (Fig. 2). This relationship between size and limb stripe color has not been previously detected in painted turtles. Prior work on stripe color focused on sex-specific differences rather than size differences, and found no differences in brightness between sexes and that males had redder forelimb stripes than females (Rowe et al. 2014). However, sexual size dimorphism might mask size-specific color differences, as adult female painted turtles are larger than males (Hoekstra et al. 2018). Indeed, when we assessed effects of sex or size without accounting for sexual dimorphism, brightness and hue did not differ between sexes or sizes. Size predicts color in other turtle species, such as European pond turtles and Spanish terrapins, though the aspects of color influenced by size vary (Ibáñez et al. 2013; Ibáñez et al. 2017). In another reptile, the common lizard, larger individuals had redder bellies than smaller individuals (Fitze et al. 2009), similar to this study.

Dietary access to carotenoids can shift the coloration of many species (e.g., Hill et al. 2002; Kopena et al. 2014). Increasing dietary access to carotenoids influences stripe and spot color of male painted turtles (Steffen et al. 2019). Larger turtles may have a different diet, and thus greater access to carotenoids, than smaller turtles, which may drive the pattern of increasing red hue of forelimb stripes with size. Still, little is known regarding specifics of painted turtle diet beyond being more omnivorous as adults (Ernst and Lovich 2009). Alternatively, changes in hue with size may result from age-dependent carotenoid allocation for camouflage (Wilson et al. 2007) or signaling (Freeman-Gallant et al. 2010). Decreased red hue with smaller size may be advantageous for predator avoidance, as red wavelengths are maximally transmitted in shallow freshwater systems, and many potential predators in these ecosystems have more red-sensitive

visual pigments (Lythgoe 1984). Predator avoidance is often the explanation for changing melanism, the darkening of skin pigments by melanin, in turtles (e.g., Rowe et al. 2014). For larger turtles with less predation pressure, this increased visibility instead may be advantageous for attracting mates. Evidence of assortative mating by age was found in painted turtles in Michigan (McGuire et al. 2014), and redder forelimb stripes may be a mechanism by which turtles can identify mates of a similar age (i.e. size, Hoekstra et al. 2018). Males could further assess female fitness via redness of the forelimb stripes, as larger females have increased reproductive output in this population (Bowden et al. 2004).

In sum, the sex-specific and size-specific relationships between physiology and color detected in this study suggest that coloration of forelimb stripes reflects physiological fitness in ways that could be used in mate choice in painted turtles. Future studies should examine relationships of coloration to both male and female reproductive success, which could rigorously evaluate our prediction that color is important for painted turtle mate choice and reflects both physiological and evolutionary fitness. Further, although this study is correlational rather than experimental, particular physiological measures (CORT, PHA) appear to more strongly predict color, thus these measures should be incorporated into future experiments of color signaling honesty in painted turtles. Overall, we present a more comprehensive analysis of physiological state and color by analyzing multiple measures of stress and immune function. That not all physiological measures predicted color, or were predictive in complex ways, is important to consider when assessing relationships between color and physiological fitness in vertebrates.

Acknowledgements

We thank R. Polich, N. Howell and J. Braland for research pond support, B. Bodensteiner for use of camera equipment, J. Pettway for photographing assistance at the TCRA, A. Toth, K.

Roe, and J. Nason for guidance and comments, and the many members of the Janzen lab for the collection and care of turtles. Funding for fieldwork was provided by National Science Foundation grants LTREB DEB-1242510 and IOS-1257857 awarded to FJJ. Physiological measures were partially funded by the ISU University Honors Program (to K. Gerwig for H:L counts). Pond building and maintenance was provided by the ISU Horticulture Research Farms. Permits for painted turtle collection at the TCRA were provided by the United States Army Corps of Engineers, the United States Fish and Wildlife Service (SUP 32576-021), and the Illinois Department of Natural Resources (NH11.0073). This research was approved by ISU IACUC (12-03-5570-J).

References

Andersson M (1986) Evolution of condition-dependent sex ornaments and mating preferences: sexual selection based on viability differences. Evolution 40:804-816 https://doi.org/10.1111/j.1558-5646.1986.tb00540.x

Balm PHM (1999). Stress physiology in animals. CRC Press, Sheffield

Beck ML, Hopkins WA, Hawley DM (2015) Relationships among plumage coloration, blood selenium concentrations and immune responses of adult and nestling tree swallows. J Exp Biol 218:3415-3424 https://doi.org/10.1242/jeb.123794

Blount JD, Metcalfe NB, Birkhead TR, Surai PF (2003) Carotenoid modulation of immune function and sexual attractiveness in zebra finches. Science 300:125-127 https://doi.org/10.1126/science.1082142

Bowden RM, Harms HK, Paitz RT, Janzen FJ (2004) Does optimal egg size vary with demographic stage because of a physiological constraint? Funct Ecol 18:522-529 https://doi.org/10.1111/j.0269-8463.2004.00861.x

Bybee SM, Yuan F, Ramstetter MD, Llorente-Bousquets J, Reed RD, Osorio D, Briscoe AD (2012) UV photoreceptors and UV-yellow wing pigments in *Heliconius* butterflies allow a color signal to serve both mimicry and intraspecific communication. Am Nat 179:38-51 https://doi.org/10.1086/663192

Campbell T, Ellis CK (2007). Avian and exotic animal hematology and cytology. 3rd edn. Blackwell Publishing, Ames

Caro T, Stoddard MC, Stuart-Fox D (2017) Animal coloration research: why it matters. Philos Trans R Soc Lond B Biol Sci 372:20160333 https://doi.org/10.1098/rstb.2016.0333

Chew BP, Park JS (2004) Carotenoid Action on the Immune Response. J Nutr 134:257S-261S https://doi.org/10.1093/jn/134.1.257S

Congdon JD, Nagle RD, Kinney OM, van Loben Sels RC, Quinter T, Tinkle DW (2003) Testing hypotheses of aging in long-lived painted turtles (*Chrysemys picta*). Exp Gerontol 38:765-772 https://doi.org/10.1016/s0531-5565(03)00106-2

Cote J, Meylan S, Clobert J, Voituron Y (2010a) Carotenoid-based coloration, oxidative stress and corticosterone in common lizards. J Exp Biol 213:2116-2124 https://doi.org/10.1242/jeb.040220

Cote J, Arnoux E, Sorci G, Gaillard M, Faivre B (2010b) Age-dependent allocation of carotenoids to coloration versus antioxidant defences. J Exp Biol 213:271-277 https://doi.org/10.1242/jeb.035188

Davis AK, Maney DL, Maerz JC (2008) The use of leukocyte profiles to measure stress in vertebrates: a review for ecologists. Funct Ecol 22:760-772 https://doi.org/10.1111/j.1365-2435.2008.01467.x

Desprat JL, Lengagne T, Mondy N (2017) Immune challenges and visual signalling in tree frogs. Sci Nat 104:21 https://doi.org/10.1007/s00114-017-1436-x

Ernst CH, Lovich JE (2009). Turtles of the United States and Canada. 2nd edn. Johns Hopkins University Press, Baltimore

Faivre B, Grégoire A, Préault M, Cézilly F, Sorci G (2003) Immune activation rapidly mirrored in a secondary sexual trait. Science 300:103 https://doi.org/10.1126/science.1081802

Fanter CE, Lin Z, Keenan SW, Janzen FJ, Mitchell TS, Warren DE (2020) Development-specific transcriptomic profiling suggests new mechanisms for anoxic survival in the ventricle of overwintering turtles. J Exp Biol 223:213918 https://doi.org/10.1242/jeb.213918

Fitze PS, Cote J, San-Jose LM, Meylan S, Isaksson C, Andersson S, Rossi JM, Clobert J (2009) Carotenoid-based colours reflect the stress response in the common lizard. PLoS One 4:e5111 https://doi.org/10.1371/journal.pone.0005111

Freeman-Gallant CR, Taff CC, Morin DF, Dunn PO, Whittingham LA, Tsang SM (2010) Sexual selection, multiple male ornaments, and age-and condition-dependent signaling in the common yellowthroat. Evolution 64:1007-1017 https://doi.org/10.1111/j.1558-5646.2009.00873.x

Gangloff EJ, Sparkman AM, Holden KG, Corwin CJ, Topf M, Bronikowski AM (2017) Geographic variation and within-individual correlations of physiological stress markers in a widespread reptile, the common garter snake (*Thamnophis sirtalis*). Comp Biochem Physiol, A: Mol Integr Physiol 205:68-76 https://doi.org/10.1016/j.cbpa.2016.12.019

Goessling JM, Kennedy H, Mendonça MT, Wilson AE, Grindstaff J (2015) A meta-analysis of plasma corticosterone and heterophil : lymphocyte ratios - is there conservation of physiological stress responses over time? Funct Ecol 29:1189-1196 https://doi.org/10.1111/1365-2435.12442

Graf V (1967) A spectral sensitivity curve and wavelength discrimination for the turtle *Chrysemys picta picta*. Vision Res 7:915-928 https://doi.org/10.1016/0042-6989(67)90010-7

Griffith SC, Parker TH, Olson VA (2006) Melanin-versus carotenoid-based sexual signals: is the difference really so black and red? Anim Behav 71:749-763 https://doi.org/10.1016/j.anbehav.2005.07.016

Hawkshaw DM, Moldowan PD, Litzgus JD, Brooks RJ, Rollinson N (2019) Discovery and description of a novel sexual weapon in the world's most widely-studied freshwater turtle. Evol Ecol 33:889-900 https://doi.org/10.1007/s10682-019-10014-3

Hill GE, McGraw KJ (2006). Bird Coloration: Function and Evolution. Harvard University Press, Cambridge

Hill GE, Inouye CY, Montgomerie R (2002) Dietary carotenoids predict plumage coloration in wild house finches. Proc R Soc B 269:1119-1124 https://doi.org/10.1098/rspb.2002.1980

Hoekstra LA, Weber RC, Bronikowski AM, Janzen FJ (2018) Sex-specific growth, shape, and their impacts on life history of a long-lived vertebrate. Evol Ecol Res 19:639–657

Hoekstra LA, Schwartz TS, Sparkman AM, Miller DA, Bronikowski AM (2020) The untapped potential of reptile biodiversity for understanding how and why animals age. Funct Ecol 34:38-54 https://doi.org/10.1111/1365-2435.13450

Ibáñez A, Marzal A, López P, Martín J (2013) Sexually dichromatic coloration reflects size and immunocompetence in female Spanish terrapins, *Mauremys leprosa*. Naturwissenschaften 100:1137-1147 https://doi.org/10.1007/s00114-013-1118-2

Ibáñez A, Polo-Cavia N, López P, Martín J (2014) Honest sexual signaling in turtles: experimental evidence of a trade-off between immune response and coloration in red-eared sliders *Trachemys scripta elegans*. Naturwissenschaften 101:803-811 https://doi.org/10.1007/s00114-014-1219-6

Ibáñez A, Martín J, Marzal A, Bertolero A (2017) The effect of growth rate and ageing on colour variation of European pond turtles. Sci Nat 104:49 https://doi.org/10.1007/s00114-017-1469-1

Johnstone CP, Reina RD, Lill A (2012) Interpreting indices of physiological stress in free-living vertebrates. J Comp Physiol, B 182:861-879 https://doi.org/10.1007/s00360-012-0656-9

Judson JM, Reding DM, Bronikowski AM (2020) Immunosenescence and its influence on reproduction in a long-lived vertebrate. J Exp Biol In Press https://doi.org/10.1242/jeb.223057

Kelly RJ, Murphy TG, Tarvin KA, Burness G (2012) Carotenoid-based ornaments of female and male American goldfinches (*Spinus tristis*) show sex-specific correlations with immune function and metabolic rate. Physiol Biochem Zool 85:348-363 https://doi.org/10.1086/666059

Kemp DJ, Herberstein ME, Grether GF (2012) Unraveling the true complexity of costly color signaling. Behav Ecol 23:233-236 https://doi.org/10.1093/beheco/arr153

Kennedy EA, Lattin CR, Romero LM, Dearborn DC (2013) Feather coloration in museum specimens is related to feather corticosterone. Behav Ecol Sociobiol 67:341-348 https://doi.org/10.1007/s00265-012-1454-9

Koch RE, Kavazis AN, Hasselquist D, Hood WR, Zhang Y, Toomey MB, Hill GE (2018) No evidence that carotenoid pigments boost either immune or antioxidant defenses in a songbird. Nat Commun 9:491 https://doi.org/10.1038/s41467-018-02974-x

Kopena R, López P, Martín J (2014) Relative contribution of dietary carotenoids and vitamin E to visual and chemical sexual signals of male Iberian green lizards: an experimental test. Behav Ecol Sociobiol 68:571-581 https://doi.org/10.1007/s00265-013-1672-9

Krinsky NI (2001) Carotenoids as antioxidants. Nutrition 17:815-817 https://doi.org/10.1016/S0899-9007(01)00651-7

Landys MM, Ramenofsky M, Wingfield JC (2006) Actions of glucocorticoids at a seasonal baseline as compared to stress-related levels in the regulation of periodic life processes. Gen Comp Endocrinol 148:132-149 https://doi.org/10.1016/j.ygcen.2006.02.013

Lessells CM, Boag PT (1987) Unrepeatable repeatabilities: a common mistake. Auk 104:116-121 https://doi.org/10.2307/4087240

Lindsay WR, Wapstra E, Silverin B, Olsson M (2016) Corticosterone: a costly mediator of signal honesty in sand lizards. Ecol Evol 6:7451-7461 https://doi.org/10.1002/ece3.2318

López G, Figuerola J, Soriguer R (2008) Carotenoid-based masks in the European goldfinch *Carduelis carduelis* reflect different information in males and females. Ardea 96:233-242 https://doi.org/10.5253/078.096.0208

López P, Gabirot M, Martín J (2009) Immune challenge affects sexual coloration of male Iberian wall lizards. J Exp Zool Part A 311A:96-104 https://doi.org/10.1002/jez.505

Lythgoe J (1984) Visual pigments and environmental light. Vision Res 24:1539-1550 https://doi.org/10.1016/S0042-6989(84)80003-6

Maney DL, Davis AK, Goode CT, Reid A, Showalter C (2008) Carotenoid-based plumage coloration predicts leukocyte parameters during the breeding season in northern cardinals (*Cardinalis cardinalis*). Ethology 114:369-380 https://doi.org/10.1111/j.1439-0310.2008.01476.x

Martín J, López P (2009) Multiple color signals may reveal multiple messages in male Schreiber's green lizards, *Lacerta schreiberi*. Behav Ecol Sociobiol 63:1743–1755 https://doi.org/10.1007/s00265-009-0794-6

Matson KD, Ricklefs RE, Klasing KC (2005) A hemolysis-hemagglutination assay for characterizing constitutive innate humoral immunity in wild and domestic birds. Dev Comp Immunol 29:275-286 https://doi.org/10.1016/j.dci.2004.07.006

Matson KD, Tieleman BI, Klasing KC (2006) Capture stress and the bactericidal competence of blood and plasma in five species of tropical birds. Physiol Biochem Zool 79:556-564 https://doi.org/10.1086/501057

McGraw K, Adkins-Regan E, Parker R (2005) Maternally derived carotenoid pigments affect offspring survival, sex ratio, and sexual attractiveness in a colorful songbird. Naturwissenschaften 92:375-380 https://doi.org/10.1007/s00114-005-0003-z

McGraw KJ, Lee K, Lewin A (2011) The effect of capture-and-handling stress on carotenoid-based beak coloration in zebra finches. J Comp Physiol, A 197:683-691 https://doi.org/10.1007/s00359-011-0631-z

McGuire JM, Congdon JD, Scribner KT, Nagle RD (2014) Female reproductive qualities affect male painted turtle (*Chrysemys picta marginata)* reproductive success. Behav Ecol Sociobiol 68:1589-1602 https://doi.org/10.1007/s00265-014-1768-x

Moldowan PD, Brooks RJ, Litzgus JD (2015) Turtles with "teeth": beak morphology of Testudines with a focus on the tomiodonts of Painted Turtles (*Chrysemys* spp.). Zoomorphology 135:121-135 https://doi.org/10.1007/s00435-015-0288-1

Mougeot F, Martinez-Padilla J, Bortolotti GR, Webster LM, Piertney SB (2010) Physiological stress links parasites to carotenoid-based colour signals. J Evol Biol 23:643-650 https://doi.org/10.1111/j.1420-9101.2009.01926.x

Padgett DA, Glaser R (2003) How stress influences the immune response. Trends Immunol 24:444-448 https://doi.org/10.1016/s1471-4906(03)00173-x

Palacios MG, Cunnick JE, Bronikowski AM (2013) Complex interplay of body condition, life history, and prevailing environment shapes immune defenses of garter snakes in the wild. Physiol Biochem Zool 86:547-558 https://doi.org/10.1086/672371

Plasman M, Reynoso VH, Nicolás L, Torres R (2015) Multiple colour traits signal performance and immune response in the Dickerson's collared lizard *Crotaphytus dickersonae*. Behav Ecol Sociobiol 69:765-775 https://doi.org/10.1007/s00265-015-1892-2

Polich RL (2016) Stress hormone levels in a freshwater turtle from sites differing in human activity. Conserv Physiol 4:1-9 https://doi.org/10.1093/conphys/cow016

Polo-Cavia N, López P, Martín J (2013) Head coloration reflects health state in the red-eared slider *Trachemys scripta elegans*. Behav Ecol Sociobiol 67:153-162 https://doi.org/10.1007/s00265-012-1435-z

Proulx SR, Day T, Rowe L (2002) Older males signal more reliably. Proc R Soc B 269:2291-2299 https://doi.org/10.1098/rspb.2002.2129

R Core Team (2019). R: A language and environment for statistical computing. R Foundation for Statistical Computing.

Refsnider JM, Palacios MG, Reding DM, Bronikowski AM (2015) Effects of a novel climate on stress response and immune function in painted turtles (*Chrysemys picta*). J Exp Zool Part A 323:160-168 https://doi.org/10.1002/jez.1902

Reinke BA, Calsbeek R, Stuart-Fox D (2017) A test of an antipredatory function of conspicuous plastron coloration in hatchling turtles. Evol Ecol 31:463-476 https://doi.org/10.1007/s10682-017-9892-5

Reinke BA, Hoekstra L, Bronikowski AM, Janzen FJ, Miller D (2019) Joint estimation of growth and survival from mark-recapture data to improve estimates of senescence in wild populations. Ecology 101:e02877 https://doi.org/10.1002/ecy.2877

Rowe JW, Bunce CF, Clark DL (2014) Spectral reflectance and substrate color-induced melanization in immature and adult Midland painted turtles (*Chrysemys picta marginata*). Amphib-Reptil 35:149-159 https://doi.org/10.1163/15685381-00002934

Saks L, Ots I, Horak P (2003) Carotenoid-based plumage coloration of male greenfinches reflects health and immunocompetence. Oecologia 134:301-307 https://doi.org/10.1007/s00442-002-1125-z

San-Jose LM, Fitze PS (2013) Corticosterone regulates multiple colour traits in *Lacerta* [*Zootoca*] *vivipara* males. J Evol Biol 26:2681-2690 https://doi.org/10.1111/jeb.12265

Schneider CA, Rasband WS, Eliceiri KW (2012) NIH Image to ImageJ: 25 years of image analysis. Nat Methods 9:671-675 https://doi.org/10.1038/nmeth.2089

Schwanz L, Warner DA, McGaugh S, Di Terlizzi R, Bronikowski A (2011) State-dependent physiological maintenance in a long-lived ectotherm, the painted turtle (*Chrysemys picta*). J Exp Biol 214:88-97 https://doi.org/10.1242/jeb.046813

Sefc KM, Brown AC, Clotfelter ED (2014) Carotenoid-based coloration in cichlid fishes. Comp Biochem Physiol, A: Mol Integr Physiol 173:42-51 https://doi.org/10.1016/j.cbpa.2014.03.006

Smith KR, Cadena V, Endler JA, Kearney MR, Porter WP, Stuart-Fox D (2016) Color change for thermoregulation versus camouflage in free-ranging lizards. Am Nat 188:668-678 https://doi.org/10.1086/688765

Steffen JE, Hultberg J, Drozda S (2019) The effect of dietary carotenoid increase on painted turtle spot and stripe color. Comp Biochem Physiol, A: Mol Integr Physiol 229:10-17 https://doi.org/10.1016/j.cbpb.2018.12.002

Steffen JE, Learn KM, Drumheller JS, Boback SM, McGraw KJ (2015) Carotenoid composition of colorful body stripes and patches in the painted turtle (*Chrysemys picta*) and red-eared slider (*Trachemys scripta*). Chelonian Conserv Biol 14:56-63 https://doi.org/10.2744/ccab-14-01-56-63.1

Stevens M, Lown AE, Wood LE (2014) Color change and camouflage in juvenile shore crabs *Carcinus maenas*. Front Ecol Evol 2:14 https://doi.org/10.3389/fevo.2014.00014

Strack AM, Sebastian RJ, Schwartz MW, Dallman MF (1995) Glucocorticoids and insulin: reciprocal signals for energy balance. Am J Physiol Regul Integr Comp Physiol 268:R142-R149 https://doi.org/10.1152/ajpregu.1995.268.1.R142

Svensson PA, Wong BBM (2011) Carotenoid-based signals in behavioural ecology: a review. Behaviour 148:131-189 https://doi.org/10.1163/000579510x548673

Troscianko J, Stevens M (2015) Image calibration and analysis toolbox - a free software suite for objectively measuring reflectance, colour and pattern. Methods Ecol Evol 6:1320-1331 https://doi.org/10.1111/2041-210X.12439

Twig G, Perlman I (2004) Homogeneity and diversity of color-opponent horizontal cells in the turtle retina: Consequences for potential wavelength discrimination. J Vis 4:403-414 https://doi.org/10.1167/4.5.5

Twig G, Levy H, Perlman I (2003) Color opponency in horizontal cells of the vertebrate retina. Prog Retin Eye Res 22:31-68 https://doi.org/10.1016/s1350-9462(02)00045-9

Weiss SL, Kennedy EA, Safran RJ, McGraw KJ (2011) Pterin-based ornamental coloration predicts yolk antioxidant levels in female striped plateau lizards (*Sceloporus virgatus*). J Anim Ecol 80:519-527 https://doi.org/10.1111/j.1365-2656.2010.01801.x

Wickham H (2016). ggplot2: Elegant Graphics for Data Analysis. Springer-Verlag New York.

Wilson D, Heinsohn R, Endler JA (2007) The adaptive significance of ontogenetic colour change in a tropical python. Biol Lett 3:40-43 https://doi.org/10.1098/rsbl.2006.0574

Zana Y, Ventura DF, De Souza JM, DeVoe RD (2001) Tetrachromatic input to turtle horizontal cells. Vis Neurosci 18:759-765 https://doi.org/10.1017/S0952523801185093

Tables and Figures

Table 1: Effects of stress response on coloration

Dependent Variable	Source of Variation	df	F	*P*-Value
Brightness	Pond	2, 39	0.68	0.5111
	Sex	1, 39	0.18	0.6749
	zPL[a]	1, 39	0.02	0.8786
	CORT[b]	1, 39	7.70	0.0084*
	Glucose	1, 39	0.83	0.3666
	H:L[c]	1, 39	1.44	0.2371
	Sex * CORT	1, 39	4.70	0.0363*
	zPL * CORT	1, 39	3.51	0.0685
	zPL * Glucose	1, 39	3.64	0.0636
Hue (Long : Medium Wavelengths)	Pond	2, 41	0.09	0.9144
	Sex	1, 41	3.86	0.0562
	zPL	1, 41	6.72	0.0132*
	CORT	1, 41	0.43	0.5170
	Glucose	1, 41	0.00	0.9971
	H:L	1, 41	2.46	0.1242
	Sex * Glucose	1, 41	4.90	0.0325*

[a] plastron length standardized by sex; [b] corticosterone concentration; [c] heterophil:lymphocyte ratio; * $P < 0.05$

Table 2: Effects of immune function on coloration

Dependent Variable	Source of Variation	df	F	*P*-Value
Brightness	Pond	2, 36	1.10	0.3442
	Sex	1, 36	1.78	0.1899
	zPL[a]	1, 36	1.08	0.3056
	Agglutination	1, 36	1.93	0.1734
	Lysis	1, 36	0.02	0.8847
	Bactericidal Competence	1, 36	0.04	0.8516
	ConA[b]	1, 36	0.18	0.6776
	PHA[c]	1, 36	0.00	0.9814
Hue (Long : Medium Wavelengths)	Pond	2, 33	0.37	0.6938
	Sex	1, 33	0.35	0.5578
	zPL	1, 33	10.02	0.0033*
	Agglutination	1, 33	2.52	0.1220
	Lysis	1, 33	0.07	0.7966
	Bactericidal Competence	1, 33	0.07	0.7980
	ConA	1, 33	0.15	0.7033
	PHA	1, 33	10.54	0.0027*
	Sex * Lysis	1, 33	3.26	0.0801
	Sex * Bactericidal Competence	1, 33	4.29	0.0462*
	zPL * PHA	1, 33	4.99	0.0324*

[a] plastron length standardized by sex; [b] lymphocyte proliferative responses to concanavalin A and [c] phytohemagglutinin; * $P < 0.05$

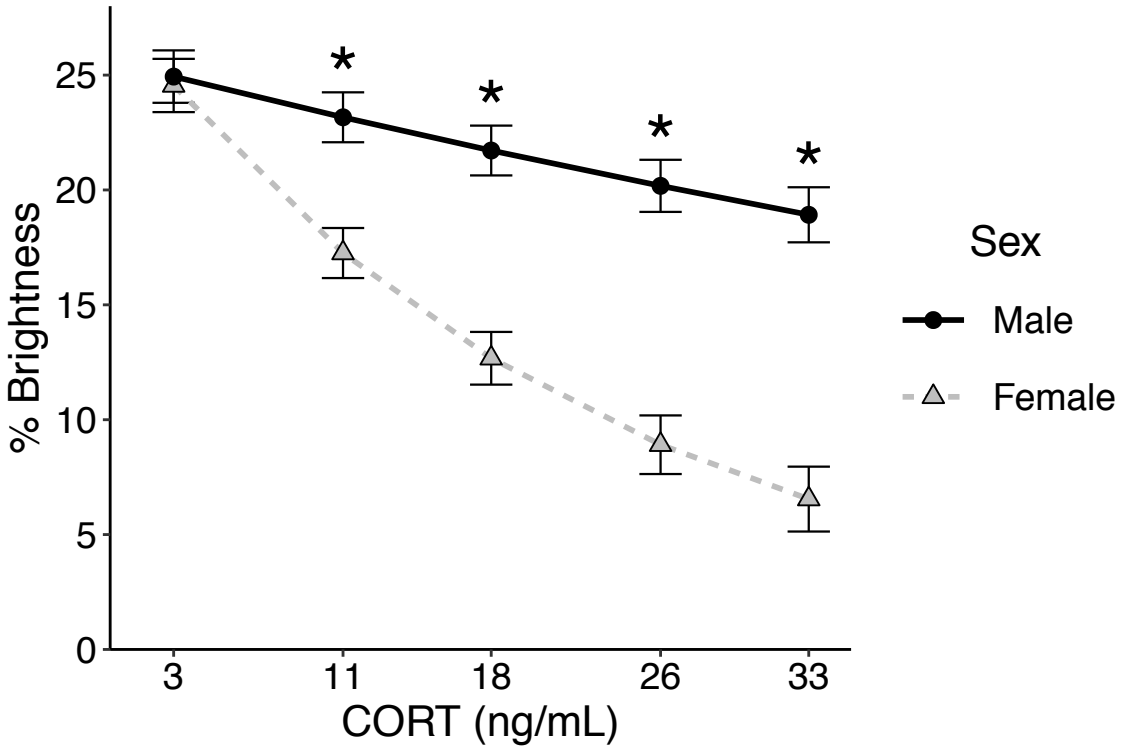

Figure 1: Relationship of baseline corticosterone (CORT) concentrations in the bloodstream versus percent brightness of the forelimb stripe of painted turtles. To visualize the interaction of CORT by sex, five evenly spaced values within the range of CORT concentrations in this study were selected. Points represent back-transformed least squares means $\pm$ SE from the brightness model in Table 1. Significant pairwise differences (all $P < 0.02$) between sexes are denoted with asterisks

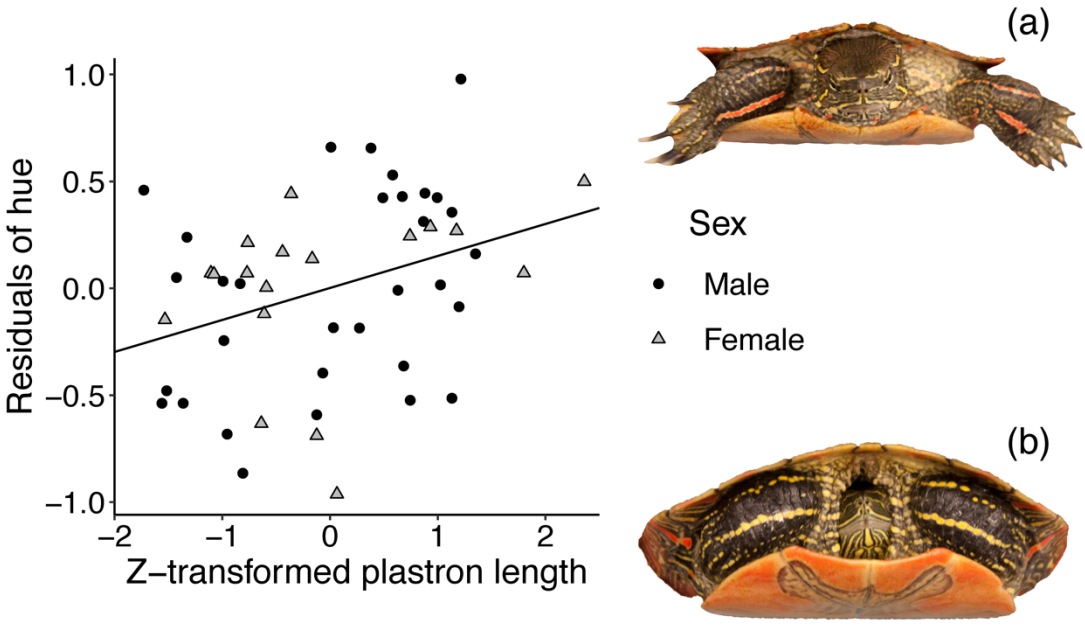

Figure 2: Relationship of size and hue of painted turtle forelimb stripes. Plastron length was z-transformed by sex (zPL), and points were obtained by calculating residuals from the model of hue excluding zPL in Table 1. Equation of line: $Y = 0.15x + 0.002$; $R^2 = 0.12$. (A) male painted turtle with highest value of hue and (B) female painted turtle with lowest value of hue for the forelimb stripe. Image backgrounds were removed using Adobe Photoshop CC 2018

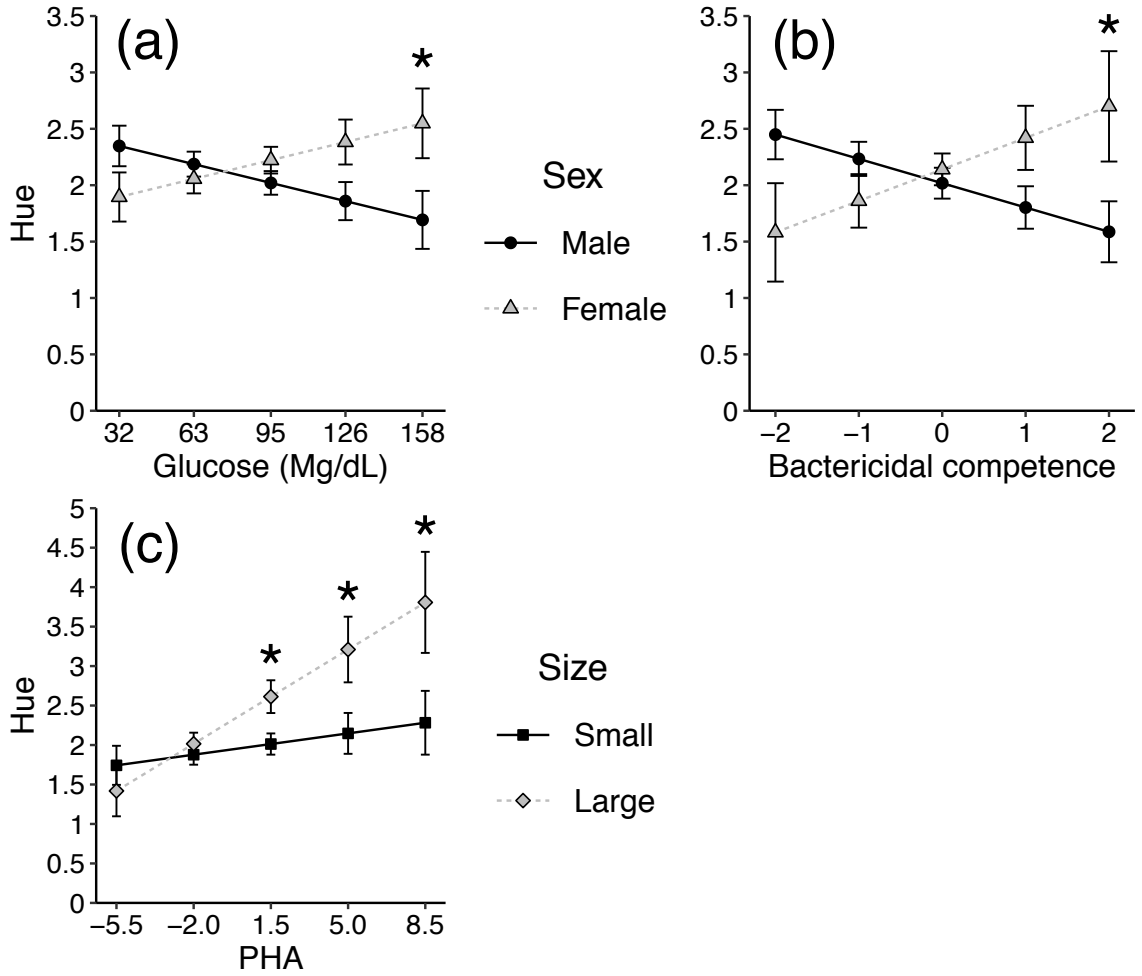

Figure 3: Interactions of sex and size with physiology influence hue of forelimb stripes. Five evenly spaced values within the range of glucose, bactericidal competence, and lymphocyte proliferative responses to a T-cell mitogen, phytohemagglutinin (PHA) in this study were chosen to plot relationships. Significant pairwise differences ($P < 0.05$) are denoted with asterisks. (A) Relationship between glucose concentrations and hue by sex. Points represent least squares means (LSM) ± SE from the hue model in Table 1. (B) Relationship between bactericidal competence and hue by sex. Points represent LSM ± SE from the hue model in Table 2. (C) Relationship between PHA and hue by size. Points represent LSM ± SE from the hue model in Table 2, and sizes were binned into small (less than mean plastron length) and large turtles (greater than mean plastron length) to plot the size interaction

Supplemental Material

Expanded Methods:

Husbandry and Physiology Sampling

We captured painted turtles for this study using hoop nets in July 2014 from the Thomson Causeway Recreation Area (TCRA) in Thomson, IL in the United States. We transported these turtles ~300 km directly west to Iowa State University (ISU), where we housed turtles in 53-liter bins filled with dechlorinated water and set lighting to mimic the photoperiod of Ames, IA. We followed all applicable ISU guidelines for the care and use of animals in this study. Turtles hibernated in cold rooms at 4°C in bins filled with water using a photoperiod mimicking that of winter photoperiod in Ames, IA during the winter of 2014. In April 2015, we seeded three semi-natural experimental ponds (19m x 15m x 1.5m; Mitchell et al. 2017) at the ISU Horticulture Research Farm with 57 painted turtles (36 males, 21 females). Turtles lived in the ponds during the summer months of 2015, consuming aquatic plants, anurans, and invertebrates that colonized the ponds along with supplementary Mazuri® Aquatic Turtle Diet. We drained all ponds and returned turtles to ISU in October 2015 for overwintering, and turtles were released back into the ponds the following April.

In July 2016, we drained all experimental ponds and removed the turtles. We obtained a blood sample from the caudal vein of each turtle with a heparin-rinsed syringe to assess baseline measures of circulating CORT and glucose. To ensure we were measuring baseline circulating CORT, we recorded handling time, which is the time from capture to completion of collection of blood, to compare with CORT measures, as CORT increases in the bloodstream within 10 minutes of handling in painted turtles (Polich 2016). We aliquoted whole blood (50μL) into tubes with 50μL of AIM V serum-free lymphocyte cell medium for lymphocyte proliferation assays (Palacios et al. 2013; Palacios and Bronikowski 2017) and made a blood smear stained

with Wright Giemsa for differential cell counts. We centrifuged the remaining whole blood (from 30-150 uL) and separated the plasma into two aliquots for CORT and immune assays before flash freezing in liquid nitrogen and storing at -80ºC. To assess age and its potential effects on color and physiology, we measured plastron length, which can be used as a proxy for age in these turtles (Hoekstra et al. 2018).

Color Analysis

We took RAW-formatted photographs (tripod-mounted Canon EOS Digital Rebel XSi camera and EF-S18-55mm lens) of each turtle's cranial region under controlled incandescent lighting and included a grey standard (18% reflectance; Insignia NS-DWB3M) in every photograph. We took two photographs of each turtle to assess repeatability and checked photographs for overexposure before analysis using the Image Calibration and Analysis Toolbox v. 1.22 (Troscianko and Stevens 2015) in ImageJ v. 1.52a (Schneider et al. 2012). The Image Calibration and Analysis Toolbox linearizes photographs to account for slight variation in lighting conditions between photographs using the grey standard and calculates reflectance (Troscianko and Stevens 2015). Reflectance is the measure of electromagnetic energy reflected off an object and is measured for each of the camera's color channels (blue, green, red). These color channels each correspond to a range of wavelengths (short wavelengths, SW; medium wavelengths, MW; long wavelengths, LW; Troscianko and Stevens 2015). For this study, we chose two regions of interest (ROIs) to measure in each photograph: the middle point of the colored stripe of the right forelimb and of the left forelimb, respectively (Fig. S1). We chose the forelimb stripes on each side because we did not measure reflectance in the ultraviolet (UV) spectrum; the limb stripes demonstrate low levels of reflectance in the UV spectrum in painted turtles and are visible to conspecifics during mating behaviors (Steffen et al. 2015). If the stripe

did not extend unbroken down the forelimb, we measured the nearest point to the middle of the stripe (Fig. S1).

We $\log_{10}$-transformed reflectance measures for the three color channels for normality before assessing repeatability (intraclass correlation coefficient, Lessells and Boag 1987) across the measures for each ROI (left or right forelimb stripe) in each color channel in R v. 3.6.1 (R Core Team 2019). Measures of reflectance were highly repeatable across photographs, with intraclass correlations between 81% and 87% across color channels, due to low variance within individuals (average SD = 0.05, see Color Analysis). Additionally, within a photograph, reflectance was repeatable across forelimb stripes, with intraclass correlations between 57% and 79% across color channels due to low variance within individuals (average SD = 0.07) and a high correlation coefficient between reflectance measures for each color channel (Pearson's $r >$ 0.6). Thus, we used reflectance measures from only the right forelimb ROI to calculate brightness and hues. We calculated brightness with non-transformed reflectance measures across color channels using the equation $\frac{(\mathrm{LW}+\mathrm{MW}+\mathrm{SW})/3}{655.35}$, which results in a brightness percentage (Stevens et al. 2014; Troscianko and Stevens 2015); high values indicate increased brightness and thus lighter color. We then $\log_{10}$-transformed these percentages to achieve normality for statistical analyses.

We calculated hue using multiple approaches that aim to assess hues visible to painted turtles through knowledge of color-opponent channels. Color-opponency refers to the contrasting polarization of retinal nerve cells in response to certain wavelengths of light; for example, in turtle chromaticity (C-type) horizontal cells, long wavelengths of light stimulate depolarization of cells, while shorter wavelengths result in hyperpolarization (Twig et al. 2003). The cells' opposing responses to different wavelengths of light allows discrimination between wavelengths,

which is hypothesized to produce different perceptions of hue. Our first measure of hue was based on one of the color-opponent channels, Red/Green, that has been established in turtle Red/Green C-type horizontal cells (Twig et al. 2003; Twig and Perlman 2004). In these cells, red light causes depolarization, and yellow and green light causes hyperpolarization. Thus, we calculated hue using the equation LW/MW, which is a ratio of the reflectance measures for the red and green color channels of the camera, respectively. This measure of hue should not be sensitive to UV wavelengths, as there is no evidence of SW- and UV-cone inputs in red/green horizontal retina cells (Zana et al. 2001), and thus should be an appropriate estimate of hue based on turtle vision. Additionally, this measure of hue includes the wavelengths for which painted turtles show maximal spectral sensitivity during behavioral trials (625 – 660nm) and for which painted turtles can behaviorally discriminate among wavelengths (can discriminate between light of 625nm and 685nm; Graf 1967). The second method of measuring hue was based on a principal components analysis (PCA) to assess the axes of color variation in the forelimb stripes (Spottiswoode and Stevens 2011; Stevens et al. 2014). We performed PCA on a covariance matrix of standardized $\log_{10}$-transformed reflectance measures for SW, MW, and LW channels in R v. 3.6.1 (R Core Team 2019), and the loadings on the principal components determined our decisions for which color-opponent channels to assess for hue.

For our second method of assessing hue, the PCA of reflectance measures resulted in three PCs. PC1 accounted for 93.9% of the variance, and as reflectance measures for all color channels load equally on this PC, this PC is equivalent to the variation in overall brightness across color channels. The second and third PCs accounted for 5.3% and 0.8% of the variance, respectively. As the third PC accounted for a low percentage of variance, we focused only on PC2. PC2 is equivalent to LW/(MW+SW). Our first measure of hue, based on known opponent

color channels in turtles (LW/MW, see Color Analysis), was highly correlated with PC2 (Pearson's $r > 0.99$). Thus, we only use the ratio LW/MW to characterize hue, which represents the ratio of long wavelengths (reds) to medium wavelengths (yellows and greens); a higher ratio represents a more reddish hue. Our final dependent variables of color are $\log_{10}$-transformed brightness and hue (LW/MW). Brightness and hue of the forelimb stripes of turtles in this study varied considerably (Fig. S1).

As these turtles were held in controlled ponds with supplemented diet, we compared our results for brightness and hue in this study to a dataset collected from the painted turtle source population at the TCRA (Judson, unpublished data). We took RAW-formatted photographs away from direct sunlight, with turtles held over a uniform grey background and the same grey standard used in the previous photographs held next to the arm stripes, using a tripod-mounted Sony α5000 camera with Sony 16-50mm F/3.5-5.6 PZ OSS E Mount lens. Although the cameras used for these two studies differed, and the photographs of turtles at the TCRA were taken outdoors in less controlled conditions, this comparison nonetheless yields a reference of variation in wild painted turtle color to assess whether diet substantially affects color variation in the turtles used in this study. Variation in brightness and hue displayed by painted turtles at the TCRA and captive turtles used in this study were similar, though the average brightness and hue across individuals varied between the two datasets. In wild TCRA painted turtles, brightness of the right forelimb ROI ranged from -3.8% to 35.8%, and in this study, brightness ranged from 7.7% to 50.5%. Hue of wild TCRA painted turtle forelimb stripes ranged from 1.59 to 3.52, and in this study, hue ranged from 1.16 to 3. The differences in average brightness and hue may be due to different cameras and photographing conditions. Nevertheless, the variance in the two datasets was not different (two-sample F-test $P > 0.22$), and thus the variation in our captive

study was representative of color variation in the wild. Additionally, the captive turtles did not appear to be more stressed than those at the TCRA, as baseline CORT values were similar to those reported across multiple studies at the TCRA (mean CORT this study=11.95 ng/mL; Refsnider et al. 2015 back-transformed least-square means=7 ng/mL; Polich 2016=27.45 ng/mL).

Physiological Measures

Stress Response: Corticosterone, Glucose, and Heterophil:Lymphocyte Ratios

Glucocorticoids, such as CORT, are common biomarkers used to assess individual health, as they mediate multiple physiological functions including an animal's stress response (Landys et al. 2006). We quantified the baseline concentration of circulating plasma CORT (ng/mL) using a double-antibody radioimmunoassay (ImmuChem Double Antibody Corticosterone I-125 RIA kit, MP Biomedicals, Irvine, CA, USA). This assay follows previously described protocols validated in painted turtles (Refsnider et al. 2015; Polich 2016). We ran all samples (N=57) in duplicate, with a pooled sample included with each batch to assess inter-assay variability. CORT was not correlated with handling time (Pearson's $r = 0.2$, $P = 0.14$).

Circulating glucose concentrations are produced by antagonism between glucocorticoids and insulin (Strack et al. 1995); appropriate concentrations of glucose are essential to both homeostatic functions and stress responses. We measured the baseline concentration of circulating glucose (Mg/dL) using 1.5µL blood plasma with a FreeStyle Lite® glucometer (Abbott Diabetes Care, Alameda, CA) and FreeStyle Lite® test strips (N=55; Gangloff et al. 2017).

Leukocyte profiles such as heterophil:lymphocyte (H:L) ratios measure physiological response to stressors (Davis et al. 2008; Polo-Cavia et al. 2013). Here, we analyzed H:L ratios via stained blood smears by identifying 100 leukocytes at 1000x magnification and counting the

number of heterophils and lymphocytes within those leukocytes (N=54; Gangloff et al. 2017). Under chronic stress conditions, a large H:L ratio is produced by glucocorticoids mobilizing lymphocytes into tissues and out of the bloodstream, while heterophils are increased in the bloodstream (Davis et al. 2008).

Innate Immune Function: Bactericidal Competence of Plasma, Natural Antibodies, and Lysis

The bactericidal competence (BC) of plasma measures constitutive innate immune function. Turtles with increased innate immune function are characterized by a high bacterial killing capacity, or competence, while individuals with depressed immune function may exhibit lower bactericidal competence (Matson et al. 2006). We assessed BC of plasma according to Palacios et al. (2011) and Refsnider et al. (2015) with a few modifications noted here. We diluted *Escherichia coli* working solution 1:160 with sterile phosphate-buffered saline (PBS) to produce a working solution containing approximately 300 colony-forming bacteria per 10µL. We prepared samples (N=54) with 10µL plasma, 90µL warm PBS, and 10µL *E. coli* working stock. We performed 3 controls for each set of samples, consisting of 100µL warm PBS and 10µL *E. coli* working stock. We incubated samples and controls for 20 minutes at 28ºC before plating each sample and control in duplicate, with 50µL on each plate. Finally, we incubated plates for 24 hours at 28ºC. We calculated proportion of bacteria killed as the mean number of bacterial colonies on the sample plates compared to the mean of the control plates, and we converted this to a proportion by subtracting from 1 (Palacios et al. 2011). We detected a batch effect due to decreased survivorship of the *E. coli* working stock over time, and thus z-transformed BC for each batch (3 batches over 3 days).

Natural antibodies (NAbs) and complement-mediated lysis (CL) are two additional measures of constitutive innate immunity; high levels of NAbs and CL activity indicate a higher

level of innate immune defense (Matson et al. 2005). We assessed these immune measures using a haemolysis-haemagglutination assay modified from Matson et al. (2005) for use in reptiles (Palacios et al. 2011), specifically painted turtles (Schwanz et al. 2011; Refsnider et al. 2015). We added 10µL plasma to the first column of a 96-well plate, and performed serial two-fold dilutions with 10µL of plasma and PBS beginning with the second column. Thus, the first column represents undiluted plasma, with each subsequent column diluted by a factor of two. We then added 10µL of a 2% sheep red blood cell (SRBC) suspension to each well. We gently mixed plates on a shaker for 2 minutes before incubating plates for 60 minutes at 28°C and then immediately scoring titers. We estimated titers as $-\log_2$ of the highest dilution factor of plasma that showed agglutination or lysis for NAbs and CL measures, respectively. As some wells showed partial agglutination or lysis, we scored intermediate titers as half scores. We ran all samples (N=52) in duplicate, with the exception of plasma-limited samples (N=3), and averaged scores across duplicates. We included a positive control (anti-SRBC antibodies diluted to 1:16, Fisher # ICN55800) and negative control (PBS) in each plate. Lysing ability of plasma samples using this method were low for our study, similar to Schwanz et al. (2011), thus we converted CL titers to a binary variable (i.e., 0 for no lysis, 1 for any lysis of SRBC).

Adaptive Immune Function: Lymphocyte proliferative ability

Lymphocyte proliferation assays measure an organism's adaptive immune function by assessing the activation and proliferation of B- and T-lymphocytes in response to a mitogen; increased proliferation indicates a stronger immune response (Palacios et al. 2013). We gauged lymphocyte proliferation ability with a whole-blood mitogenic stimulation assay (Palacios et al. 2013; Palacios and Bronikowski 2017) performed within 24 hours of blood collection. We assayed samples (N=54) in triplicate in a 96-well plate format. We used two T-cell mitogens, concanavalin A (ConA) and phytohemagglutinin (PHA), and one B-cell mitogen,

lipopolysaccharide (LPS). Detailed methods for mitogens and concentrations can be found in Palacios et al. (2013). Briefly, we incubated mitogen- and control-treated triplicates for 96 hours total at 28°C in a 7% CO2 humidified atmosphere, and we pulsed plates with tritiated [^{3}H] thymidine (0.5 μCi/well) for the final 24 hours of incubation. We harvested triplicates with glass-fiber filters using a cell harvester (Combi Cell Harvester; Skatron Instruments, Sterling, VA) and quantified thymidine incorporation in counts per minute (cpm) using a liquid scintillation counter (Palacios et al. 2013; Palacios and Bronikowski 2017). The proliferative ability of lymphocytes is expressed as a stimulation index (SI; Palacios et al. 2013), which is a ratio that compares mean cpm of mitogen-stimulated samples and non-stimulated controls. Samples with no difference in stimulation compared to controls received an SI of one. To control for differences in the initial number of lymphocytes in each sample, we estimated total leukocyte counts using the indirect Phloxin B method (Campbell and Ellis 2007) with 0.1% phloxin stain (Vetlab Supply, Palmetto Bay, FL) and hemocytometer (Palacios et al. 2013). We used slide preparations from the H:L assay to calculate the starting number of lymphocytes by multiplying the total leukocyte count by the proportion of lymphocytes for each individual. For the three individuals for which we could not detect enough cells on the slide preparations, we averaged the proportion of lymphocytes across all individuals and used that proportion to calculate starting number of lymphocytes. To correct the SI for starting number of lymphocytes, as greater numbers of lymphocytes should increase SI, we performed a linear regression of starting number of lymphocytes versus SI for each mitogen. We use the residuals from those models as values for SI of the three mitogens.

Statistics

We used SAS v. 9.4 (SAS Institute, Cary, NC) for all statistical analyses described here. We assessed the influence of independent variables on $\log_{10}$-transformed brightness and the

multiple measures of hue with general linear models in PROC GLM. First, we removed outliers that were less than or greater than three standard deviations from the mean (N=1 for BC, H:L, CORT, SI_{ConA}; N=2 for SI_{PHA}, SI_{LPS}). We calculated correlations among all physiological variables to assess our prediction that stress measures and immune function measures are associated with one another and to avoid multicollinearity in the models. To more effectively test the influence of separate immune and stress responses, we ran two sets of models including either the stress-response measures or the immune-system measures with brightness or hue as the dependent variable. For all models, we included sex and the pond in which each turtle was kept as fixed effects. We also included plastron length standardized by sex (zPL) using a sex-specific z-transformation, as female painted turtles attain larger body sizes than males (Hoekstra et al. 2018). The original models for stress response included pond, sex, zPL, CORT, glucose, and H:L ratio. We also included interactions among sex, zPL, and the stress measures, as interactions among these factors may differentially influence color depending upon the sex or size of the individual, as was found in Spanish terrapins (Ibáñez et al. 2013). There were no strong correlations among stress variables (Supplemental Table 1), and we found no multicollinearity in the models. We removed non-significant interactions ($P > 0.1$) and kept all main effects in the models. The final models for stress response are summarized in Table 1.

The original models for immune function included pond, sex, zPL, standardized BC, NAbs, CL, SI_{ConA}, SI_{PHA}, and all two-way interactions among sex, zPL, and these immune measures. We excluded SI_{LPS} from the models, as it was strongly correlated with SI_{PHA} (Pearson's $r = 0.69$; Supplemental Table 1) and model results were the same when including either SI_{PHA} or SI_{LPS}. We removed non-significant interactions ($P > 0.1$) and kept all main

effects. The final models for immune function are summarized in Table 2. We graphed significant relationships using ggplot2 (Wickham 2016) in R version 3.6.1 (R Core Team 2019).

Supplemental References

Campbell T, Ellis CK (2007). Avian and exotic animal hematology and cytology. 3rd edn. Blackwell Publishing, Ames

Davis AK, Maney DL, Maerz JC (2008) The use of leukocyte profiles to measure stress in vertebrates: a review for ecologists. Funct Ecol 22:760-772 doi: 10.1111/j.1365-2435.2008.01467.x

Gangloff EJ, Sparkman AM, Holden KG, Corwin CJ, Topf M, Bronikowski AM (2017) Geographic variation and within-individual correlations of physiological stress markers in a widespread reptile, the common garter snake (*Thamnophis sirtalis*). Comp Biochem Physiol, A: Mol Integr Physiol 205:68-76 doi: 10.1016/j.cbpa.2016.12.019

Graf V (1967) A spectral sensitivity curve and wavelength discrimination for the turtle *Chrysemys picta picta*. Vision Res 7:915-928 doi: 10.1016/0042-6989(67)90010-7

Hoekstra LA, Weber RC, Bronikowski AM, Janzen FJ (2018) Sex-specific growth, shape, and their impacts on life history of a long-lived vertebrate. Evol Ecol Res 19:639–657

Ibáñez A, Marzal A, López P, Martín J (2013) Sexually dichromatic coloration reflects size and immunocompetence in female Spanish terrapins, *Mauremys leprosa*. Naturwissenschaften 100:1137-1147 doi: 10.1007/s00114-013-1118-2

Landys MM, Ramenofsky M, Wingfield JC (2006) Actions of glucocorticoids at a seasonal baseline as compared to stress-related levels in the regulation of periodic life processes. Gen Comp Endocrinol 148:132-149 doi: 10.1016/j.ygcen.2006.02.013

Lessells CM, Boag PT (1987) Unrepeatable repeatabilities: a common mistake. Auk 104:116-121 doi: 10.2307/4087240

Matson KD, Ricklefs RE, Klasing KC (2005) A hemolysis-hemagglutination assay for characterizing constitutive innate humoral immunity in wild and domestic birds. Dev Comp Immunol 29:275-286 doi: 10.1016/j.dci.2004.07.006

Matson KD, Tieleman BI, Klasing KC (2006) Capture stress and the bactericidal competence of blood and plasma in five species of tropical birds. Physiol Biochem Zool 79:556-564 doi: 10.1086/501057

Mitchell TS, Refsnider JM, Sethuraman A, Warner DA, Janzen FJ (2017) Experimental assessment of winter conditions on turtle nesting behaviour. Evol Ecol Res 18:271-280

Palacios MG, Bronikowski AM (2017) Immune variation during pregnancy suggests immune component-specific costs of reproduction in a viviparous snake with disparate life-history strategies. J Exp Zool Part A 327:513-522 doi: 10.1002/jez.2137

Palacios MG, Sparkman AM, Bronikowski AM (2011) Developmental plasticity of immune defence in two life-history ecotypes of the garter snake, *Thamnophis elegans* - a common-environment experiment. J Anim Ecol 80:431-437 doi: 10.1111/j.1365-2656.2010.01785.x

Palacios MG, Cunnick JE, Bronikowski AM (2013) Complex interplay of body condition, life history, and prevailing environment shapes immune defenses of garter snakes in the wild. Physiol Biochem Zool 86:547-558 doi: 10.1086/672371

Polich RL (2016) Stress hormone levels in a freshwater turtle from sites differing in human activity. Conserv Physiol 4:1-9 doi: 10.1093/conphys/cow016

Polo-Cavia N, López P, Martín J (2013) Head coloration reflects health state in the red-eared slider *Trachemys scripta elegans*. Behav Ecol Sociobiol 67:153-162 doi: 10.1007/s00265-012-1435-z

R Core Team (2019). R: A language and environment for statistical computing. R Foundation for Statistical Computing.

Refsnider JM, Palacios MG, Reding DM, Bronikowski AM (2015) Effects of a novel climate on stress response and immune function in painted turtles (*Chrysemys picta*). J Exp Zool Part A 323:160-168 doi: 10.1002/jez.1902

Schneider CA, Rasband WS, Eliceiri KW (2012) NIH Image to ImageJ: 25 years of image analysis. Nat Methods 9:671-675 doi: 10.1038/nmeth.2089

Schwanz L, Warner DA, McGaugh S, Di Terlizzi R, Bronikowski A (2011) State-dependent physiological maintenance in a long-lived ectotherm, the painted turtle (*Chrysemys picta*). J Exp Biol 214:88-97 doi: 10.1242/jeb.046813

Spottiswoode CN, Stevens M (2011) How to evade a coevolving brood parasite: egg discrimination versus egg variability as host defences. Proc R Soc B 278:3566-3573 doi: 10.1098/rspb.2011.0401

Steffen JE, Learn KM, Drumheller JS, Boback SM, McGraw KJ (2015) Carotenoid composition of colorful body stripes and patches in the painted turtle (*Chrysemys picta*) and red-eared slider (*Trachemys scripta*). Chelonian Conserv Biol 14:56-63 doi: 10.2744/ccab-14-01-56-63.1

Stevens M, Lown AE, Wood LE (2014) Color change and camouflage in juvenile shore crabs *Carcinus maenas*. Front Ecol Evol 2:14 doi: 10.3389/fevo.2014.00014

Strack AM, Sebastian RJ, Schwartz MW, Dallman MF (1995) Glucocorticoids and insulin: reciprocal signals for energy balance. Am J Physiol Regul Integr Comp Physiol 268:R142-R149 doi: 10.1152/ajpregu.1995.268.1.R142

Troscianko J, Stevens M (2015) Image calibration and analysis toolbox - a free software suite for objectively measuring reflectance, colour and pattern. Methods Ecol Evol 6:1320-1331 doi: 10.1111/2041-210X.12439

Twig G, Perlman I (2004) Homogeneity and diversity of color-opponent horizontal cells in the turtle retina: Consequences for potential wavelength discrimination. J Vis 4:403-414 doi: 10.1167/4.5.5

Twig G, Levy H, Perlman I (2003) Color opponency in horizontal cells of the vertebrate retina. Prog Retin Eye Res 22:31-68 doi: 10.1016/s1350-9462(02)00045-9

Wickham H (2016). ggplot2: Elegant Graphics for Data Analysis. Springer-Verlag New York.

Zana Y, Ventura DF, De Souza JM, DeVoe RD (2001) Tetrachromatic input to turtle horizontal cells. Vis Neurosci 18:759-765 doi: 10.1017/S0952523801185093

Supplemental Table 1: Pearson's *r*, *P* = probability, N = sample size. Correlations with $P < 0.05$ in bold. CORT = corticosterone, H:L = heterophil:lymphocyte ratio, BC = bactericidal competence, SI = lymphocyte stimulation index for respective mitogen (ConA, PHA, LPS) standardized by number of lymphocytes.

	CORT	Glucose	H:L Ratio	Agglutination	Lysis	BC	SI_{ConA}	SI_{PHA}	SI_{LPS}
CORT	1								
P	—								
N	56								
Glucose	0.12674	1							
P	0.3611	—							
N	54	55							
H:L	**0.28957**	-0.19513	1						
P	**0.0373**	0.17	—						
N	**52**	51	53						
Agglutination	**0.43308**	0.1012	0.00901	1					
P	**0.0015**	0.4844	0.951	—					
N	**51**	50	49	52					
Lysis	0.0969	0.0314	0.11826	0.19385	1				
P	0.4987	0.8286	0.4184	0.1685	—				
N	51	50	49	52	52				
BC	0.16028	-0.01717	0.17005	**0.35745**	**0.47077**	1			
P	0.2563	0.9048	0.2378	**0.01**	**0.0005**	—			
N	52	51	50	**51**	**51**	53			
SI_{ConA}	0.07592	0.08213	-0.07469	-0.2025	0.06881	-0.19849	1		
P	0.5927	0.5667	0.61	0.1675	0.6421	0.1716	—		
N	52	51	49	48	48	49	53		
SI_{PHA}	0.07986	0.10738	-0.01626	-0.0681	0.06838	0.00105	**-0.42223**	1	
P	0.5775	0.4579	0.9117	0.6456	0.6442	0.9943	**0.002**	—	
N	51	50	49	48	48	49	**51**	52	
SI_{LPS}	0.05309	0.03963	-0.12668	0.05998	0.20632	0.03846	-0.11337	**0.68787**	1
P	0.7114	0.7847	0.3857	0.6855	0.1595	0.793	0.4283	**<.0001**	—
N	51	50	49	48	48	49	51	**52**	52

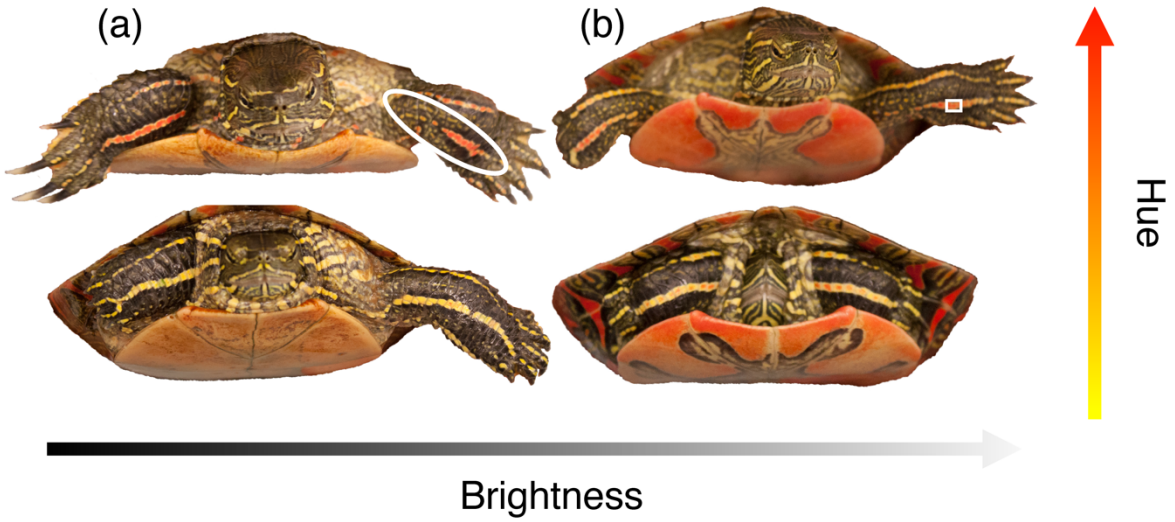

Figure S1: Four example images of turtles from this study arranged by overall percent brightness and hue of their forelimb stripes. a) An example of a turtle whose stripe does not extend unbroken down the forelimb. In those cases, the largest region of color closest to the midpoint was measured. b) An example of a measured region of interest (ROI) is shown by the white box. Backgrounds for all images were removed using Adobe Photoshop CC 2018

CHAPTER 3. PHENOTYPIC AND ENVIRONMENTAL PREDICTORS OF REPRODUCTIVE SUCCESS IN PAINTED TURTLES

Jessica M. Judson, Luke A. Hoekstra, Kaitlyn G. Holden, and Fredric J. Janzen

Department of Ecology, Evolution, and Organismal Biology, Iowa State University, Ames, Iowa, USA

Modified from a manuscript submitted to *Behavioral Ecology*

Abstract

Sexual selection is often assumed to elicit sexually dimorphic traits. However, most work on this assumption in tetrapod vertebrates has focused on birds. In this field experiment, we assessed relationships between both sexually dimorphic (body size, claw length) and non-dimorphic traits (forelimb stripe color, baseline corticosterone concentrations) and reproductive success in adult painted turtles to explicate the roles of these phenotypes in mate choice and the evolution of sexual dimorphism. We also modified adult sex ratios in experimental ponds to elucidate the role of biased sex ratios on reproductive success, which is a timely test of the potential threat of biased sex ratios on population persistence in a species with temperature-dependent sex determination. We found no strong influence of male phenotypes on male siring success, but female body size and baseline corticosterone concentrations predicted female clutch sizes. We find weak evidence that adult sex ratio influences male siring success, with a male-biased sex ratio producing lower male siring success than a female-biased sex ratio. This study offers evidence that female mate choice may not be an important selective force on male phenotypes, but that instead selection occurs on female phenotypes, particularly body size and corticosterone concentrations. Further, biased adult sex ratios can influence reproductive success

of both sexes. Finally, the use of Kompetitive Allele Specific PCR (KASP) was highly successful in parentage analysis, which adds reptiles to the growing list of taxa successfully genotyped with this new technology.

Introduction

Sexually dimorphic traits frequently inspire studies of sexual selection. While some sexually dimorphic traits can be explained by sexual selection on males (e.g., White et al. 2018), others do not influence male reproductive success, and instead may reflect selection on females (Blanckenhorn 2005). Phenotypes that do not exhibit sexual dimorphism can also influence male or female reproductive success (e.g., Kelly et al. 2012). Furthermore, the environmental context of mating, such as adult sex ratio, can affect reproductive success, shaping population dynamics and persistence (Szekely et al. 2014).

Large body size is typically a strong predictor of male reproductive success (e.g., Shine et al. 2000; White et al. 2018), particularly in species where male-male competition for mates or territories occurs, or where forced matings are common. However, under female-biased sexual size dimorphism (SSD), female choice may determine reproductive success (Berry and Shine 1980). Male body size may still be important for mate choice in such species, but female-biased SSD can evolve due to fecundity selection on females (Blanckenhorn 2005). In these situations, large female body size predicts increased reproductive output (e.g., Cox et al. 2003). In addition to SSD, other sexually dimorphic traits, including color, can affect reproductive success. Male color influences reproductive success in many vertebrates (e.g., Siefferman and Hill 2003; Salvador et al. 2007).

Non-dimorphic phenotypes also may be important for reproductive success of males and females. In species with high biparental investment in care of offspring, both sexes should be

choosy in selecting mates (Johnstone et al. 1996). Brightly colored ornaments exhibited by both sexes can send similar or different signals of quality to potential mates (Kelly et al. 2012). However, in vertebrates without heavy investment in parental care, the relationship between color and reproductive success is less well understood. In some species of brightly colored pond turtles, for example, color may not vary between the sexes (Judson et al. In review), yet female choice of males is often invoked as generating bright colors on the skin and plastron (e.g., Polo-Cavia et al. 2013). Thus, color may still play a role in reproductive success even when color is not sexually dimorphic.

Beyond morphology, physiological phenotypes associated with stress responses may predict reproductive success. Stress hormones (i.e., glucocorticoids) in vertebrates are essential mediators of energy balance in response to both acute stressors and other common activities, including feeding and reproduction (Landys et al. 2006). Glucocorticoids are often studied in the context of trade-offs, as acutely or chronically stressed iteroparous organisms may need to allocate energetic resources toward survival at the expense of reproduction (Wingfield and Sapolsky 2003). The CORT-Fitness Hypothesis (Bonier et al. 2009) posits that stressed vertebrates may experience decreased fitness as a result of increased stress (often measured by concentrations of corticosterone; CORT). However, increased CORT during reproductive activity can also facilitate reproductive behaviors and have positive effects on fitness (Bonier et al. 2009). Thus, elevation of glucocorticoids is not in and of itself indicative of a negative acute or chronic life event, and context matters. Although CORT can directly mediate reproductive physiology and behavior, it can also interact with mating signals, including color, to influence mate choice and, ultimately, fitness (Moore and Hopkins 2009; reviewed in Leary and Baugh 2020).

In addition to phenotype, environmental conditions can substantially influence individual reproductive success. Resource availability often strongly determines reproductive success (e.g., Hoset et al. 2017). In some populations, the adult sex ratio (ASR) may be biased, thus the availability of mates may be an important resource dictating reproductive success and future population dynamics. Biased ASR can modify the frequency of intrasexual (Weir et al. 2011) and intersexual competition (Le Galliard et al. 2005) and change the dynamics of mate choice (Atwell and Wagner 2014; Grant and Grant 2019), which can have long-term consequences for population persistence (e.g., Steifetten and Dale 2006; reviewed in Szekely et al. 2014). In common lizards, for example, increased competition due to skewed ASR changed behavior and increased intersexual aggression, leading to population declines (Le Galliard et al. 2005). Many vulnerable species exhibit biased ASR due to skewed death rates of males or females (e.g., Heinsohn et al. 2019). In reptiles with temperature-dependent sex determination (TSD), biased ASR might be exacerbated by ongoing climate warming producing skewed offspring sex ratios (Janzen 1994; Schwanz et al. 2010). These biased ASRs also could contribute to decreased effective population sizes and trap populations in an extinction vortex (Grayson et al. 2014). Understanding the influence of skewed ASR on reproductive success, particularly in species with TSD, is thus important in both basic and applied contexts.

In this study of a pond turtle with female-biased SSD, we measured body size, claw length, forelimb stripe color, and baseline CORT concentrations to quantify their relative influence on male and female reproductive success. Furthermore, using semi-natural experimental ponds, we modified the ASR to test its influence on reproductive success and potential impact on population dynamics of a species with TSD. Finally, we assigned parentage of offspring by developing a set of SNPs from population-level RADseq data and used a

genotyping technology new to reptiles, Kompetitive Allele Specific PCR (KASP), to genotype all individuals included in this study.

Methods

Study System

The painted turtle (*Chrysemys picta*) is widespread in North America (Ernst and Lovich 2009). Adults are sexually dimorphic: males have elongated foreclaws and females are larger, suggesting forcible insemination is likely uncommon (Berry and Shine 1980; but see Hawkshaw et al. 2019). Visual and tactile courtship displays performed before mating offer the potential for female choice based on male traits, including his body size, claw length, and color (Ernst and Lovich 2009). Females can store sperm, which could allow for cryptic female choice, and some clutches in the wild exhibit multiple paternity (~13%, Pearse et al. 2001; >30%, Pearse et al. 2002; ~14.1%, McGuire et al. 2014), typically with two sires represented in a single clutch. Males may choose females based upon female size (McGuire et al. 2014), as size is an indicator of female reproductive output (e.g., Hoekstra et al. 2018), or by coloration (Judson et al. In review). Alternatively, males may instead attempt mating with as many females as possible (Bateman 1948) based on encounter rate, or may mate randomly with respect to female traits. Predictors of reproductive success for painted turtles beyond female size remain elusive. The brightness and hue of adult forelimb stripes indicate aspects of stress and immune health (Judson et al. In review), and thus could signal mate quality, though the influence of color on reproductive success has not been evaluated. Moreover, social context, especially the ASR (e.g., Szekely et al. 2014), can influence mating systems generally, but its influence on reproductive success in painted turtles is not well understood. Incubation temperature determines hatchling sex ratios in painted turtles (e.g., Janzen 1994), which in turn affect ASR (Schwanz et al. 2010),

and climate change models predict a warming environment that could further skew sex ratios over time (Refsnider and Janzen 2016).

Turtle Husbandry and Sampling

The following research methods were approved by Iowa State University (ISU) IACUC (12-03-5570-J). We constructed three semi-natural experimental ponds (19m × 15m × 1.5m) at the ISU Horticulture Farm surrounded by 25m x 55m x 1m silt fencing with aluminum flashing to prevent movement of turtles between ponds and to allow females adequate area surrounding the ponds to construct nests (Judson et al. In review; Fig. 1). In April 2016, we released 63 adults (26 females, 37 males), collected from the Thomson Causeway Recreation Area (TCRA) in Thomson, IL, USA, into the ponds. Permits for painted turtle collection were provided by the United States Army Corps of Engineers, the United States Fish and Wildlife Service (SUP 32576-021), and the Illinois Department of Natural Resources (NH11.0073). We classified all turtles as sexually mature using a combination of size, presence of sexually-dimorphic characters (e.g. elongated claws in males), and annual rings on plastral scutes (Moll 1973). We placed turtles into the ponds with differing ecologically-relevant ratios of females to males recorded in wild populations (e.g., Hughes 2011; Dupuis-Désormeaux et al. 2017), which we refer to as an ASR treatment: male-biased (M > F), female-biased (M < F), and approximately equal number of males and females (M = F; Fig. 1). We supplemented the turtles' diet with Mazuri® Aquatic Turtle Diet for the duration of the experiment, which did not measurably change forelimb stripe coloration between captive and wild turtles (Judson et al. In review). In May and June of 2016, we monitored ponds for nesting activity hourly 0600-2200 h. After a female finished nesting, we obtained a blood sample with a heparin-rinsed syringe from the caudal vein for genotyping. We removed eggs from each nest, placed them into plastic containers filled with moist vermiculite (-

150 kPa), and incubated them at 28°C until hatching at ISU. Following incubation, we sampled tissue from 207 hatchlings for genotyping, excluding undeveloped embryos and infertile eggs (N=20).

In July 2016, following the nesting season, we removed the turtles from the ponds and collected a blood sample within 10 minutes of capture. This 10-minute limit was to assess baseline measures of CORT in the bloodstream, which rise after 10 minutes of handling in painted turtles (Polich 2016). We centrifuged the blood to separate the plasma before snap freezing plasma and red blood cells in liquid nitrogen and storing at -80ºC for CORT measures and genotyping, respectively. We also measured other aspects of stress and immune function (Judson et al. In review), but we do not consider these variables here, as we did not have strong a priori predictions for their influence on reproductive output in painted turtles, and post-hoc analysis of the effects of unreported physiological variables on reproductive success did not affect our conclusions regarding the effects of CORT. Finally, we measured plastron length for all turtles and length of the third claw of each forelimb to the nearest mm for males, which is usually the longest claw (McTaggart 2000; Hughes 2011). We averaged the two claw measures, excluding any claws that were broken in our averages (N=5).

Color Analysis

For color analysis, we followed the methods of Judson et al. (In review). Briefly, we used a tripod-mounted Canon EOS Digital Rebel XSi camera and EF-S18-55mm lens to take RAW-formatted photographs of each turtle's cranial region under controlled incandescent lighting with a grey standard (18% reflectance; Insignia NS-DWB3M) in every photograph. We used the Image Calibration and Analysis Toolbox v. 1.22 (Troscianko and Stevens 2015) in ImageJ v. 1.52a (Schneider et al. 2012) to linearize photographs and obtain reflectance measures. We

measured reflectance as close as possible to the middle point of the right forelimb stripe, which appears yellow, orange, or red to the human eye. We performed the above process for all except six turtles, who either were ill (N=2: 1 female, 1 male) and thus not photographed, or were not recovered from the ponds (N=4 females, likely due to predation; F. Janzen personal observation) and thus were not photographed or measured for CORT. We used two measures to represent color variation of forelimb stripes with long wavelength (LW), medium wavelength (MW) and short wavelength (SW) reflectance measures: overall percent brightness, calculated as $\frac{(LW+MW+SW)/3}{655.35}$ (Troscianko and Stevens 2015; Judson et al. In review), and hue, calculated as LW/MW (Judson et al. In revision). High values of percent brightness indicate lighter stripe color, whereas high values of hue indicate increased redness and decreased yellowness of the forelimb stripe.

Corticosterone

CORT levels reflect vertebrate stress responses, but also function in concert with other physiological factors to facilitate reproductive behaviors, feeding, and maintenance of homeostasis (Moore and Jessop 2003; Landys et al. 2006). To quantify baseline concentrations of circulating plasma CORT (ng/mL), we used a double-antibody radioimmunoassay (ImmuChem Double Antibody Corticosterone I-125 RIA kit, MP Biomedicals, Irvine, CA, USA (Polich 2016; Judson et al. In review). We quantified samples (N=59) in duplicate and included a pooled sample to assess inter-assay variability (average coefficient of variation 4.0%).

Parentage Analysis

We used Kompetitive Allele Specific PCR (KASP) all-inclusive services to extract DNA and genotype 96 SNP loci in all 63 adults and 207 hatchlings (Semagn et al. 2014). KASP has been successful for genotyping many crop species (McCouch et al. 2010; Khera et al. 2013), and its use in vertebrates is increasingly common (e.g., Wielstra et al. 2016; Bourgeois et al. 2018). To determine the 96 SNP loci that confidently assign parentage, we used RADseq data of known parent-offspring pairs from this population (FJ Janzen, unpublished data). Our SNP filtering of RADseq data was adapted from GATK Best Practices (McKenna et al. 2010; DePristo et al. 2011). Briefly, we used a minGQ filter of 20, kept only biallelic sites, allowed only 1% missing genotypes for each site, and used a minor allele frequency filter of 0.4 to select SNPs with high heterozygosity in the population. This filtering yielded 801 SNPs. Next, we used the SAMtools v. 1.4 (Li et al. 2009) faidx command to query the surrounding sequence of each SNP from the *C. picta* draft genome v. 3.0.3 (Shaffer et al. 2013). We removed any SNPs with missing data or ambiguous sequence in the 50 bp upstream or downstream of the SNP of interest. We further reduced the SNP set by removing SNPs of interest that had >1 SNP in the flanking regions for a final set of N=150. We measured linkage disequilibrium of these SNPs in PLINK v. 1.9 (Purcell et al. 2007) to ensure that none were linked ($r^2 < 0.5$, average r^2 across all SNPs = 0.04). We selected 96 SNPs from this set, a number that yielded high parentage assignment success in other studies of vertebrates (Hauser et al. 2011). We compared flanking primer sequences for these SNPs to the *C. picta* draft genome using BLAST to eliminate multiple matches.

To analyze genotypes obtained from KASP, we used the pedigree program Cervus v. 3.0.7 (Kalinowski et al. 2007). We recorded maternity assignment for all clutches during nesting observations, and Cervus assigned these recorded mothers to the correct clutches in all cases. Thus, we tested paternity with known maternal genotypes in Cervus with default settings. We

also analyzed sibship among hatchlings using the full likelihood method of COLONY v. 2.0.6.5 (Jones and Wang 2010) to confirm multiple paternity and provide insight into relationships among hatchlings resulting from sperm storage that were not sired by males included in the experimental ponds.

Statistics

For all statistical analyses and plotting, we used R version 4.0.2 (R Core Team 2020). Our final sample sizes for inclusion in statistical analyses were 22 females and 37 males recovered from the ponds (see Color Analysis). As we expected that predictors of reproductive success would differ between males and females, we modeled the sexes separately. We standardized the continuous predictor variables (plastron length, CORT concentrations, forelimb stripe brightness and hue, and male claw length) by sex to mean of zero and unit variance so that slopes could be directly compared among variables (Grueber et al. 2011). We checked for outliers in continuous predictors using a threshold of three standard deviations from the mean for each sex, and found one male outlier for forelimb stripe brightness, which we removed.

Female reproductive success - We assessed correlations among female measures, and found that no predictor variables were strongly correlated ($-0.63 < r < 0.52$). For females, the measure of reproductive success was the clutch size (including infertile eggs and undeveloped embryos), and the full model conditional upon female clutch size being greater than zero was as follows:

$$Y = \mu + ASR\ Treatment + zPlastron\ Length + zCORT + zBrightness + zHue + \varepsilon$$

where μ represents the grand mean and ε the error term, and "z" precedes standardized continuous predictors. We included ASR treatment as a fixed effect. We included plastron length, as body size is an important predictor of clutch size in female painted turtles (e.g.,

Hoekstra et al. 2018). Clutch size was under-dispersed, as is typical of reproductive data (Brooks et al. 2019), and three females that were recovered from the ponds did not oviposit. Thus, to account for a zero-inflated, under-dispersed count distribution, we assessed generalized linear models using 'glmmTMB' v 1.0.2.1 (Brooks et al. 2017; Brooks et al. 2019). We used an all-subset approach to model selection, which included every combination of variables from the full model and intercept-only models which assess only the constant and residual variance (Grueber et al. 2011), with a zero-inflated Conway-Maxwell-Poisson error distribution to account for under-dispersion and zero-inflation in clutch size using 'dredge' from 'MuMIn' v 1.43.17 (Bartoń 2020). The zero-inflation model included an intercept-only zero-inflation model (~1; Brooks et al. 2019) with no other predictors included, as only a small number of females did not reproduce, and increased zero-inflation model complexity induced model convergence issues. We selected the best-fitting model(s) using AIC_c (Burnham and Anderson 2002). To compare models using AIC_c, we removed the female for which we did not have color measures from all model comparisons, as comparisons among models are only valid when the same data are included for each model (Symonds and Moussalli 2011). We tested the full and best-fitting models for dispersion and model fit with 'DHARMa' v 0.3.3.0 (Hartig 2020) and for multicollinearity using 'performance' v 0.5.0 (Lüdecke et al. 2020). We also calculated Akaike model and parameter weights for all model subsets using 'MuMIn' v 1.43.17. We report parameter estimates for the models within two ΔAIC_c units from the best submodel, excluding any nested models included in that threshold (Arnold 2010).

Male reproductive success - For males, we checked correlations and assessed multicollinearity in the same manner as for females. We found no strong correlations amongst predictor variables ($-0.58 < r < 0.53$). The measure of reproductive success was the number of

offspring sired (i.e., absolute fitness; e.g. Noble et al. 2013) as determined by parentage analysis, and the full model conditional upon the number of offspring sired being greater than zero was as follows:

$$Y = \mu + ASR\ Treatment + zPlastron\ Length + zCORT + zBrightness + zHue + zMean\ Claw\ Length + \varepsilon$$

We modeled males in the same manner as females with a few exceptions. Number of offspring sired was both zero-inflated and over-dispersed, thus we assessed full conditional model fit with zero-inflated Poisson, Conway-Maxwell-Poisson, and negative binomial error distributions. A zero-inflated Conway-Maxwell-Poisson error distribution best fit the full conditional model according to dispersion tests in 'DHARMa' v 0.3.3.0 and comparison among error distributions using AIC_c, so we used this error distribution for all model subsetting comparisons. We excluded three males due to missing data from subsetted models (see Color Analysis). The zero-inflation model for males included the same predictors as the male full conditional model, and intercept-only conditional and zero-inflation models were included in model comparisons. We also performed model subsetting comparisons with an intercept-only zero-inflation model for comparison. We created all figures of results using 'ggplot2' v. 3.3.2 (Wickham 2016).

Opportunity for Selection - Finally, we measured the Opportunity for Selection using a new index, ΔI, which allows comparison between males and females when sex ratios are unequal (Waples 2020). We used the same offspring life stage comparison for males and females, the number of hatchlings, for this index.

Results

The 26 females laid 22 clutches during the nesting season, resulting in 227 eggs laid. Clutch sizes ranged from 0-14 eggs, with a mean of 10.3 eggs among ovipositing females (Fig. 2). Of the 227 eggs laid, 207 offspring successfully hatched, split between the male-biased pond (74 offspring), equal sex-ratio pond (69 offspring), and female-biased pond (64 offspring; Fig. 1).

The final panel of SNPs consisted of 88 loci, as 8 of the 96 loci were not successfully genotyped due to unclear separation of clusters or poor amplification during KASP genotyping. We genotyped all 207 hatchlings, though 5 individuals genotyped at fewer than 50 loci could not be assigned to a single sire. These 5 hatchlings were thus excluded from statistical analyses of males. We assigned paternity for all remaining hatchlings with high confidence, with the exception of two clutches (14 hatchlings) that did not have likely sires among the males in this study. Offspring within each of these two clutches were full siblings with a probability of 1; there was no evidence of half siblings between the two clutches, suggesting that the sires were different individuals whose sperm was stored and that these clutches did not exhibit multiple paternity. Among the males in our study, 21 sired no offspring, and 16 sired between 1 and 34 offspring in 1 to 4 different clutches, with a mean of 11.8 offspring sired (Fig. 2). The incidence of multiple paternity was 18%, or 4 out of 22 clutches, with two multiply-sired clutches each from the male-biased and equal-ratio ponds. Opportunity for Selection (ΔI) was 0.12 for females and 2.33 for males.

Females

The best-fitting model according to AIC_c included plastron length and CORT (Table 1). Larger females and those with lower CORT concentrations laid more eggs (Table 2; Fig. 3).

Pond ASR and females' forelimb stripe brightness and hue did not predict female reproductive success, as indicated by low Akaike weights of these variables (0.09, 0.14, and 0.24, respectively) compared to plastron length (0.99) and CORT (0.46). We detected no multicollinearity in either the full or best-fitting model nor issues with model fit, as dispersion tests were non-significant (Figs. S1, S2).

Males

Best-fitting models according to AIC_c included either ASR treatment or forelimb stripe brightness (Table 1). However, model weights were low for all models (≤ 0.05), and parameter weights were all ≤ 0.50, suggesting considerable model uncertainty. Additionally, the null model including only intercepts for the conditional and zero-inflation parameter was 2.5 ΔAIC_c units from the best-fitting model (Table 1), suggesting the included variables are weak predictors of male reproductive success. Notwithstanding, according to these models, female-biased ASR and greater forelimb stripe brightness increased individual reproductive success (Table 3, Fig. 4). As with the female models, we detected no multicollinearity in conditional and zero-inflated full and best-fitting models and no issues with model fit as indicated by non-significant dispersion tests (Figs. S3, S4). Model ΔAIC_c rankings for the best-fitting models with an intercept-only zero-inflation model used in model subsetting were the same as those including a zero-inflation model that matched the full conditional model.

Discussion

We quantified two sexually-dimorphic traits, body size and male claw length, in addition to plasma CORT and color of forelimb stripes in adult painted turtles in a field experiment in which we manipulated ASR to assess the impact of these factors on measures of individual fitness. Female reproductive success was positively related to body size and negatively related to

plasma CORT, whereas male reproductive success was not strongly predicted by any measured phenotypes or by ASR. Our results suggest directional selection on morphology and physiology in females, and are thus congruent with the perspective that sexual dimorphism in traits could arise from selection on just one sex, rather than on both (Janzen and Paukstis 1991).

The ratio of reproducing males to females was approximately 1:1.4, with 22 of 26 females and 16 of 37 males successfully reproducing. Reproductive success varied widely among turtles, but was more skewed in males than females, such that the Opportunity for Selection (ΔI) was much greater in males than females. Most females reproduced, and the mean number of eggs laid by nesting females (10.4) and the range of eggs laid (0-14) were similar to results of other studies of painted turtles from the TCRA population (mean 10.9 eggs, range 1-14 per nest, Pearse et al. 2002; mean ~10 eggs per nest across lifetime, Delaney et al. In Press). For males, reproductive success ranged from 0 to 34 offspring, with a mean of 11.8 offspring sired across successful males, and fewer than half of the males in this study sired any offspring. These results are similar to a 4-year study of painted turtles from southeastern Michigan, which found that successful males sired on average 8.6 offspring with a range of 1 to 32 offspring (McGuire et al. 2014). Given the considerable variation in male reproductive success, our experiment had ample scope to identify any selection on the male traits we measured, yet we found none.

We also detected multiple paternity in 18% of the clutches, which is similar to estimates of multiple paternity prevalence in free-ranging painted turtles from this population (10.7% observed, 30.1% estimated, Pearse et al. 2002). Interestingly, despite this experiment taking place following the third summer of holding turtles in the ASR treatment ponds (Judson et al. In review) to prevent the use of stored sperm, we found two instances of probable long-term sperm storage in the equal ASR pond, as the genotypes of two sires were not matched by the males in

our experiment. Sperm storage has been documented for up to three years in female painted turtles at the TCRA, and recent matings sire the initial clutches of offspring in a 'last in, first out' pattern (Pearse et al. 2001). Thus, the two females in our study probably did not mate with males in their pond, and instead utilized stored sperm. The reason for this is unclear, but the decision to use stored sperm deserves further study in wild populations. Overall, given the similar patterns of reproductive success in our experiment and studies of wild populations, our husbandry of turtles should be representative of potential phenotypes influencing reproductive success in the wild.

Sexually-dimorphic phenotypes - We investigated two sexually dimorphic phenotypes in this study, body size (as measured by plastron length) and male claw length, to assess their role in reproductive success. Body size was strongly positively associated with the number of eggs laid by females. This finding is consistent with prior studies (e.g., McGuire et al. 2014; Hoekstra et al. 2018) and aligns with phylogenetic analyses supporting the role of fecundity selection in the evolution of SSD in emydid turtles (e.g., Stephens and Wiens 2009). In contrast, male body size and male claw length did not predict male siring success, and body size was not predictive of whether a male sired offspring or not (t-test P=0.79). Similarly, carapace length (which is strongly correlated with plastron length, Hoekstra et al. 2018) did not differ between successful and unsuccessful free-ranging males at the TCRA in an earlier study (Pearse et al. 2002). As plastron length is a proxy for age in this population (Hoekstra et al. 2018), these results imply that female reproductive success increases with age due to increasing body size, whereas male reproductive success does not increase with age. Successful male painted turtles from northwestern Ontario had shorter carapaces (McTaggart 2000), but another study of the same population found no clear relationship between male plastron length and reproductive success (Hughes 2011). Thus, small males appear to accrue no reproductive advantage, and

female choice of male body size is not supported in this study. If male coercion were important for copulation, large males would be expected to have increased reproductive success (Hawkshaw et al. 2019). Still, male mating strategy could shift with size from courtship behaviors, where claw length may be more important, to coercion as males grow, which is supported by behavioral differences in courtship in Hughes (2011) and would obscure a generalized influence of size and claw length on male reproductive success.

Coloration - Conspicuous coloration commonly signals male health and competitive ability (e.g., McGraw and Ardia 2003; Plasman et al. 2015). Males with bright colors or specific hues experience increased fitness through female choice (e.g., Safran et al. 2005). Female color also may be important for male mate choice and reproductive success (Lüdtke and Foerster 2019). Indeed, color and health are associated in pond turtles of both sexes. For example, female red-eared slider turtles displayed decreased brightness of chin stripes following an immune challenge (Ibáñez et al. 2014). In painted turtles, stress biomarkers and immune function predict brightness and hue of forelimb stripes in sex- and size-dependent contexts (Judson et al. In review). Even so, we detected no substantive covariances between either male or female reproductive success and forelimb stripe color, which casts doubt on the long-presumed function of forelimb stripe coloration in pond turtles as a mate attractant (e.g., Ibáñez et al. 2014; Steffen et al. 2015; Judson et al. In review).

Forelimb stripe color might affect fitness separate from signaling mate quality in emydid turtles. Color may be a species recognition signal, such that heterospecific matings are reduced in areas where multiple sympatric species of similarly sized turtles interact (e.g., Vogt 1993), as is the case for much of the painted turtle's geographic range (Ernst and Lovich 2009). Alternatively, painted turtle limb and head stripes may function in crypsis (Rowe et al. 2014),

though no evidence of their cryptic advantage exists to date. Our methods precluded turtle visual system modeling (i.e., visual-system specific quantum catches) due to absence of UV measures, and thus we measured the forelimb stripes, which show little UV reflectance (Steffen et al. 2015) and predict health state in painted turtles (Judson et al. In review), so our results should not be limited by the absence of UV measures. However, head stripes, which we did not measure in this experiment and which have much greater UV reflectance (Steffen et al. 2015), might affect reproductive success in painted turtles. The impact of head stripe coloration on reproductive success should be assessed to further elucidate the role of coloration in mate choice of freshwater turtles.

Though color of forelimb stripes does not appear to influence reproductive success, we found support for the CORT-Fitness Hypothesis (Bonier et al. 2009) in female painted turtles. Females with higher baseline CORT concentrations laid fewer eggs and thus had lower fitness (Fig. 3). Importantly, this finding is based on measuring CORT after the nesting season, rather than right after a nesting event. Thus, in an otherwise aquatic turtle, our measures are distinct from immediate stress responses to terrestrial reproductive effort (e.g., Polich 2018) and may better reflect baseline levels of stress. Experimentally increased baseline CORT concentrations are associated with decreased female reproductive success in other reptiles, including garter snakes (Robert et al. 2009) and eastern fence lizards (MacLeod et al. 2018). Decreased offspring survivorship after application of CORT to recently oviposited painted turtle eggs suggests increased maternal CORT may also limit offspring fitness (Polich et al. 2018), further decreasing lifetime fitness of these iteroparous turtles. Interestingly, although baseline CORT and stripe brightness are negatively associated in these painted turtles (Judson et al. In review), stripe brightness was not associated with reproductive success. CORT is often proposed to be a

mediator of signal honesty through its influence on allocation of resources toward self-maintenance and away from reproduction (e.g., ornamentation to attract mates, reviewed in Leary and Baugh 2020). Thus, CORT might affect female brightness by advertising reproductive quality to male painted turtles while also directly mediating maternal allocation to reproductive bouts.

Adult sex ratio - Environmental contexts strongly influence reproductive success in many species, and glucocorticoids might mediate the interaction of environmental stress with reproductive effort (Bonier et al. 2009). Environmental stressors, including lack of resources, extreme temperatures, and adverse social contexts, can affect CORT concentrations and reduce reproductive success (Henderson et al. 2017; Lea et al. 2018). Skewed ASRs can be another environmental stressor via increased mate competition or harassment from conspecifics (e.g., Le Galliard et al. 2005; Lea et al. 2018). We manipulated ASR of three experimental ponds to explore the influence of ASR on reproductive success of both sexes. We found no evidence that ASR affected female clutch size using a model selection approach, but we could not model factors influencing whether or not a female oviposited as only three females recovered from the ponds did not oviposit. However, two of these turtles exhibited some of the highest CORT concentrations of females in this study (Fig. 3), all three were kept in the female-biased ASR pond, in addition to one female that did not reproduce and was not recovered from the pond (Fig. 2), and turtles from this pond tended to have higher CORT concentrations compared to those from the equal and male-biased ponds (Fig. S5). Although not statistically significant, the effects of a female-biased ASR should be studied, particularly in this species and other turtles that have TSD. Climate warming presumably will produce increasingly female-biased ASR in such turtles, as warmer incubation conditions yield female hatchlings (Janzen 1994; Schwanz et al. 2010).

The female-biased pond also did not yield any clutches with multiple paternity, which may suggest a lack of re-mating opportunities due to limited male availability (Uller and Olsson 2008).

We detected weak evidence that ASR influenced male reproductive success, as model weights were low. Males in the male-biased ASR pond achieved lower reproductive success on average than males in the female-biased pond (Fig. 4), and the variance in male reproductive success was greater in the female-biased pond than in the male-biased or equal ratio ponds (Fig. 2). This result contrasts with the hypothesis that increased male availability should enhance female choice and thus increase variance in male reproductive success (Kvarnemo and Ahnesjö 2002). A simulation study of male painted turtle reproductive success in varying ASR found that, consistent with our results, males in a female-biased population exhibited increased average reproductive success and increased variance in reproductive success (Hughes 2011). This pattern was attributed to increased male encounters of females in a female-biased population, allowing more opportunities for mating. Although female choice cannot be ruled out as a factor by us or by Hughes (2011), it is not necessary to invoke female choice as driving any of the reproductive patterns we detected with ASR treatments or with the phenotypes measured. Importantly, we cannot disentangle density effects from ASR effects, as there were differing numbers of turtles in each pond. Thus, future studies should evaluate whether density or ASR plays a greater role in reproductive success (Wacker et al. 2013), and whether females' responses to prolonged skew in ASR include changes in use of stored sperm in future reproductive bouts.

We assessed relationships between multiple traits, ASR, and reproductive success in sexually dimorphic painted turtles under semi-natural conditions to understand how phenotypes and ASR might affect male and female reproductive success. We found strong evidence that

female body size and CORT concentration influenced clutch size, whereas relationships for males were weaker and only suggested a trend toward male-biased ASR reducing male reproductive success. Despite many hypothesized relationships between the phenotypes quantified in this study (e.g., male claw length and forelimb coloration) and potential female mate choice in painted turtles, we detected no evidence of female mate choice. Thus, reproductive dynamics in turtles may be more complex than is often assumed.

Acknowledgements

This work was supported by the National Science Foundation (LTREB DEB-1242510 and IOS-1257857 to FJJ), the National Institutes of Health (R01-AG049416 to AM Bronikowski), and the Iowa Science Foundation (ISF 17-16 to JMJ and FJJ). We thank R. Polich, T. Mitchell, D. Warner, N. Howell and J. Braland for pond building and maintenance at the ISU Horticulture Farm, B. Bodensteiner for camera equipment, C. Adams for nest monitoring, A. Toth, K. Roe, and J. Nason for project guidance and comments, R. Waples for guidance on Opportunity for Selection indices, E. Gangloff and A. McCombs for statistical advice, A. Bronikowski for manuscript feedback, and the many past and present members of the Janzen lab for the collection and care of turtles.

References

Arnold TW. 2010. Uninformative parameters and model selection using Akaike's Information Criterion. J Wildl Manage. 74:1175-1178.

Atwell A, Wagner WE. 2014. Female mate choice plasticity is affected by the interaction between male density and female age in a field cricket. Anim Behav. 98:177-183.

Bartoń K. 2020. MuMIn: Multi-Model Inference. R package, v. 1.43.17. https://cran.r-project.org/package=MuMIn

Bateman AJ. 1948. Intra-sexual selection in Drosophila. Heredity. 2:349-368.

Berry JF, Shine R. 1980. Sexual size dimorphism and sexual selection in turtles (Order Testudines). Oecologia. 44:185-191.

Blanckenhorn WU. 2005. Behavioral causes and consequences of sexual size dimorphism. Ethology. 111:977-1016.

Bonier F, Martin PR, Moore IT, Wingfield JC. 2009. Do baseline glucocorticoids predict fitness? Trends Ecol Evol. 24:634-642.

Bourgeois S, Senn H, Kaden J, Taggart JB, Ogden R, Jeffery KJ, Bunnefeld N, Abernethy K, McEwing R. 2018. Single-nucleotide polymorphism discovery and panel characterization in the African forest elephant. Ecol Evol. 8:2207-2217.

Brooks ME, Kristensen K, Darrigo MR, Rubim P, Uriarte M, Bruna E, Bolker BM. 2019. Statistical modeling of patterns in annual reproductive rates. Ecology. 100:e02706.

Brooks ME, Kristensen K, van Benthem KJ, Magnusson A, Berg CW, Nielsen A, Skaug HJ, Maechler M, Bolker BM. 2017. glmmTMB balances speed and flexibility among packages for zero-inflated generalized linear mixed modeling. The R Journal. 9:378-400.

Burnham KP, Anderson DR. 2002. Model selection and multimodel inference : a practical information-theoretic approach. 2nd ed. New York: Springer.

Burnham KP, Anderson DR, Huyvaert KP. 2011. AIC model selection and multimodel inference in behavioral ecology: some background, observations, and comparisons. Behav Ecol Sociobiol. 65:23-35.

Cox RM, Skelly SL, John-Alder HB. 2003. A comparative test of adaptive hypotheses for sexual size dimorphism in lizards. Evolution. 57:1653-1669.

DePristo MA, Banks E, Poplin R, Garimella KV, Maguire JR, Hartl C, Philippakis AA, del Angel G, Rivas MA, Hanna M, et al. 2011. A framework for variation discovery and genotyping using next-generation DNA sequencing data. Nat Genet. 43:491-498.

Dupuis-Désormeaux M, D'Elia V, Cook C, Pearson J, Adhikari V, MacDonald S. 2017. Remarkable male bias in a population of midland painted turtles (*Chrysemys picta marginata*) in Ontario, Canada. Herpetol Conserv Biol. 12:225–232.

Ernst CH, Lovich JE. 2009. Turtles of the United States and Canada. 2nd ed. Baltimore: Johns Hopkins University Press.

Grant PR, Grant BR. 2019. Adult sex ratio influences mate choice in Darwin's finches. Proc Natl Acad Sci USA. 116:12373-12382.

Grayson KL, Mitchell NJ, Monks JM, Keall SN, Wilson JN, Nelson NJ. 2014. Sex ratio bias and extinction risk in an isolated population of Tuatara (Sphenodon punctatus). PLoS One. 9:e94214.

Grueber C, Nakagawa S, Laws R, Jamieson I. 2011. Multimodel inference in ecology and evolution: challenges and solutions. J Evol Biol. 24:699-711.

Hartig F. 2020. DHARMa: Residual Diagnostics for Hierarchical (Multi-Level / Mixed) Regression Models. R package, v. 0.3.3.0. https://cran.r-project.org/package=DHARMa

Hauser L, Baird M, Hilborn R, Seeb LW, Seeb JE. 2011. An empirical comparison of SNPs and microsatellites for parentage and kinship assignment in a wild sockeye salmon (Oncorhynchus nerka) population. Mol Ecol Resour. 11:150-161.

Hawkshaw DM, Moldowan PD, Litzgus JD, Brooks RJ, Rollinson N. 2019. Discovery and description of a novel sexual weapon in the world's most widely- studied freshwater turtle. Evol Ecol. 33:889-900.

Heinsohn R, Olah G, Webb M, Peakall R, Stojanovic D. 2019. Sex ratio bias and shared paternity reduce individual fitness and population viability in a critically endangered parrot. J Anim Ecol. 88:502-510.

Henderson L, Evans N, Heidinger B, Herborn K, Arnold K. 2017. Do glucocorticoids predict fitness? Linking environmental conditions, corticosterone and reproductive success in the blue tit, Cyanistes caeruleus. Royal Soc Open Sci. 4:170875.

Hoekstra LA, Weber RC, Bronikowski AM, Janzen FJ. 2018. Sex-specific growth, shape, and their impacts on life history of a long-lived vertebrate. Evol Ecol Res. 19:639–657.

Hoset KS, Villers A, Wistbacka R, Selonen V. 2017. Pulsed food resources, but not forest cover, determine lifetime reproductive success in a forest- dwelling rodent. J Anim Ecol. 86:1235-1245.

Hughes E. 2011. The effect of sex ratio on male reproductive success in painted turtles (*Chrysemys picta*) [dissertation]. [Guelph (ON)]: University of Guelph.

Ibáñez A, Polo-Cavia N, López P, Martín J. 2014. Honest sexual signaling in turtles: experimental evidence of a trade-off between immune response and coloration in red-eared sliders *Trachemys scripta elegans*. Naturwissenschaften. 101:803-811.

Janzen FJ. 1994. Climate change and temperature-dependent sex determination in reptiles. Proc Natl Acad Sci USA. 91:7487-7490.

Janzen FJ, Paukstis GL. 1991. Environmental sex determination in reptiles: ecology, evolution, and experimental design. Q Rev Biol. 66:149-179.

Johnstone RA, Reynolds JD, Deutsch JC. 1996. Mutual mate choice and sex differences in choosiness. Evolution. 50:1382-1391.

Jones OR, Wang J. 2010. COLONY: a program for parentage and sibship inference from multilocus genotype data. Mol Ecol Resour. 10:551-555.

[dataset]. Judson JM, Hoekstra LA, Holden KG, Janzen FJ. 2020. Iowa State University Data Repository.

Kalinowski ST, Taper ML, Marshall TC. 2007. Revising how the computer program CERVUS accommodates genotyping error increases success in paternity assignment. Mol Ecol. 16:1099-1106.

Kelly RJ, Murphy TG, Tarvin KA, Burness G. 2012. Carotenoid-based ornaments of female and male American goldfinches (Spinus tristis) show sex-specific correlations with immune function and metabolic rate. Physiol Biochem Zool. 85:348-363.

Khera P, Upadhyaya HD, Pandey MK, Roorkiwal M, Sriswathi M, Janila P, Guo Y, McKain MR, Nagy ED, Knapp SJ, et al. 2013. Single nucleotide polymorphism–based genetic diversity in the reference set of peanut (spp.) by developing and applying cost-effective kompetitive allele specific polymerase chain reaction genotyping assays. Plant Genome. 6:1-11.

Kvarnemo C, Ahnesjö I. 2002. Operational sex ratios and mating competition. In: Hardy ICW, editor. Sex ratios: concepts and research methods. New York: Cambridge University Press.

Landys MM, Ramenofsky M, Wingfield JC. 2006. Actions of glucocorticoids at a seasonal baseline as compared to stress-related levels in the regulation of periodic life processes. Gen Comp Endocrinol. 148:132-149.

Le Galliard JF, Fitze PS, Ferriere R, Clobert J. 2005. Sex ratio bias, male aggression, and population collapse in lizards. Proc Natl Acad Sci USA. 102:18231-18236.

Lea JM, Walker SL, Kerley GI, Jackson J, Matevich SC, Shultz S. 2018. Non- invasive physiological markers demonstrate link between habitat quality, adult sex ratio and poor population growth rate in a vulnerable species, the Cape mountain zebra. Funct Ecol. 32:300-312.

Leary CJ, Baugh AT. 2020. Glucocorticoids, male sexual signals, and mate choice by females: Implications for sexual selection. Gen Comp Endocrinol. 288:113354.

Li H, Handsaker B, Wysoker A, Fennell T, Ruan J, Homer N, Marth G, Abecasis G, Durbin R, Genome Project Data Processing S. 2009. The Sequence Alignment/Map format and SAMtools. Bioinformatics. 25:2078-2079.

Lüdecke D, Makowski D, Waggoner P, Patil I. 2020. performance: Assessment of Regression Models Performance. R package, v. 0.5.0. https://cran.r-project.org/package=performance

Lüdtke DU, Foerster K. 2019. A female color ornament honestly signals fecundity. Front Ecol Evol. 7

MacLeod K, Sheriff MJ, Ensminger D, Owen D, Langkilde T. 2018. Survival and reproductive costs of repeated acute glucocorticoid elevations in a captive, wild animal. Gen Comp Endocrinol. 268:1-6.

McCouch SR, Zhao K, Wright M, Tung C-W, Ebana K, Thomson M, Reynolds A, Wang D, DeClerck G, Ali ML, et al. 2010. Development of genome-wide SNP assays for rice. Breed Sci. 60:524-535.

McGraw KJ, Ardia DR. 2003. Carotenoids, immunocompetence, and the information content of sexual colors: an experimental test. Am Nat. 162:704-712.

McGuire JM, Congdon JD, Scribner KT, Nagle RD. 2014. Female reproductive qualities affect male painted turtle (*Chrysemys picta marginata*) reproductive success. Behav Ecol Sociobiol. 68:1589-1602.

McKenna A, Hanna M, Banks E, Sivachenko A, Cibulskis K, Kernytsky A, Garimella K, Altshuler D, Gabriel S, Daly M, et al. 2010. The Genome Analysis Toolkit: a MapReduce framework for analyzing next-generation DNA sequencing data. Genome Res. 20:1297-1303.

McTaggart S. 2000. Good genes or sexy sons? Testing the benefits of female mate choice in the painted turtle, *Chrysemys picta* [thesis]. [Guelph (ON)]: University of Guelph.

Moll E. 1973. Latitudinal and intersubspecific variation in reproduction of the painted turtle, *Chrysemys picta*. Herpetologica. 29:307-318.

Moore IT, Jessop TS. 2003. Stress, reproduction, and adrenocortical modulation in amphibians and reptiles. Horm Behav. 43:39-47.

Moore IT, Hopkins WA. 2009. Interactions and trade-offs among physiological determinants of performance and reproductive success. Integr Comp Biol. 49:441-451.

Noble DW, Wechmann K, Keogh JS, Whiting MJ. 2013. Behavioral and morphological traits interact to promote the evolution of alternative reproductive tactics in a lizard. Am Nat. 182:726-742.

Pearse D, Janzen F, Avise J. 2002. Multiple paternity, sperm storage, and reproductive success of female and male painted turtles (*Chrysemys picta*) in nature. Behav Ecol Sociobiol. 51:164-171.

Pearse DE, Janzen FJ, Avise JC. 2001. Genetic markers substantiate long-term storage and utilization of sperm by female painted turtles. Heredity. 86:378-384.

Plasman M, Reynoso VH, Nicolás L, Torres R. 2015. Multiple colour traits signal performance and immune response in the Dickerson's collared lizard *Crotaphytus dickersonae*. Behav Ecol Sociobiol. 69:765-775.

Polich RL. 2016. Stress hormone levels in a freshwater turtle from sites differing in human activity. Conserv Physiol. 4:1-9.

Polich RL. 2018. Fluctuating hormone levels during reproduction in freshwater turtles. J Herpetol. 52:74-78.

Polich RL, Bodensteiner BL, Adams CI, Janzen FJ. 2018. Effects of augmented corticosterone in painted turtle eggs on offspring development and behavior. Physiol Behav. 183:1-9.

Polo-Cavia N, López P, Martín J. 2013. Head coloration reflects health state in the red-eared slider Trachemys scripta elegans. Behav Ecol Sociobiol. 67:153-162.

Purcell S, Neale B, Todd-Brown K, Thomas L, Ferreira MA, Bender D, Maller J, Sklar P, de Bakker PI, Daly MJ, et al. 2007. PLINK: a tool set for whole-genome association and population-based linkage analyses. Am J Hum Genet. 81:559-575.

R Core Team. 2020. R: A language and environment for statistical computing. https://www.r-project.org/

Refsnider JM, Janzen FJ. 2016. Temperature-dependent sex determination under rapid anthropogenic environmental change: Evolution at a turtle's pace? J Hered. 107:61-70.

Robert KA, Vleck C, Bronikowski AM. 2009. The effects of maternal corticosterone levels on offspring behavior in fast-and slow-growth garter snakes (*Thamnophis elegans*). Horm Behav. 55:24-32.

Rowe JW, Bunce CF, Clark DL. 2014. Spectral reflectance and substrate color-induced melanization in immature and adult Midland painted turtles (*Chrysemys picta marginata*). Amphib-Reptil. 35:149-159.

Safran RJ, Neuman CR, McGraw KJ, Lovette IJ. 2005. Dynamic paternity allocation as a function of male plumage color in barn swallows. Science. 309:2210-2212.

Salvador A, Díaz JA, Veiga JP, Bloor P, Brown RP. 2007. Correlates of reproductive success in male lizards of the alpine species *Iberolacerta cyreni*. Behav Ecol. 19:169-176.

Schneider CA, Rasband WS, Eliceiri KW. 2012. NIH Image to ImageJ: 25 years of image analysis. Nat Methods. 9:671-675.

Schwanz LE, Spencer RJ, Bowden RM, Janzen FJ. 2010. Climate and predation dominate juvenile and adult recruitment in a turtle with temperature-dependent sex determination. Ecology. 91:3016-3026.

Semagn K, Babu R, Hearne S, Olsen M. 2014. Single nucleotide polymorphism genotyping using Kompetitive Allele Specific PCR (KASP): overview of the technology and its application in crop improvement. Mol Breed. 33:1-14.

Shaffer HB, Minx P, Warren DE, Shedlock AM, Thomson RC, Valenzuela N, Abramyan J, Amemiya CT, Badenhorst D, Biggar KK, et al. 2013. The western painted turtle genome, a model for the evolution of extreme physiological adaptations in a slowly evolving lineage. Genome Biol. 14:R28.

Shine R, Olsson M, Moore I, LeMaster M, Greene M, Mason R. 2000. Body size enhances mating success in male garter snakes. Anim Behav. 59:F4-F11.

Siefferman L, Hill GE. 2003. Structural and melanin coloration indicate parental effort and reproductive success in male eastern bluebirds. Behav Ecol. 14:855-861.

Steffen JE, Learn KM, Drumheller JS, Boback SM, McGraw KJ. 2015. Carotenoid composition of colorful body stripes and patches in the painted turtle (*Chrysemys picta*) and red-eared slider (*Trachemys scripta*). Chelonian Conserv Biol. 14:56-63.

Steifetten Ø, Dale S. 2006. Viability of an endangered population of ortolan buntings: The effect of a skewed operational sex ratio. Biol Conserv. 132:88-97.

Stephens PR, Wiens JJ. 2009. Evolution of sexual size dimorphisms in emydid turtles: ecological dimorphism, Rensch's Rule, and sympatric divergence. Evolution. 63:910-925.

Symonds MR, Moussalli A. 2011. A brief guide to model selection, multimodel inference and model averaging in behavioural ecology using Akaike's information criterion. Behav Ecol Sociobiol. 65:13-21.

Szekely T, Weissing FJ, Komdeur J. 2014. Adult sex ratio variation: implications for breeding system evolution. J Evol Biol. 27:1500-1512.

Troscianko J, Stevens M. 2015. Image calibration and analysis toolbox - a free software suite for objectively measuring reflectance, colour and pattern. Methods Ecol Evol. 6:1320-1331.

Uller T, Olsson M. 2008. Multiple paternity in reptiles: patterns and processes. Mol Ecol. 17:2566-2580.

Vogt RC. 1993. Systematics of the false map turtles (Graptemys pseudogeographica complex: Reptilia, Testudines, Emydidae). Ann Carnegie Mus. 62:1-46.

Wacker S, Mobley K, Forsgren E, Myhre LC, de Jong K, Amundsen T. 2013. Operational sex ratio but not density affects sexual selection in a fish. Evolution. 67:1937-1949.

Waples RS. 2020. An estimator of the Opportunity for Selection that is independent of mean fitness. Evolution. 74:1942-1953.

Weir LK, Grant JWA, Hutchings JA. 2011. The influence of operational sex ratio on the intensity of competition for mates. Am Nat. 177:167-176.

White KN, Rothermel BB, Zamudio KR, Tuberville TD. 2018. Male body size predicts reproductive success but not within-clutch paternity patterns in gopher tortoises (Gopherus polyphemus). J Hered

Wickham H. 2016. ggplot2: Elegant Graphics for Data Analysis. New York: Springer.

Wielstra B, Burke T, Butlin RK, Schaap O, Shaffer HB, Vrieling K, Arntzen JW. 2016. Efficient screening for 'genetic pollution' in an anthropogenic crested newt hybrid zone. Conserv Genet Resour. 8:553-560.

Wingfield JC, Sapolsky RM. 2003. Reproduction and resistance to stress: When and how. J Neuroendocrinol. 15:711-724.

Tables and Figures

Table 1: Full, intercept-only, and 5 best-fitting models for female and male painted turtle reproductive success ranked according to AIC_c

Conditional Model	Zero-inflation Model	*df*	ΔAIC_c	Weight
Females				
~ PL[1] + CORT[2]	~ 1	5	0.00	0.33
~ PL	~ 1	4	0.41	0.27
~ PL + Hue	~ 1	5	1.86	0.13
~ PL + CORT + Brightness	~ 1	6	3.75	0.05
~ PL + CORT + Hue	~ 1	6	3.76	0.05
~ 1	~ 1	3	12.20	0.00
~ ASR[3] + PL + CORT + Brightness + Hue	~ 1	9	15.73	0.00
Males				
~ ASR	~ 1	5	0.00	0.05
~ Brightness	~ 1	4	0.39	0.04
~ ASR + Brightness	~ 1	6	1.70	0.02
~ ASR + Hue	~ 1	6	1.82	0.02
~ Brightness + CORT	~ 1	5	1.96	0.02
~ 1	~ 1	3	2.50	0.01
~ ASR + PL + CORT + Brightness + Hue + MCL[4]	~ ASR + PL + CORT + Brightness + Hue + MCL	17	53.43	0.00

All continuous predictors standardized by sex. [1]plastron length; [2]baseline corticosterone concentration; [3]adult sex ratio treatment; [4]mean claw length

Table 2: Parameter estimates for models of female painted turtle reproductive success within two ΔAIC_c units of the best-fitting submodel

Parameters	Estimate	SE	z
Model 1 (ΔAIC_c=0)			
Conditional Model			
Intercept	2.32	0.03	80.92
PL[1]	0.12	0.03	4.27
CORT[2]	–0.07	0.04	–2.07
Zero-inflation Model			
Intercept	–2.25	0.74	–3.03
Model 2 (ΔAIC_c=0.41)			
Conditional Model			
Intercept	2.34	0.03	76.39
PL	0.13	0.03	4.83
Zero-inflation Model			
Intercept	–2.25	0.74	–3.03

More complex submodels excluded when nested submodels had lower AIC values; given philosophical difference between model selection and null hypothesis significance testing (Burnham et al. 2011), we do not report p-values here. [1]plastron length; [2]baseline corticosterone concentration

Table 3: Parameter estimates for models of male painted turtle reproductive success within two ΔAIC_c units of the best-fitting submodel

Parameters	Estimate	SE	z
Model 1 (ΔAIC_c=0)			
Conditional Model			
Intercept	2.56	0.25	10.41
ASR[1]: F > M	0.72	0.35	2.04
ASR: M > F	–0.40	0.32	–1.24
Zero-inflation Model			
Intercept	0.33	0.35	0.95
Model 2 (ΔAIC_c=0.39)			
Conditional Model			
Intercept	2.51	0.15	16.35
Brightness	0.42	0.18	2.40
Zero-inflation Model			
Intercept	0.33	0.35	0.93

More complex submodels excluded when nested submodels had lower AIC values; [1]adult sex ratio treatment

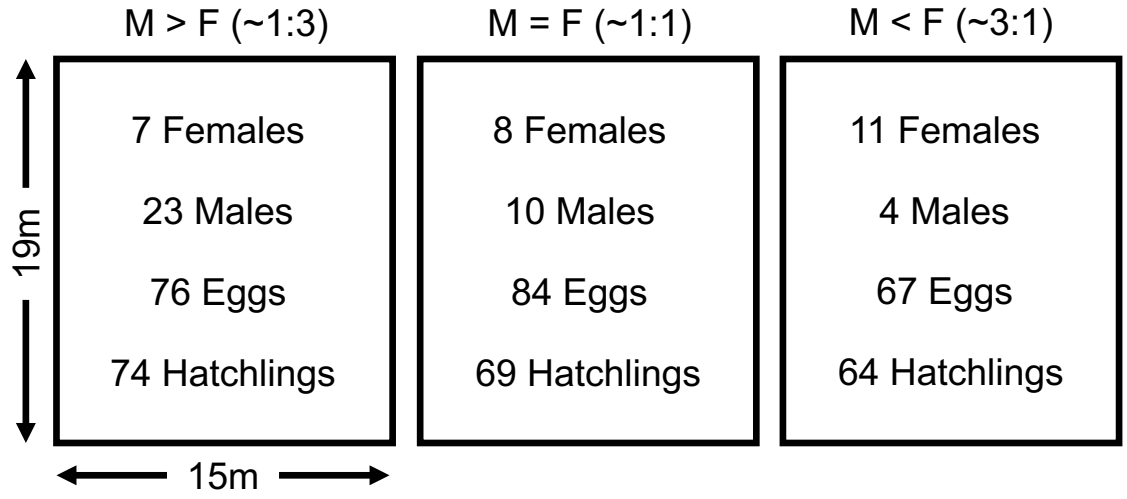

Figure 1: Diagram of adult sex ratio treatment. Number of female and male painted turtles released into each pond, the number of eggs laid, and number of offspring successfully hatched from each pond. Arrows indicate dimensions of each pond in meters.

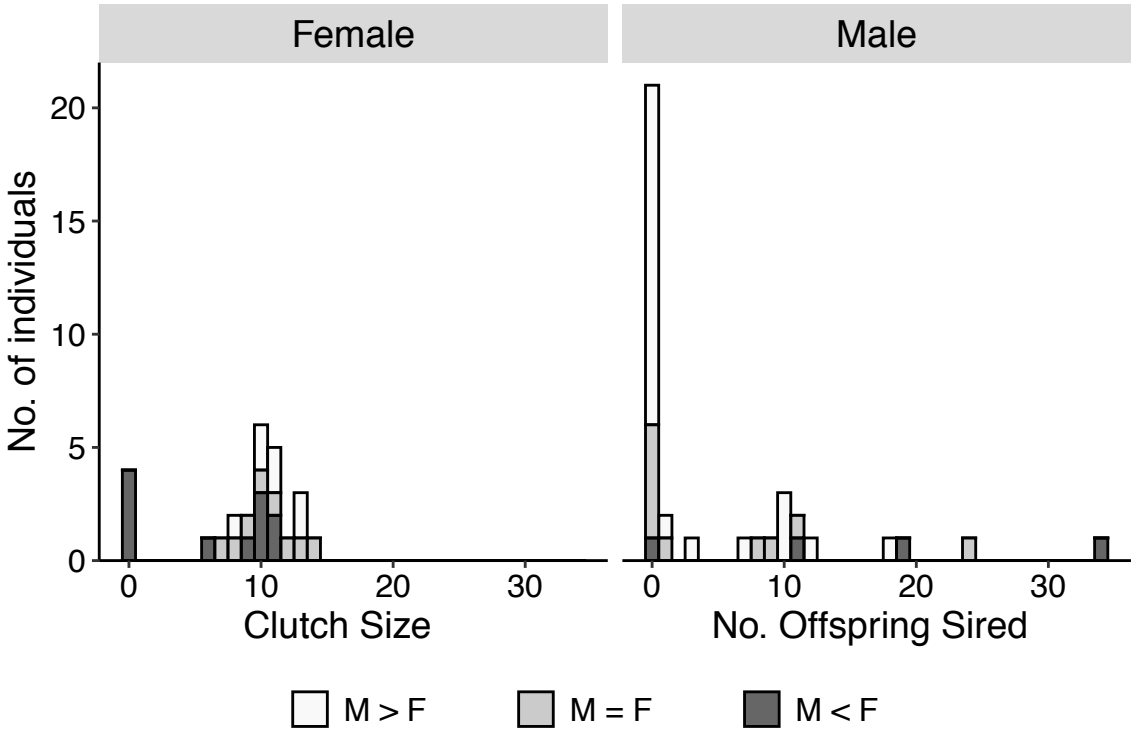

Figure 2: Stacked histogram of female and male reproductive output for adult painted turtles in this study (N=63) labeled by adult sex ratio treatment.

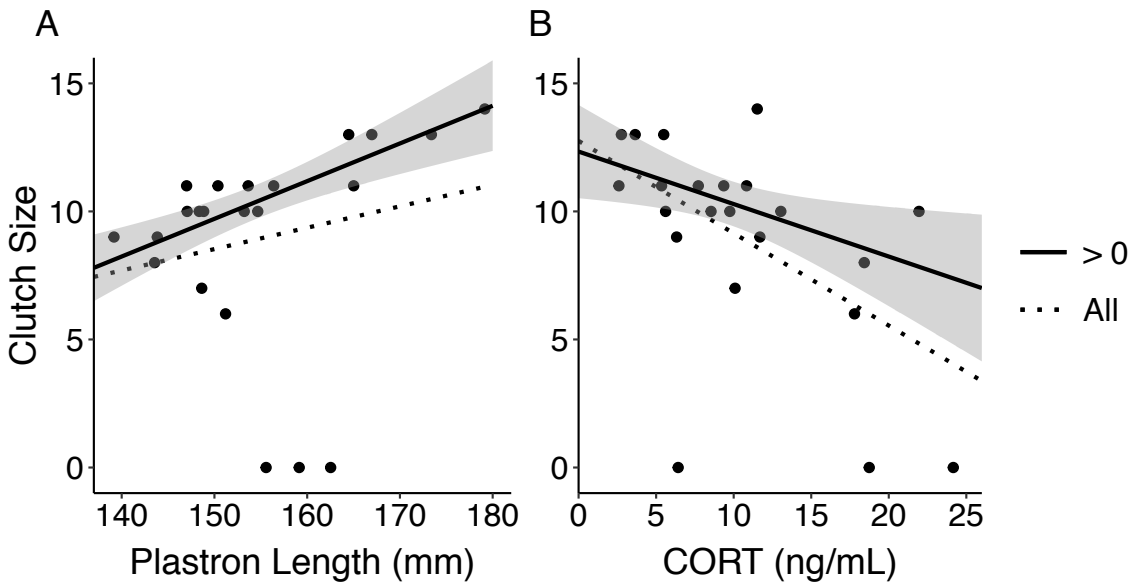

Figure 3: Relationship between number of eggs laid by female painted turtles and plastron length (A) or corticosterone concentrations (CORT; B). Raw values are plotted, and lines depict a simple linear regression using all females (All, dashed line) or excluding females that did not lay eggs (> 0, solid line). Gray shading depicts 95% confidence interval.

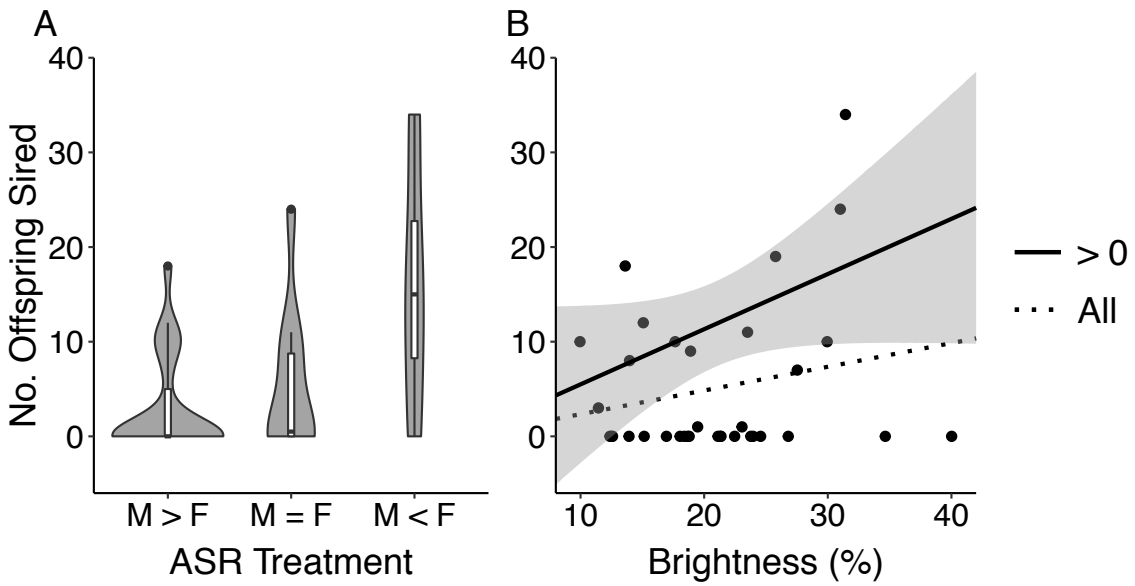

Figure 4: Violin plot for number of offspring sired by male painted turtles from each adult sex ratio (ASR) treatment (A), and relationship between male percent brightness of the forelimb stripe and number of offspring sired (B). Boxplots are inset within violin plots, and raw values are plotted for both panels. Lines in panel B depict a simple linear regression using all males (All) or excluding males that did not sire offspring (> 0). Gray shading depicts 95% confidence interval. One outlier for brightness was removed.

Supplemental Material

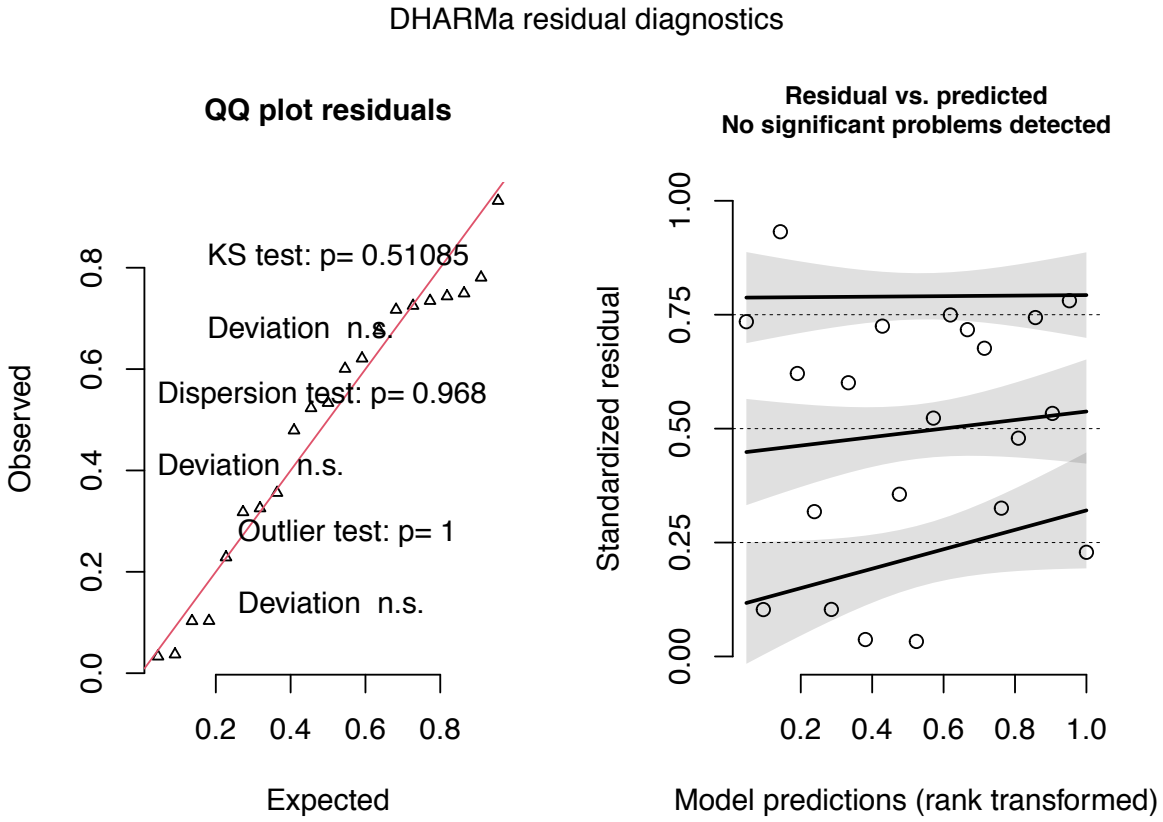

Figure S1: Model fit test for full female model

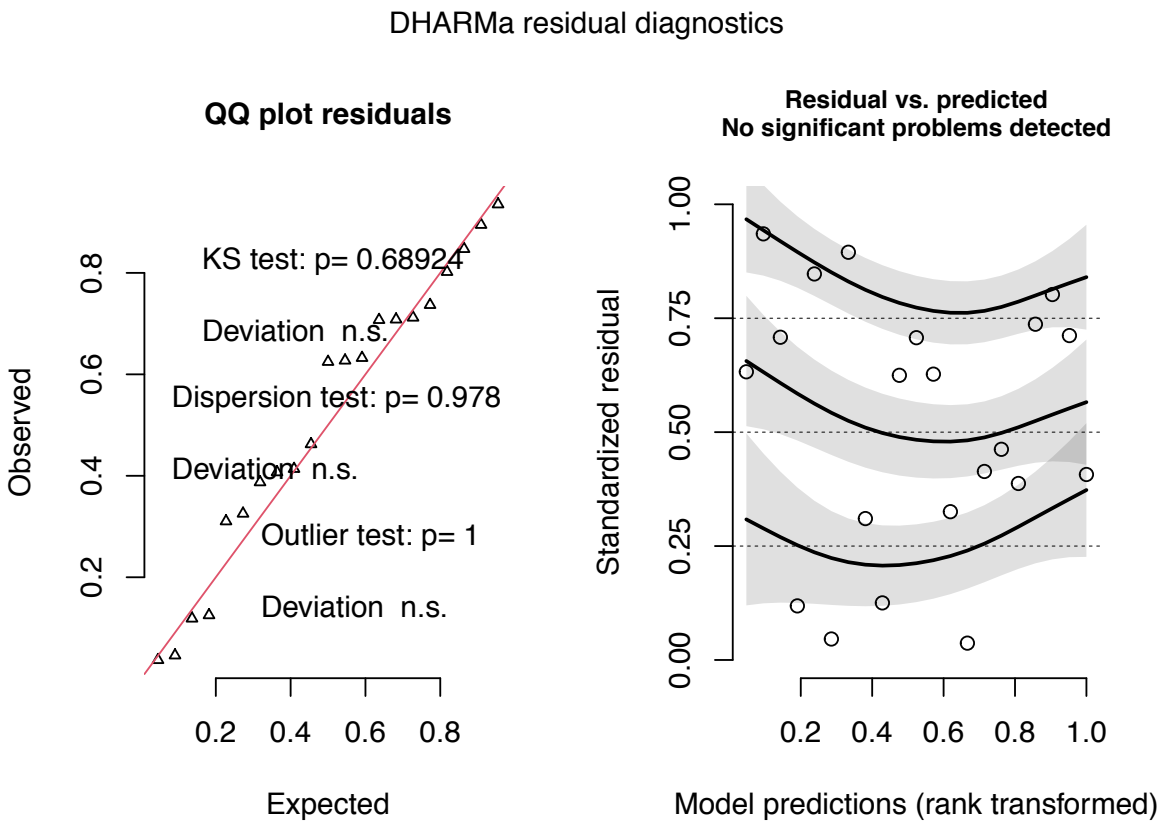

Figure S2: Model fit test for best-fitting female model

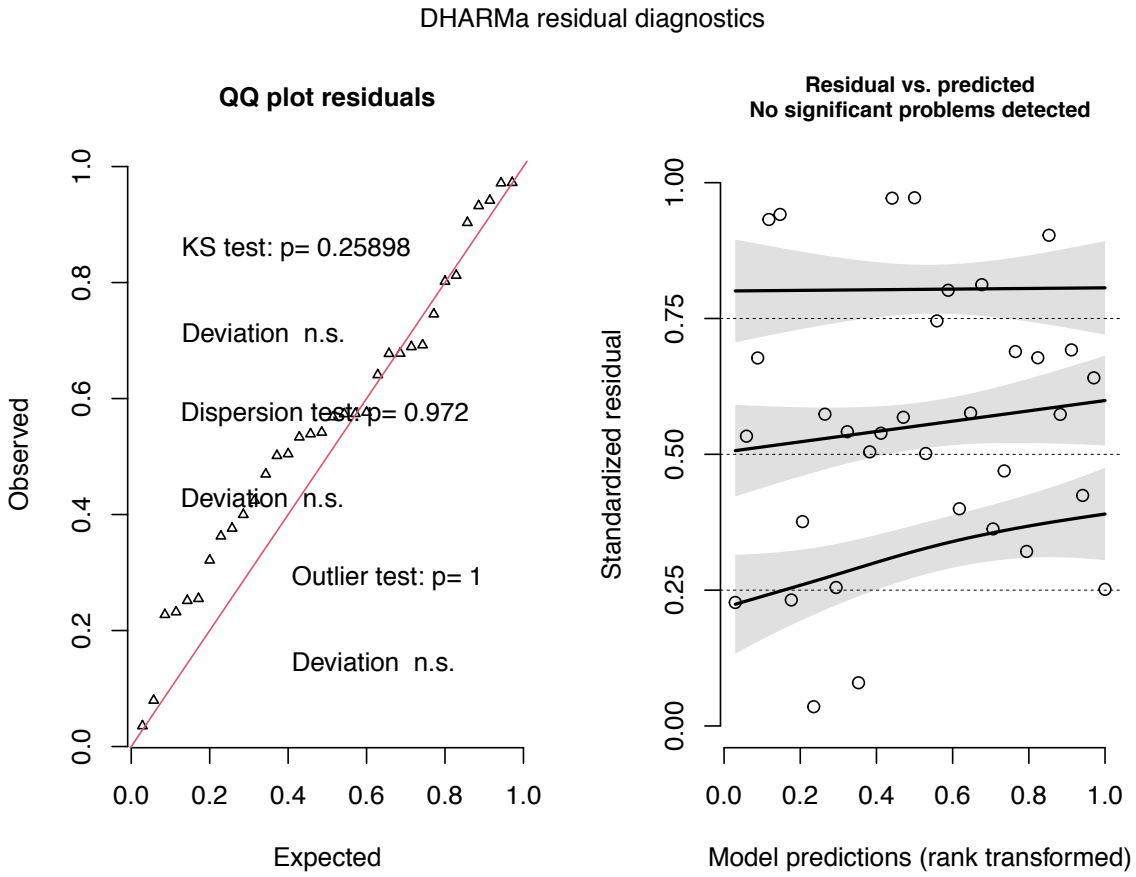

Figure S3: Model fit test for full male model

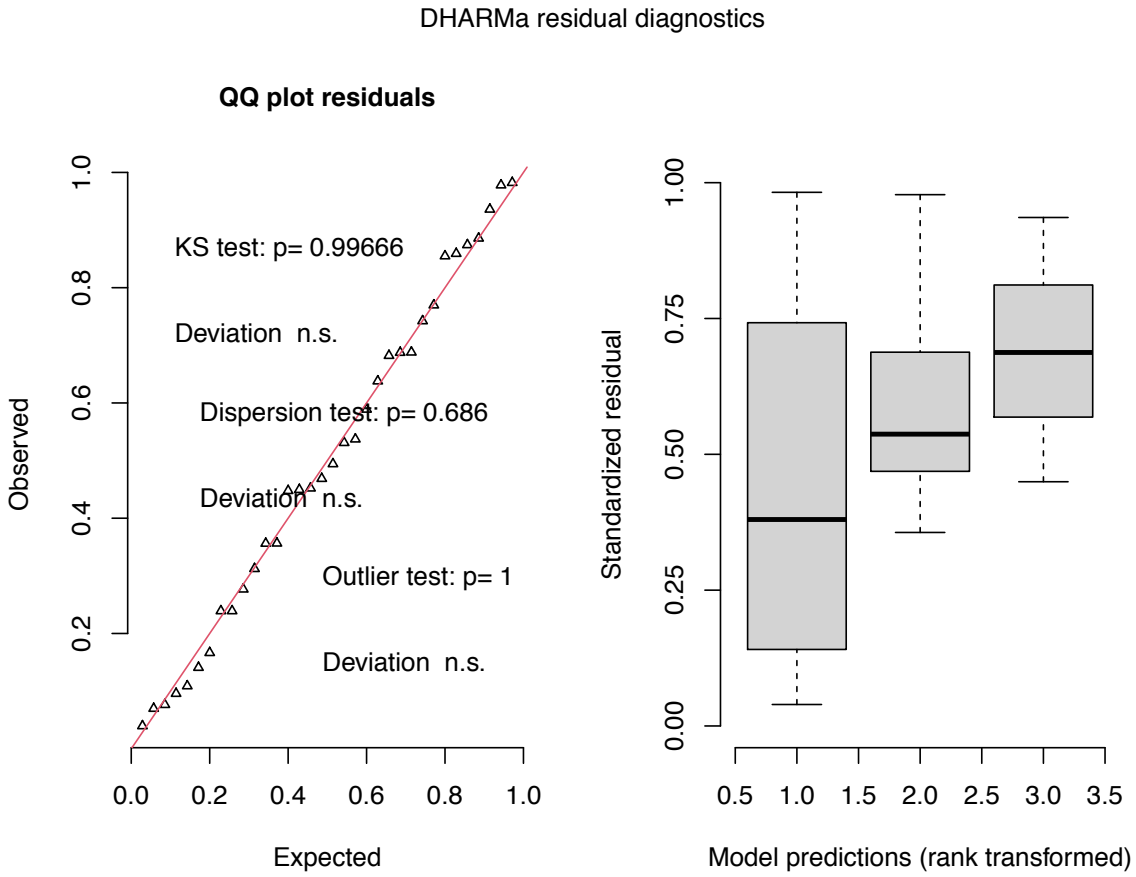

Figure S4: Model fit test for best-fitting male model

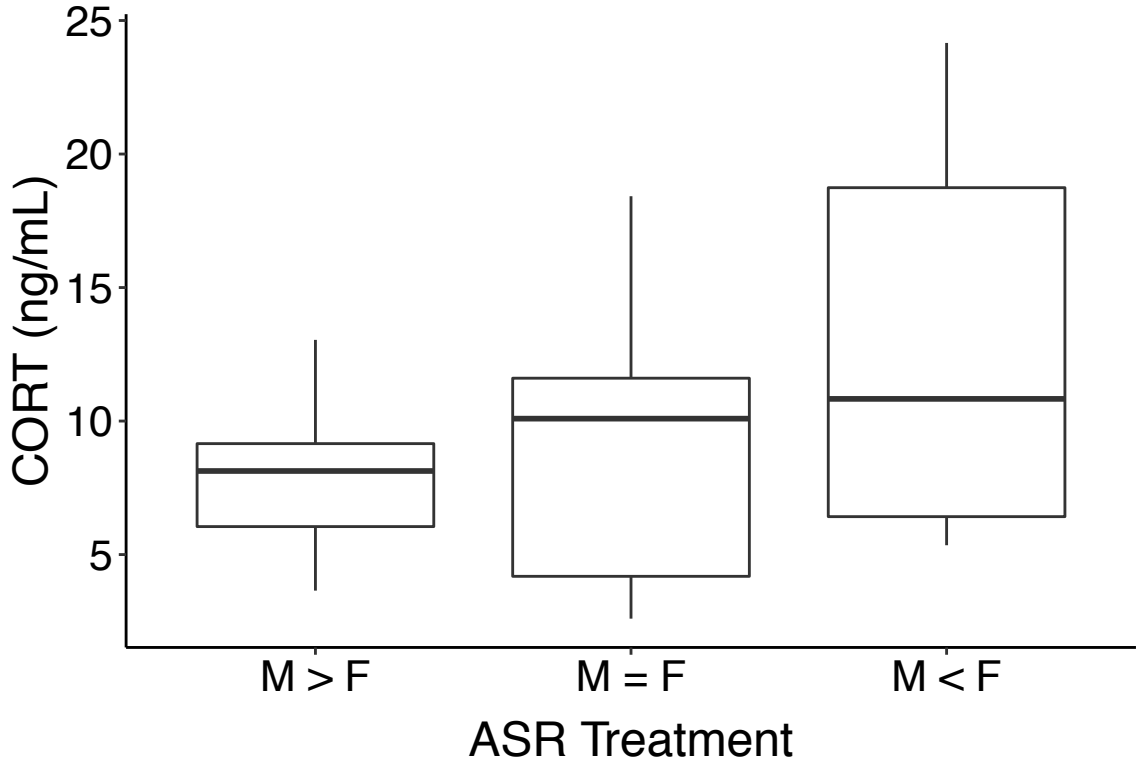

Figure S5: Comparison of female baseline corticosterone (CORT) concentrations across adult sex ratio (ASR) treatments.

CHAPTER 4. DEMOGRAPHIC HISTORY SHAPES POPULATION GENOMIC STRUCTURE IN A LONG-LIVED AQUATIC VERTEBRATE

Jessica M. Judson, Luke A. Hoekstra, and Fredric J. Janzen

Department of Ecology, Evolution, and Organismal Biology, Iowa State University, Ames, Iowa, USA

Modified from a manuscript to be submitted to *Journal of Heredity*

Abstract

In long-lived iteroparous organisms, phenotypic plasticity allows organisms to respond to environmental stressors within generations. However, much remains to be understood about the contribution of local adaptation to the current distributions of these long-lived organisms, particularly in ectothermic vertebrates. As ectothermic vertebrates are among the most vulnerable to rapid changes in environmental conditions, it is critical to understand the contributions of local adaptation to population survival. In this study, we investigated the population genomic structure of western populations of painted turtles (*Chrysemys picta*) to understand past demography and assess molecular genomic evidence of local adaptation. Despite the extensive phenotypic variation observed among populations of painted turtles across the western range of the species' distribution, we found little evidence of local adaptation, as measured by F_{ST} outliers. Instead, we found strong support for the role of historical demography in shaping population genomic structure; genotypic patterns of outlier loci and runs of homozygosity across the genome indicated that serial founder effects and gene surfing at range edges contributed to the observed genomic divergence among populations in an east-to-west pattern. As the glaciers receded in the late Pleistocene, painted turtle populations expanded

westward, and the phenotypic divergence observed may be the result of phenotypic plasticity rather than local adaptation to these distinct macro-environments. Phenotypic plasticity may thus be critical to survival of painted turtle populations in western North America, as low standing genetic variation due to repeated bottlenecks may render these populations unable to evolutionarily adapt to future environmental conditions.

Introduction

Sources of selection vary widely across the landscape, from temperature extremes to precipitation and resource availability, and yet some species have spread across and inhabit entire continents. To respond to these considerable shifts in environment, many populations have locally adapted, such that transplanting individuals from one population to another would result in a decrease in their fitness compared to native individuals (Hereford 2009). Particularly when migration is uncommon, populations are expected to locally adapt toward a fitness optimum for their environment, independent of the selective pressures faced by other populations (Orr 1998). While phenotypic divergence among populations of a widespread species is often attributed to local adaptation, individuals can also respond to diverse environmental challenges through phenotypic plasticity (Price et al. 2003; Torres-Dowdall et al. 2012). Species with short generation times and large population sizes have increased potential for rapid adaptive evolution in response to climatic shifts and environmental fluctuations (Catullo et al. 2019), but in long-lived iteroparous species, phenotypic plasticity is an important mechanism for adjusting to diverse environmental conditions experienced within an individual's lifetime (Nussey et al. 2007; Gunderson and Stillman 2015; but see Radchuk et al. 2019). Further, as phenotypic plasticity is when the same genotype produces different phenotypes in response to environmental change (e.g., Nussey et al. 2007), plasticity can result in not only different phenotypes produced

by the same individual throughout its lifetime, but also different phenotypes in individuals with the same genotype across geographic distance. To understand both the historic evolutionary pressures and the future risk of extinction from anthropogenic climate change, it is essential to assess the contributions of both phenotypic plasticity and local adaptation to phenotypic evolution in long-lived species. Species with widespread geographic distributions offer an opportunity to assess these contributions across a wide range of natural environmental conditions.

The predicted survival outcome for many reptiles and amphibians appears bleak due to the rapid pace of climatic shifts exacerbated by habitat loss and decreased population sizes (Gibbons et al. 2000; Sinervo et al. 2010; Böhm et al. 2016). However, for reptiles, most studies investigating potential responses to climate change suggest that plasticity plays an important, and perhaps predominant, role in mediating organismal responses to temperature (e.g., Refsnider and Janzen 2012; Urban et al. 2014; Refsnider and Janzen 2016; Janzen et al. 2018). Thermosensitive traits such as temperature-dependent sex determination (TSD) in many reptiles complicate predictions of survival, as temperature changes of only a few degrees could destabilize sex ratios rapidly, especially in small populations (Mitchell et al. 2010; Mitchell and Janzen 2010). While plasticity is likely important for the survival of reptiles with long generation times, the potential contribution of local adaptation to future survival in reptiles is less understood than the contribution of phenotypic plasticity (Urban et al. 2014). We currently have limited understanding of the amount of standing genetic variation in long-lived reptile populations and the degree to which this might contribute to local adaptation across populations. Investigating genomic evidence of local adaptation in long-lived reptiles can inform the next steps in management of these charismatic species (Macdonald et al. 2018).

Painted turtles (*Chrysemys picta*) – long-lived ectotherms with TSD - are an excellent model to evaluate the extent to which local adaptation, relative to phenotypic plasticity, of notable traits has contributed to population survival. The species' geographic range is widespread across North America, with populations subjected to disparate macro-environmental conditions. Divergence in color, scute patterns, nesting phenology, adult body size, reproductive effort, characteristics of TSD reaction norms (e.g., transitional range of temperatures), and thermal reaction norms for hatchling body mass and incubation time have been documented across populations (Iverson and Smith 1993; Ultsch et al. 2001; Ernst and Lovich 2009; Edge et al. 2017; Janzen et al. 2018; Bodensteiner et al. 2019; Carter et al. 2019). Phenotypic plasticity explains some variation in phenotypes among populations (e.g., nesting behavior, Refsnider and Janzen 2012; date of first nesting, Janzen et al. 2018). However, molecular genetic evidence of local adaptation among populations has not yet been assessed in this species. With genomic approaches, we can now uncover the genomic patterns and prevalence of local adaptation in long-lived vertebrates for which reciprocal transplant or common-garden experiments are difficult or infeasible (Savolainen et al. 2013). If this widespread species expresses little evidence of among-population genomic divergence, then phenotypic plasticity may be the mechanism by which populations of *C. picta* inhabit such distinct macro-environments. In this study, we investigate population genomic structure and genomic signatures of selection in seven locations spanning the western range of painted turtles to understand the role of local adaptation in population persistence of this long-lived ectotherm.

Methods

Study Organism

Painted turtles (*Chrysemys picta*) have a unique distribution among turtles, with the widest range of any North American turtle species (Ernst and Lovich 2009). The current distribution encompasses the entire eastern coast of the United States and stretches west across the northcentral United States and southern Canada, with a patchy distribution in the southwestern United States (see Carter et al. 2019). Fossil evidence suggests the species predates the Pleistocene glaciation period, and limited genetic evidence points to multiple range contractions as glaciers expanded (Starkey et al. 2003). This previous genetic study using one mitochondrial locus indicated an east-to-west pattern of oldest to youngest populations of the species. Further, very low genetic divergence was detected, particularly in the western half of its range, despite the species' age and widespread distribution. This result suggests that glaciation contracted populations in the east, followed by a rapid westward radiation of painted turtles. Additionally, the reference genome for painted turtles shows slow rates of sequence evolution compared to other vertebrate lineages, which may further compound a putative lack of genetic diversity observed among populations (Shaffer et al. 2013). More recent studies of genetic structure in painted turtles, again with limited number of markers, have consistently reported low divergence across much of the range (Jensen et al. 2015), including a few western populations (Reid et al. 2019). The recent study by Reid et al. (2019) corroborates the hypothesis that the western populations are the result of a rapid radiation westward following glaciation. Taken together, previous work on the genetic structure of this species has relied on a small number of neutral markers.

In addition to the potential of past demographic fluctuations with range expansion influencing the population genetic structure of painted turtles, phenotypes vary across locations

from the species' western range. For example, body size of adult painted turtles was positively correlated with latitude and elevation and negatively correlated with mean annual temperature in western populations (Iverson and Smith 1993). Additionally, thermal reaction norms for painted turtle hatchling phenotypes of western locations varied in common-garden conditions; responses of incubation duration and hatchling mass to temperature varied among hatchlings from different locations, but in a pattern inconsistent with latitude (Bodensteiner et al. 2019). As a model of a long-lived ectothermic amniote with an exceptional fossil record, a genome-wide study of genetic differentiation in painted turtles is warranted to allow tests of the relative roles of genetic drift, local adaptation, phenotypic plasticity, and biogeography in shaping population persistence.

Sample Collection

We collected clutches of painted turtle hatchlings or eggs from seven locations across the western 2/3 of the species' range (Table 1) and incubated eggs at Iowa State University (ISU) until hatching (see Refsnider et al. 2014; Bodensteiner et al. 2019). We stored hatchlings in 70% ethanol until DNA extraction. All research followed IACUC protocols of ISU with appropriate sampling permits from the associated agencies of each sampling location. To avoid any bias of relatedness, we genotyped only one hatchling from each clutch for this study, with sample sizes ranging from 5 to 38 hatchlings from each location (Table 1). We extracted DNA from hatchling liver tissue using a DNeasy Blood and Tissue Kit (Qiagen, Germantown, MD) or a phenol-chloroform DNA extraction protocol (Sambrook et al. 1989). We quantified DNA with a NanoDropTM 2000 Spectrophotometer and assessed DNA purity and quality using a 1% agarose gel before we performed DNA sequencing on 164 individuals.

RAD Processing and Variant Calling

We used a restriction site-associated DNA sequencing (RADseq) approach with a single-restriction enzyme, MseI, ligated resulting fragments with two barcode adapters, and pooled samples for size selection. We assessed resulting libraries for quality before paired-end 150 bp sequencing on an Illumina HiSeq platform (Illumina, San Diego, CA). Following sequencing, we removed raw reads that contained more than 10% unknown bases, removed reads with more than 50% low quality bases ($Q \leq 5$), and trimmed adapter sequences with cutadapt v2.5 (Martin 2011). Finally, we used the BWA-mem algorithm (Li 2013) in bwa v0.7.17 (Li and Durbin 2009; Li and Durbin 2010) to align reads to the painted turtle reference genome v3.0.3 downloaded from NCBI (Shaffer et al. 2013).

We processed aligned reads for variant calling by removing unmapped and improperly paired reads, reads not in primary alignment, and alignments with mapping quality (MAPQ) < 30 using SAMtools v1.9 (Li et al. 2009). To call variants, we used a modified Sentieon DNAseq workflow (v201808.01; https://support.sentieon.com/manual/DNAseq_usage/dnaseq/). We used Sentieon's Haplotyper algorithm to generate genomic variant call format files (GVCFs), including only sites with a minimum base quality > 20, and generated a VCF with raw variant calls across all samples with the GVCFtyper algorithm. We created a mask file containing both confident variant and invariant reference sites using '–emit_mode confident'. Following genotyping, we applied hard filters to single nucleotide polymorphisms (SNPs) and indels/mixed sites separately using GATK's VariantFiltration and SelectVariants (v4.0.4.0, McKenna et al. 2010; DePristo et al. 2011). We removed SNPs if they fit any of the following characteristics: low variant confidence (QD < 2.0), strand bias (FS > 60.0 or SOR > 4.0), low mapping quality (MQ < 40.0), large differences between reference and variant mapping quality (MQRankSum < -

12.5), or bias in position of alleles within reads (ReadPosRankSum < -8.0; e.g., Pfeifer et al. 2018). We removed indels if QD < 2, FS > 200, or ReadPosRankSum < -20.

We further filtered the variant and invariant VCFs using VCFtools v0.1.14 (Danecek et al. 2011). We removed individuals with low average depth (< 2X), excluded variants with mean genotype quality < 20.0, and restricted to biallelic sites where applicable. We then removed indels (filtered above), as well as 3bp upstream and downstream of the indel, from both the SNP and the invariant sites VCFs. Next, we removed SNPs with excess heterozygosity (Hardy-Weinberg-Equilibrium $P < 10^{-7}$). As the sampled locations are extremely geographically distant, we set this threshold low to ensure we did not remove real variants generated by substantial population genomic structure (e.g., Martin et al. 2018). We removed sites fixed for the non-reference allele and both variant and invariant sites with >25% of genotypes missing across individuals. This procedure yielded 41,546,386 accessible sites across the painted turtle genome. We then applied a stricter set of hard filters to ensure a high-quality set for population genomic analyses (Pfeifer et al. 2018), which are outlined here. First, we assigned SNP genotypes with a depth less than 4 or greater than 100 as missing to avoid including any low coverage reads or paralogous regions. Second, we partitioned the painted turtle genome scaffolds into 1.5kb blocks and assigned all SNPs and monomorphic sites to their corresponding blocks using a custom R script (v3.6.3; R Core Team 2020) with “dplyr” v0.7.5 (Wickham et al. 2018). We removed any blocks with a median distance between SNPs less than 3 or with less than 150 accessible sites (both variant and invariant) to prevent the inclusion of SNPs in repetitive or misaligned regions. This approach produced a dataset with 37,832,754 invariant and 566,852 variant sites over 153,416 blocks, which was used for calculating nucleotide diversity.

For analyses using only variants, we reduced missing data among SNPs and individuals by removing SNPs with greater than 10% missing genotypes and ensured that individuals had greater than 75% SNPs genotyped in the resulting dataset. The resulting VCF file contained 253,365 SNPs across 161 individuals. Then, we applied a minor allele frequency (MAF) filter such that singletons were excluded, and we retained only one SNP with the least missing data per 1.5kb block to avoid linkage among markers, for a final 48,060 SNPs used for population genomic analyses. A summary of filtering can be found in the Supplemental Material (Table S1).

Population Genomic and Demographic Analyses

To calculate intrapopulation (π) average nucleotide diversity values, we used VCFtools v0.1.14 --site-pi (Danecek et al. 2011) to calculate per-site nucleotide diversity for each population and then weight-averaged the estimate by the number of accessible sites (38,399,606; Martin et al. 2018). We used this same set and weight-averaging to calculate interpopulation (d_{xy}) nucleotide diversity in the R package "PopGenome" v2.7.5 (Pfeifer et al. 2014). We used the final filtered SNP dataset to calculate summary statistics for each population using "vcfR" v1.12.0 (Knaus and Grünwald 2017), "poppr" v2.8.7 (Kamvar et al. 2014), "adegenet" v2.1.3 (Jombart and Ahmed 2011), "heirfstat" v0.5.7 (Goudet and Jombart 2020) and "SNPRelate" v1.22.0 (Zheng et al. 2012) in R. These statistics include average percentage of missing genotypes per individual, number of private variable sites in each population, percentage of polymorphic SNP loci, expected (H_E) and observed (H_O) heterozygosity, average inbreeding coefficient (F_{IS}), and Weir and Cockerham's overall and pairwise F_{ST} (Weir and Cockerham 1984).

We performed a principal components analysis (PCA) in R using "SNPRelate" v1.22.0 (Zheng et al. 2012) downloaded from BiocManager v1.30.10 (Morgan 2019) to evaluate

population differentiation. We further assessed groupings in our data using the program STRUCTURE v2.3.4 (Pritchard et al. 2000) with the admixture model and the following parameters: 100,000 burn-in and 100,000 repetitions for each run of K from K=1 to K=10, correlated allele frequencies among populations, the alternative, population-specific ancestry prior (which entails allowing a separate alpha for each population; POPALPHAS=1), and an initial alpha value of 0.14, where alpha is the result of 1/K and K is the assumed number of populations. These settings were chosen to account for unequal sampling sizes from the seven locations (Wang 2017). Each value of K was run 20 times using the above parameters, as recommended by Gilbert et al. (2012). To select the optimal K from the STRUCTURE runs, we used multiple methods (Janes et al. 2017): we assessed the posterior probabilities for each K (Pritchard et al. 2000) and plotted Ln Pr(X|K) (Pritchard and Wen 2003) and ΔK (Evanno et al. 2005) using CLUMPAK v. 1.1 (Kopelman et al. 2015) and STRUCTURE HARVESTER (Earl and Vonholdt 2012).

We built a maximum likelihood population tree using TreeMix v. 1.13, which uses a graph-based approach to model both gene flow and population splits (Pickrell and Pritchard 2012). We used 500 bootstrap replicates, and assumed no migration given the distance among sampled locations. We tested for isolation by distance (IBD) using a Mantel test comparing straight-line geographic distance (km) between locations to pairwise genetic differentiation, $F_{ST}/(1-F_{ST})$ (Rousset 1997), implemented in "vegan" v.2.5.7 (Oksanen et al. 2020) with 10,000 permutations. Finally, we assessed runs of homozygosity (ROH) in the variant dataset with all filters except the final filter retaining one SNP per block using PLINK v1.9 (Purcell et al. 2007). Runs of homozygosity are tracts of homozygosity along the genome, and ROH can be informative of both past demographic changes (e.g., bottlenecks) and recent inbreeding among

individuals within populations (reviewed in Ceballos et al. 2018). Specifically, long tracts of homozygosity are generated by recent inbreeding loops among individuals, while more numerous short ROH can be indicative of coalescence among individuals during population bottlenecks further back in time. We used the –homozyg algorithm in PLINK with the following settings: window size of 25 SNPs, defined windows as homozygous if one or less heterozygous sites were found in the window, allowed no more than 5 missing sites within a window, and set the window threshold for a SNP being defined as in a homozygous segment of a chromosome (hit rate) at 0.05. For a region to be defined as a ROH, segments must include ≥ 25 SNPs, cover ≥ 1,000 kb, contain a maximum of one heterozygous site, contain minimum SNP density of 1 per 50 kb, and have maximum distance between two adjacent SNPs of ≤ 1,000 kb (Grossen et al. 2018).

Selection Scans

To detect outlier loci potentially linked to selection across the sampled locations, we first applied the Bayesian approach of BayeScan v2.1 (Foll and Gaggiotti 2008). For this analysis, we used the variant dataset that contained all filtering steps described above except the final filter retaining one SNP per block (212,670 SNPs; Table S1). We included these potentially linked SNPs in this analysis to give increased support for any detected outlier SNPs; if selection is causing a deviation from the population mean F_{ST}, the surrounding SNPs should deviate in a similar manner (Storfer et al. 2018). We used a burn-in of 50,000, 100,000 iterations, and prior odds of 100 for the neutral model to reduce the number of false positives. We evaluated convergence using the R package CODA (Plummer et al. 2006), and any loci with a q-value less than 0.05 were identified for further analysis. We plotted results of all analyses using "ggplot2" v3.3.3 (Wickham 2016) in R.

Results

Sampling and RAD Variants

In total, 164 painted turtle hatchlings representing 7 sampling locations were sequenced for this project (Table 1), with an average of 3.77 million high-quality reads per individual and 3.5 million reads mapped to the reference genome. Joint genotyping yielded 3.53 million SNP loci; individual depth filters (which removed three individuals) and site filters resulted in a final dataset of 48,060 SNPs from 161 individuals with an average of 4.43% missing genotypes across individuals (Table 1, Table 2, Table S1). With such a large number of SNPs, a representation of genetic diversity in these locations was likely captured even in locations where the number of individuals sampled was small (Nazareno et al. 2017).

Population Genomic and Demographic Analyses

Summary statistics suggested that genetic variation varied widely among locations. Polymorphism ranged from 31% to 87% (Table 2), with the lowest values of polymorphism and private alleles in the northwestern populations and the highest in the Illinois population. The Illinois population had much greater genetic variation than the other sampled locations, with private alleles an order of magnitude more numerous than any other population. Weir and Cockerham's overall weighted F_{ST} across locations was 0.136 and average F_{ST} across loci was 0.089.

Pairwise F_{ST}, d_{xy}, PCA, and STRUCTURE results all depicted a similar pattern of genetic structure across the sampled locations. Pairwise F_{ST} values suggested moderate to high differentiation among many populations (Table 3). However, Illinois, Nebraska, Minnesota, and Kansas had lower levels of differentiation than other pairwise comparisons, and Oregon and

Idaho pairwise F_{ST} was similarly low. The first three principal components (PC) explained 20% of the variation in the dataset, with percentages of 9.4%, 6.2% and 4.5% of the variance explained, respectively (Fig. 1A). The first PC was consistent with positioning of populations from east to west, with most populations grouping in the middle of PC1 and Illinois and the northwestern populations residing on either end of the PC. The second PC separated the New Mexico population from the more northern populations, and the third PC separated New Mexico individuals from Nebraska, Kansas, and Minnesota individuals. The results of the various estimators of best K for the STRUCTURE runs suggested the number of populations in these data is 6 (Fig. 1C; SI Fig. 1-5). ΔK suggested the optimal K was 2, but this result is not convincing given the frequent recovery of K=2 using this method (Janes et al. 2017) and other estimators suggesting K=6 to be the best number of populations in these data. Painted turtles from the Oregon and Idaho locations were similar in allele frequencies; these individuals overlapped in the PCA and displayed low pairwise F_{ST} and d_{xy} (Table 3). Two individuals from Oregon were distinguished from the other Oregon individuals in both the PCA and STRUCTURE analyses (Fig. 1). We calculated individual relatedness using PLINK, and both individuals appeared not to be closely related.

The population tree from the TreeMix analysis explained 99.8% of the covariance in allele frequencies among locations. There was substantial drift among populations, with Oregon and Idaho grouping closely and the remaining populations showing branching consistent with their east-west location (Fig. 2). The Mantel test of IBD supported a significant relationship between pairwise geographic distance and pairwise genetic distance ($P = 0.012$; Fig. 1B). When investigating the demographic history and relatedness among individuals, the total length of ROH was correlated with the number of ROH (R^2=0.5821; Fig. 3A). The relationship was linear,

with individuals from the most genetically variable population (IL) having shorter and fewer ROH, individuals from Oregon and Idaho having more of their genome in ROH and more numerous ROH, and other populations displaying ROH patterns consistent with their geographic distance from the IL population (Fig. 3A). ROH were then partitioned into either small and intermediate ROH < 5 megabases (MB) or long ROH > 5 MB, the latter of which indicate recent inbreeding (e.g., McQuillan et al. 2008; Grossen et al. 2018). When comparing long ROH, populations did not vary in the total length of long ROH in the genome, as would be expected under a scenario of increased inbreeding among individuals within certain populations (Fig. 3B). Instead, populations varied in the total length of the genome that resides in short and intermediate ROH, with Oregon and Idaho individuals having much more numerous ROH < 5MB than other populations (Fig. 3C). This result, coupled with the linear relationship of total ROH length to number of ROH increasing with geographic distance among populations (Fig. 3A), strongly supports a role of repeated bottlenecks through serial founder effects in the demographic history of painted turtle populations as the species' range spread westward.

Selection Scans

After validating convergence, Bayescan identified 43 F_{ST} outlier loci at the 0.05 false discovery rate (FDR) (Fig. 4; Table S2). Six loci derived from defined chromosomes of the painted turtle genome assembly, and the remainder were found on scaffolds. We further investigated the location of these SNPs in the genome for proximity to genic regions. Of these outliers, 26 corresponded to genic regions, but only one variant (in the RBBP6 gene) was located in a coding region. This variant, however, does not change the amino acid sequence of the gene. We investigated genotypic patterns among populations at the 43 outlier loci and found that all 43 outlier loci were segregating in the Illinois population. The patterns of segregation were

consistent with genetic drift, as populations geographically closer to the Illinois population had less variation than the Illinois population at these loci, and New Mexico and northwest populations were usually fixed for one of the two alleles represented in the Illinois population.

Given two remarkable aspects of the biology of painted turtles that conceivably could be linked to adaptation to macro-environmental conditions across the geographic range, we further explored potential adaptation at the candidate gene level. First, we queried coverage of genes implicated in the sex-determination mechanism, as these genes may play a role in differentiation of the transitional range of temperatures across these populations (Carter et al. 2019). We found coverage of DMRT1 in our dataset, with 22 variant sites, though none were in coding regions. These variants did not appear to be correlated with sex of sampled hatchlings, though most hatchlings were incubated in field conditions, and thus we cannot assess the influence of genotype on sex at the pivotal temperature of ~28°C (when theoretical sex ratio is 1:1; Telemeco et al. 2013). Second, we had coverage of ANKRD1, ATF3, CA1, SYR61, ENDOD, PTGS2, S100A1, and TNC, which are all identified as differentially expressed during anoxia or re-oxygenation in painted turtles (Fanter et al. 2020). One variant in CA1 was located in a coding region, and changed an amino acid from proline to glutamine. This variant was found in 5 Illinois individuals, 7 Minnesota individuals, and 1 Nebraska individual. Four other variants associated with amino acid changes in coding regions of CYR61 and TNC were found at low frequency in one to three individuals.

Discussion

With genomic data, we can now investigate in greater detail the genomic architecture of local adaptation among populations of widespread species and understand past demographic changes that led to species distributions. In this study, we used RADseq to sequence thousands

of markers in painted turtles from 7 locations across the western range of the species. Populations were genetically differentiated, with patterns of divergence consistent with latitudinal and longitudinal distance among populations. There was sparse evidence of selection on variants across the genome, measured by significant genetic differentiation (F_{ST}) among populations, few of which were associated with changes in coding regions. Further, the loci with highest F_{ST} among populations were all segregating in the Illinois population, and were subsequently fixed in populations farther west in a pattern consistent with serial founder effects driving genomic differentiation. These results suggest that population demographic history, rather than local adaptation, largely shapes genomic divergence among western populations of painted turtles. Given the phenotypic differences noted among these populations, phenotypic plasticity is likely a major contributor to the success of painted turtles in colonizing a large geographic range across North America, allowing accommodation to substantially different macro-environmental conditions.

Population Genomics of Painted Turtles

In many widespread species, populations are characterized by strong genetic differentiation from the co-occurring forces of selection and genetic drift (e.g., Rödin-Mörch et al. 2019). During range expansions, and in the absence of significant gene flow, reduction in genetic diversity is often observed at range edges due to serial founder effects (DeGiorgio et al. 2011). Genetic surfing from differential fixation of alleles along the expanding range front during range expansion creates distinct population genetic structure, and can even drive patterns of stronger genetic structure in populations at range edges than those from the original range (e.g., Graciá et al. 2013; reviewed in Excoffier et al. 2009). Understanding the population genetic

structure and past demography of widespread species is important when investigating local adaptation, as many patterns that could be interpreted as local adaptation (e.g., variation at allele frequencies along clines in environmental conditions) could also be driven by serial founder effects (Hoban et al. 2016). Thus, we first investigated the population genomic structure of the western range of painted turtles to test past biogeographic hypotheses of the species' range in North America.

Previous analyses of population genetic differentiation among western painted turtle populations have consistently revealed low genetic divergence. Starkey et al. (2003) investigated the phylogeography of painted turtles across the species' range using a single mitochondrial marker (control region CR) and reported pairwise divergence of 0.151–1.368% within the western populations. Over 60 individuals sampled had the same haplotype, with 28 individuals sharing haplotypes with one or two differences from this main haplotype (Starkey et al. 2003). The authors conclude that this lack of divergence suggests a recent radiation of painted turtles into the western United States and Canada, despite fossil evidence suggesting their presence in the Great Plains as long ago as 1.9 million years (Holman 1995). A more recent study expanded sampling to include a nuclear marker, PAX-P1, and found that the western range of painted turtles also included low haplotype diversity, though populations did not distinctly group together (Jensen et al. 2015). However, tests of demographic history based on the mitochondrial and nuclear marker suggested no evidence of population expansion in the western populations. Finally, Reid et al. (2019) included eleven microsatellite loci to further elucidate population differentiation. While fewer populations were sampled west of the Mississippi River (N=3), the results were similar to those presented here; populations were arranged from east to west in a principal coordinates analysis, and there was a significant relationship between F_{ST} and

geographic distance (r = 0.85, Reid et al. 2019). Ecological niche modeling and demographic modeling suggested a single glacial refugium followed by population expansion, in contrast to Jensen et al. (2015).

Despite the low genetic variation found in the western range of previous studies, our study genetically distinguished most populations except those from Oregon and Idaho. Indeed, the F_{ST} values found among populations were high in some cases, particularly when comparing Oregon and Idaho populations with other populations. Importantly, we detected patterns of genetic variation largely consistent with serial founder events driving genetic isolation by distance. In the most geographically isolated northwestern populations, instead of strong genetic patterns of local adaptation, as proposed in Jensen et al. (2015), we detected excess ROH suggesting that demography rather than selection has largely shaped genetic variation in western painted turtles. The length of these ROH is consistent with bottlenecks via serial founder effects leading to the current low levels of genetic variation in Oregon and Idaho, and to a lesser extent in the New Mexico population. Further, reductions in observed heterozygosity were consistent with geographic distance from the hypothesized origin of western painted turtle populations in the eastern United States. Thus, the conclusion of Reid et al. (2019) that the species' widespread range is the result of the spread of populations westward after the retraction of glaciers following the late Pleistocene is upheld by the genome-wide sequencing performed here.

We also find evidence consistent with multiple instances of human-mediated translocation of painted turtles from one population to another. Given the level of admixture in the two admixed Oregon individuals, they appear to be the result of at least second-generation offspring of translocated individuals, where one grandparent was sourced from one of the Midwestern populations. Individuals sequenced in a previous study also indicated potential

evidence of human-mediated dispersal in the western range (Jensen et al. 2015). This result highlights the importance of managing and reducing the release of pet turtles into native populations, as this practice undermines the genetic integrity of these populations. This concern was raised in the conservation assessment for the western painted turtle in Oregon (Gervais et al. 2009), and we can now establish that introductions have occurred even in areas that previously were not suspected of introductions in Oregon.

Local Adaptation in Painted Turtles

While the goal of this study was to evaluate genomic evidence for local adaptation in western populations of painted turtles, which might be expected given the measurable phenotypic variation among populations (e.g., Iverson and Smith 1993; Janzen et al. 2018), we found little evidence of local adaptation in a scan for outlier loci (43 out of 212,670 SNPs). Indeed, the genotypic patterns of the outlier loci instead are all consistent with genetic surfing (Excoffier et al. 2009). Further, none of the outlier genomic variants induce amino acid changes in genic coding regions. Even the genes associated with important phenotypes (e.g., TSD and anoxia-tolerance genes) were not highly variable among sampled populations. Based on the extensive evidence for serial founder effects and the lack of outlier loci demonstrating patterns distinct from genetic surfing, demography is likely the strongest driver of genetic variation among these populations of painted turtles, rather than local adaptation. A similar pattern has been found in invasive house finch populations, which demonstrated outlier loci fitting patterns consistent with genetic drift from founder events rather than local adaptation (Shultz et al. 2016).

Both local adaptation and population demography can induce genetic differentiation among populations. However, in species that have undergone range expansions, genetic drift is predicted to both increase genetic differentiation among populations and decrease genetic

diversity within populations (Hallatschek et al. 2007; Excoffier and Ray 2008). This pattern was not only found in this study, but also in others investigating the genetic structure of Testudines that experienced post-glacial colonization of northern ranges. For example, in the spur-thighed tortoise, populations in the northern range were characterized by reduced genetic diversity, strong population differentiation, and clinal variation from southern to northern populations in allele frequencies, all patterns consistent with genetic surfing (Graciá et al. 2013). Similar patterns were reported at microsatellite loci in the European pond turtle (Pereira et al. 2018). The genome of the painted turtle suggests a slow substitution rate relative to other vertebrate lineages (Shaffer et al. 2013), which supports a stronger role of genetic drift driving genetic differentiation, rather than local adaptation, during range expansion in Testudines.

While we do not find evidence of local adaptation, the demographic patterns of serial founder effects on the genome greatly hinder the ability to detect local adaptation in selection scans (Hoban et al. 2016). The patterns of local adaptation on F_{ST} among populations can be indistinguishable from those generated from genetic surfing, as certain populations become fixed for one allele or another due to the neutral process of drift, rather than selection (Excoffier et al. 2009; Hofer et al. 2009). Indeed, all F_{ST} outlier tests perform poorly, with many false positives, when range expansion shaped population genetic structure (Lotterhos and Whitlock 2014). Identification of local adaptation is thus particularly difficult using F_{ST} outlier approaches in species with complex demographic history, including past range expansions. In Alpine ibex, a species that experienced a recent bottleneck due to overharvesting, the influence of bottlenecks on genetic variation largely prevented the accurate identification of loci under selection (Leigh et al. 2021). Further, in geographically isolated populations with little gene flow, we would anticipate that local adaptation of a trait would be achieved through divergence at very few large-

effect loci and many more small-effect loci (Savolainen et al. 2013). Small-effect loci are often missed in F_{ST} outlier tests (Kemper et al. 2014), and thus we may not be able to effectively identify evidence of local adaptation in the phenotypes that vary among populations using these methods. Finally, in this study we used reduced-representation sequencing, which is an excellent tool for understanding population genetic structure (Catchen et al. 2017), but may miss regions of large differentiation consistent with phenotypic adaptation. Whole-genome sequencing may provide increased resolution for loci of large effect, and genome-wide association studies may be a better method for addressing local adaptation in complex phenotypes in species with a history of serial founder effects (Berg and Coop 2014).

Phenotypic Plasticity or Local Adaptation?

Given the confirmation of serial founder effects in painted turtles, we cannot rule out local adaptation leading to phenotypic differentiation among populations. However, even with analyzing > 200,000 loci across the genome, we found no strong evidence of local adaptation. This seems to contrast with the notable phenotypic variation among these populations for multiple traits. If local adaptation is not germane in these instances, then plasticity, maternal effects, or epigenetic modification may be stronger forces driving phenotypic variation of traits likely under selection (Mitchell et al. 2015; Hu and Barrett 2017; Enbody et al. 2021). This is particularly true in species with slow mutation rates and histories of population bottlenecks, as low standing genetic variation and few mutations may limit future adaptive ability without plasticity (Lande and Shannon 1996; Merila and Hendry 2014). Phenotypic plasticity is an important mechanism for surviving temperature variation in ectotherms, including turtles, and may be essential for survival as the global climate continues to rapidly change (but see Urban et al. 2014; Gunderson and Stillman 2015). However, populations at the range edges of widespread

species may be particularly vulnerable to extinction, as low genetic variation may compromise their ability to adapt to an ever-changing environment.

Acknowledgements

This work was supported by grants from the National Science Foundation (LTREB DEB-1242510 and IOS-1257857) and the National Institutes of Health (R01-AG049416). We thank the many people who participated in the collection of samples from sampling locations (B. Bodensteiner, J. Iverson, C. Milne-Zelman, T. Mitchell, J. Refsnider, D. Warner) and A. Bronikowski and members of the Janzen and Bronikowski lab groups who provided comments on drafts of this manuscript. We also thank Elena Thornhill for writing the protocol included in the supplemental material and both Elena and Kelsi Hagerty for assistance with optimizing the protocol for DNA extraction.

References

Berg JJ, Coop G. 2014. A population genetic signal of polygenic adaptation. PLoS Genet. 10:e1004412.

Bodensteiner BL, Warner DA, Iverson JB, Milne-Zelman CL, Mitchell TS, Refsnider JM, Janzen FJ. 2019. Geographic variation in thermal sensitivity of early life traits in a widespread reptile. Ecol Evol. 9:2791-2802.

Böhm M, Cook D, Ma H, Davidson AD, García A, Tapley B, Pearce-Kelly P, Carr J. 2016. Hot and bothered: using trait-based approaches to assess climate change vulnerability in reptiles. Biol Conserv. 204:32-41.

Carter AL, Bodensteiner BL, Iverson JB, Milne-Zelman CL, Mitchell TS, Refsnider JM, Warner DA, Janzen FJ. 2019. Breadth of the thermal response captures individual and geographic variation in temperature-dependent sex determination. Funct Ecol. 33:1928-1939.

Catchen JM, Hohenlohe PA, Bernatchez L, Funk WC, Andrews KR, Allendorf FW. 2017. Unbroken: RADseq remains a powerful tool for understanding the genetics of adaptation in natural populations. Mol Ecol Resour. 17:362-365.

Catullo RA, Llewelyn J, Phillips BL, Moritz CC. 2019. The potential for rapid evolution under anthropogenic climate change. Curr Biol. 29:R996-R1007.

Ceballos FC, Joshi PK, Clark DW, Ramsay M, Wilson JF. 2018. Runs of homozygosity: windows into population history and trait architecture. Nat Rev Genet. 19:220.

Danecek P, Auton A, Abecasis G, Albers CA, Banks E, DePristo MA, Handsaker RE, Lunter G, Marth GT, Sherry ST, et al. 2011. The variant call format and VCFtools. Bioinformatics. 27:2156-2158.

DeGiorgio M, Degnan JH, Rosenberg NA. 2011. Coalescence-time distributions in a serial founder model of human evolutionary history. Genetics. 189:579-593.

DePristo MA, Banks E, Poplin R, Garimella KV, Maguire JR, Hartl C, Philippakis AA, del Angel G, Rivas MA, Hanna M, et al. 2011. A framework for variation discovery and genotyping using next-generation DNA sequencing data. Nat Genet. 43:491-498.

Earl DA, Vonholdt BM. 2012. STRUCTURE HARVESTER: a website and program for visualizing STRUCTURE output and implementing the Evanno method. Conserv Genet Resour. 4:359-361.

Edge CB, Rollinson N, Brooks RJ, Congdon JD, Iverson JB, Janzen FJ, Litzgus JD. 2017. Phenotypic plasticity of nest timing in a post-glacial landscape: how do reptiles adapt to seasonal time constraints? Ecology. 98:512-524.

Enbody ED, Pettersson ME, Sprehn CG, Palm S, Wickström H, Andersson L. 2021. Ecological adaptation in European eels is based on phenotypic plasticity. Proc. Nat. Acad. Sci. 118:e2022620118.

Ernst CH, Lovich JE. 2009. Turtles of the United States and Canada. 2nd ed. Baltimore: Johns Hopkins University Press.

Evanno G, Regnaut S, Goudet J. 2005. Detecting the number of clusters of individuals using the software STRUCTURE: a simulation study. Mol Ecol. 14:2611-2620.

Excoffier L, Ray N. 2008. Surfing during population expansions promotes genetic revolutions and structuration. Trends Ecol Evol. 23:347-351.

Excoffier L, Foll M, Petit RJ. 2009. Genetic consequences of range expansions. Annu Rev Eco Evol Syst. 40:481-501.

Fanter CE, Lin Z, Keenan SW, Janzen FJ, Mitchell TS, Warren DE. 2020. Development-specific transcriptomic profiling suggests new mechanisms for anoxic survival in the ventricle of overwintering turtles. J Exp Biol. 223:213918.

Foll M, Gaggiotti O. 2008. A genome-scan method to identify selected loci appropriate for both dominant and codominant markers: a Bayesian perspective. Genetics. 180:977-993.

Gervais J, Rosenberg D, Barnes S, Puchy C, Stewart E. 2009. Conservation Assessment for the Western Painted Turtle in Oregon. U.S.D.A. Forest Service:4-61.

Gibbons JW, Scott DE, Ryan TJ, Buhlmann KA, Tuberville TD, Metts BS, Greene JL, Mills T, Leiden Y, Poppy S, et al. 2000. The Global Decline of Reptiles, Déjà Vu Amphibians. Bioscience. 50

Gilbert KJ, Andrew RL, Bock DG, Franklin MT, Kane NC, Moore JS, Moyers BT, Renaut S, Rennison DJ, Veen T, et al. 2012. Recommendations for utilizing and reporting population genetic analyses: the reproducibility of genetic clustering using the program STRUCTURE. Mol Ecol. 21:4925-4930.

Goudet J, Jombart T. 2020. hierfstat: Estimation and Tests of Hierarchical F-Statistics. v. 0.5.7. https://cran.r-project.org/package=hierfstat

Graciá E, Botella F, Anadón JD, Edelaar P, Harris DJ, Giménez A. 2013. Surfing in tortoises? Empirical signs of genetic structuring owing to range expansion. Biol Lett. 9:20121091.

Grossen C, Biebach I, Angelone-Alasaad S, Keller LF, Croll D. 2018. Population genomics analyses of European ibex species show lower diversity and higher inbreeding in reintroduced populations. Evol Appl. 11:123-139.

Gunderson AR, Stillman JH. 2015. Plasticity in thermal tolerance has limited potential to buffer ectotherms from global warming. Proc Biol Sci. 282:20150401.

Hallatschek O, Hersen P, Ramanathan S, Nelson DR. 2007. Genetic drift at expanding frontiers promotes gene segregation. Proc Nat Acad Sci. 104:19926-19930.

Hereford J. 2009. A quantitative survey of local adaptation and fitness trade-offs. Am Nat. 173:579-588.

Hoban S, Kelley JL, Lotterhos KE, Antolin MF, Bradburd G, Lowry DB, Poss ML, Reed LK, Storfer A, Whitlock MC. 2016. Finding the Genomic Basis of Local Adaptation: Pitfalls, Practical Solutions, and Future Directions. Am Nat. 188:379-397.

Hofer T, Ray N, Wegmann D, Excoffier L. 2009. Large Allele Frequency Differences between Human Continental Groups are more Likely to have Occurred by Drift During range Expansions than by Selection. Ann Hum Genet. 73:95-108.

Holman JA. 1995. Pleistocene amphibians and reptiles in North America. Oxford University Press New York.

Hu J, Barrett RDH. 2017. Epigenetics in natural animal populations. J Evol Biol. 30:1612-1632.

Iverson JB, Smith GR. 1993. Reproductive ecology of the painted turtle (*Chrysemys picta*) in the Nebraska Sandhills and across its range. Copeia:1-21.

Janes JK, Miller JM, Dupuis JR, Malenfant RM, Gorrell JC, Cullingham CI, Andrew RL. 2017. The K = 2 conundrum. Mol Ecol. 26:3594-3602.

Janzen FJ, Hoekstra LA, Brooks RJ, Carroll DM, Gibbons JW, Greene JL, Iverson JB, Litzgus JD, Michael ED, Parren SG, et al. 2018. Altered spring phenology of North American freshwater turtles and the importance of representative populations. Ecol Evol. 8:5815-5827.

Jensen EL, Govindarajulu P, Russello MA. 2015. Genetic assessment of taxonomic uncertainty in painted turtles. J Herpetol. 49:314-324.

Jombart T, Ahmed I. 2011. adegenet 1.3-1: new tools for the analysis of genome-wide SNP data. Bioinformatics. 27:3070-3071.

Kamvar ZN, Tabima JF, Grünwald NJ. 2014. Poppr: an R package for genetic analysis of populations with clonal, partially clonal, and/or sexual reproduction. PeerJ. 2:e281.

Kemper KE, Saxton SJ, Bolormaa S, Hayes BJ, Goddard ME. 2014. Selection for complex traits leaves little or no classic signatures of selection. BMC Genomics. 15:1-14.

Knaus BJ, Grünwald NJ. 2017. vcfr: a package to manipulate and visualize variant call format data in R. Mol Ecol Resour. 17:44-53.

Kopelman NM, Mayzel J, Jakobsson M, Rosenberg NA, Mayrose I. 2015. Clumpak: a program for identifying clustering modes and packaging population structure inferences across K. Mol Ecol Resour. 15:1179-1191.

Lande R, Shannon S. 1996. The role of genetic variation in adaptation and population persistence in a changing environment. Evolution. 50:434-437.

Leigh DM, Lischer HEL, Guillaume F, Grossen C, Günther T. 2021. Disentangling adaptation from drift in bottlenecked and reintroduced populations of Alpine ibex. bioRxiv:2021.2001.2026.428274.

Li H. 2013. Aligning sequence reads, clone sequences and assembly contigs with BWA-MEM. ArXiv. 1303.3997v1 [q-bio.GN]

Li H, Durbin R. 2009. Fast and accurate short read alignment with Burrows-Wheeler transform. Bioinformatics. 25:1754-1760.

Li H, Durbin R. 2010. Fast and accurate long-read alignment with Burrows-Wheeler transform. Bioinformatics. 26:589-595.

Li H, Handsaker B, Wysoker A, Fennell T, Ruan J, Homer N, Marth G, Abecasis G, Durbin R, Genome Project Data Processing S. 2009. The Sequence Alignment/Map format and SAMtools. Bioinformatics. 25:2078-2079.

Lotterhos KE, Whitlock MC. 2014. Evaluation of demographic history and neutral parameterization on the performance of FST outlier tests. Mol Ecol. 23:2178-2192.

Macdonald SL, Llewelyn J, Phillips BL. 2018. Using connectivity to identify climatic drivers of local adaptation. Ecol Lett. 21:207-216.

Martin HC, Batty EM, Hussin J, Westall P, Daish T, Kolomyjec S, Piazza P, Bowden R, Hawkins M, Grant T, et al. 2018. Insights into Platypus Population Structure and History from Whole-Genome Sequencing. Mol Biol Evol. 35:1238-1252.

Martin M. 2011. Cutadapt removes adapter sequences from high-throughput sequencing reads. EMBnet J. 17:10-12.

McKenna A, Hanna M, Banks E, Sivachenko A, Cibulskis K, Kernytsky A, Garimella K, Altshuler D, Gabriel S, Daly M, et al. 2010. The Genome Analysis Toolkit: a MapReduce framework for analyzing next-generation DNA sequencing data. Genome Res. 20:1297-1303.

McQuillan R, Leutenegger A-L, Abdel-Rahman R, Franklin CS, Pericic M, Barac-Lauc L, Smolej-Narancic N, Janicijevic B, Polasek O, Tenesa A. 2008. Runs of homozygosity in European populations. Am J Hum Genet. 83:359-372.

Merila J, Hendry AP. 2014. Climate change, adaptation, and phenotypic plasticity: the problem and the evidence. Evol Appl. 7:1-14.

Mitchell NJ, Janzen FJ. 2010. Temperature-dependent sex determination and contemporary climate change. Sex Dev. 4:129-140.

Mitchell NJ, Allendorf FW, Keall SN, Daugherty CH, Nelson NJ. 2010. Demographic effects of temperature-dependent sex determination: will tuatara survive global warming? Global Change Biol. 16:60-72.

Mitchell TS, Maciel JA, Janzen FJ. 2015. Maternal effects influence phenotypes and survival during early life stages in an aquatic turtle. Funct Ecol. 29:268-276.

Morgan M. 2019. BiocManager: Access the Bioconductor Project Package Repository. v. 1.30.10. https://cran.r-project.org/package=BiocManager

Nazareno AG, Bemmels JB, Dick CW, Lohmann LG. 2017. Minimum sample sizes for population genomics: an empirical study from an Amazonian plant species. Mol Ecol Resour. 17:1136-1147.

Nussey DH, Wilson AJ, Brommer JE. 2007. The evolutionary ecology of individual phenotypic plasticity in wild populations. J Evol Biol. 20:831-844.

Oksanen J, Guillaume Blanchet F, Friendly M, Kindt R, Legendre P, McGlinn D, Minchin PR, O'Hara RB, Simpson GL, Solymos P, et al. 2020. vegan: Community Ecology Package. v. 2.5.7. https://cran.r-project.org/package=vegan

Orr HA. 1998. The population genetics of adaptation: The distribution of factors fixed during adaptive evolution. Evolution. 52:935-949.

Pereira P, Teixeira J, Velo-Antón G. 2018. Allele surfing shaped the genetic structure of the European pond turtle via colonization and population expansion across the Iberian Peninsula from Africa. J Biogeogr. 45:2202-2215.

Pfeifer B, Wittelsbürger U, Ramos-Onsins SE, Lercher MJ. 2014. PopGenome: an efficient Swiss army knife for population genomic analyses in R. Mol Biol Evol. 31:1929-1936.

Pfeifer SP, Laurent S, Sousa VC, Linnen CR, Foll M, Excoffier L, Hoekstra HE, Jensen JD. 2018. The Evolutionary History of Nebraska Deer Mice: Local Adaptation in the Face of Strong Gene Flow. Mol Biol Evol. 35:792-806.

Pickrell JK, Pritchard JK. 2012. Inference of population splits and mixtures from genome-wide allele frequency data. PLoS Genet. 8:e1002967.

Plummer M, Best N, Cowles K, Vines K. 2006. CODA: convergence diagnosis and output analysis for MCMC. R News. 6:5.

Price TD, Qvarnström A, Irwin DE. 2003. The role of phenotypic plasticity in driving genetic evolution. Proc R Soc London B. 270:1433-1440.

Pritchard JK, Wen W. 2003. Documentation for STRUCTURE Software: Version 2. http://web.stanford.edu/group/pritchardlab/software/structure2_1.html

Pritchard JK, Stephens M, Donnelly P. 2000. Inference of population structure using multilocus genotype data. Genetics. 155:945-959.

Purcell S, Neale B, Todd-Brown K, Thomas L, Ferreira MA, Bender D, Maller J, Sklar P, de Bakker PI, Daly MJ, et al. 2007. PLINK: a tool set for whole-genome association and population-based linkage analyses. Am J Hum Genet. 81:559-575.

R Core Team. 2020. R: A language and environment for statistical computing. https://www.r-project.org/

Radchuk V, Reed T, Teplitsky C, Van De Pol M, Charmantier A, Hassall C, Adamík P, Adriaensen F, Ahola MP, Arcese P. 2019. Adaptive responses of animals to climate change are most likely insufficient. Nat Commun. 10:1-14.

Refsnider JM, Janzen FJ. 2012. Behavioural plasticity may compensate for climate change in a long-lived reptile with temperature-dependent sex determination. Biol Conserv. 152:90-95.

Refsnider JM, Janzen FJ. 2016. Temperature-dependent sex determination under rapid anthropogenic environmental change: Evolution at a turtle's pace? J Hered. 107:61-70.

Refsnider JM, Milne-Zelman C, Warner DA, Janzen FJ. 2014. Population sex ratios under differing local climates in a reptile with environmental sex determination. Evol Ecol. 28:977-989.

Reid B, Kass J, Wollney S, Jensen E, Russello M, Viola E, Pantophlet J, Iverson J, Peery M, Raxworthy C. 2019. Disentangling the genetic effects of refugial isolation and range expansion in a trans-continentally distributed species. Heredity. 122:441-457.

Rödin-Mörch P, Luquet E, Meyer-Lucht Y, Richter-Boix A, Höglund J, Laurila A. 2019. Latitudinal divergence in a widespread amphibian: Contrasting patterns of neutral and adaptive genomic variation. Mol Ecol. 28:2996-3011.

Rousset F. 1997. Genetic differentiation and estimation of gene flow from F-statistics under isolation by distance. Genetics. 145:1219-1228.

Sambrook J, Fritsch E, Maniatis T. 1989. Molecular Cloning: a Laboratory Manual, 2nd edn. New York: Cold Spring Harbor Laboratory Press.

Savolainen O, Lascoux M, Merila J. 2013. Ecological genomics of local adaptation. Nat Rev Genet. 14:807-820.

Shaffer HB, Minx P, Warren DE, Shedlock AM, Thomson RC, Valenzuela N, Abramyan J, Amemiya CT, Badenhorst D, Biggar KK, et al. 2013. The western painted turtle genome, a model for the evolution of extreme physiological adaptations in a slowly evolving lineage. Genome Biol. 14:R28.

Shultz AJ, Baker AJ, Hill GE, Nolan PM, Edwards SV. 2016. SNPs across time and space: population genomic signatures of founder events and epizootics in the House Finch (*Haemorhous mexicanus*). Ecology and Evolution. 6:7475-7489.

Sinervo B, Mendez-de-la-Cruz F, Miles DB, Heulin B, Bastiaans E, Villagran-Santa Cruz M, Lara-Resendiz R, Martinez-Mendez N, Calderon-Espinosa ML, Meza-Lazaro RN, et al. 2010. Erosion of lizard diversity by climate change and altered thermal niches. Science. 328:894-899.

Starkey DE, Shaffer HB, Burke RL, Forstner MRJ, Iverson JB, Janzen FJ, Rhodin AGJ, Ultsch GR. 2003. Molecular Systematics, Phylogeography, and the Effects of Pleistocene Glaciation in the Painted Turtle (*Chrysemys Picta*) Complex. Evolution. 57

Storfer A, Patton A, Fraik AK. 2018. Navigating the Interface Between Landscape Genetics and Landscape Genomics. Front Genet. 9:68.

Telemeco RS, Abbott KC, Janzen FJ. 2013. Modeling the effects of climate change–induced shifts in reproductive phenology on temperature-dependent traits. Am Nat. 181:637-648.

Torres-Dowdall J, Handelsman CA, Reznick DN, Ghalambor CK. 2012. Local adaptation and the evolution of phenotypic plasticity in Trinidadian guppies (*Poecilia reticulata*). Evolution. 66:3432-3443.

Ultsch GR, Ward GM, LeBerte CM, Kuhajda BR, Stewart ER. 2001. Intergradation and origins of subspecies of the turtle *Chrysemys picta*: morphological comparisons. Can J Zool. 79:485-498.

Urban MC, Richardson JL, Freidenfelds NA. 2014. Plasticity and genetic adaptation mediate amphibian and reptile responses to climate change. Evol Appl. 7:88-103.

Wang J. 2017. The computer program structure for assigning individuals to populations: easy to use but easier to misuse. Mol Ecol Resour. 17:981-990.

Weir BS, Cockerham CC. 1984. Estimating F-Statistics for the Analysis of Population Structure. Evolution. 38:1358-1370.

Wickham H. 2016. ggplot2: Elegant Graphics for Data Analysis. New York: Springer.

Wickham H, François R, Henry L, Müller K. 2018. dplyr: A Grammar of Data Manipulation. v. 0.7.5. https://cran.r-project.org/package=dplyr

Zheng X, Levine D, Shen J, Gogarten SM, Laurie C, Weir BS. 2012. A high-performance computing toolset for relatedness and principal component analysis of SNP data. Bioinformatics. 28:3326-3328.

Tables and Figures

Table 1: Sampling information for painted turtle (*Chrysemys picta*) hatchlings in this study, arranged by longitude from east to west.

Sampling Location	Location Abbr.	N	Final N (Post-Filtering)	Location Description	Longitude	Latitude
Illinois	IL	38	37	Thomson Causeway Recreation Area	-90.116389	41.94806
Minnesota	MN	30	30	Tamarac National Wildlife Refuge	-95.6483095	46.956219
Kansas	KS	5	5	Ross National History Area	-96.20854	38.294774
Nebraska	NE	27	27	Crescent Lake National Wildlife Refuge	-102.436622	41.761369
New Mexico	NM	12	12	Bosque del Apache National Wildlife Refuge	-106.89174	33.7818896
Idaho	ID	30	30	Round Lake State Park	-116.644995	48.1625864
Oregon	OR	22	20	Smith & Bybee Wetlands Nature Area	-122.726986	45.6203489
Total		164	161			

Abbreviation for sampling locations, sample size of sequencing (N) and after filtering (Final N).

Table 2: Summary genomic statistics for painted turtle sampling locations.

Location	% Missing	Private Alleles	% Poly	H_E	H_O	F_{IS}	π*
IL	4.00	9596	86.79	0.1765	0.1683	0.0511	0.0026
MN	4.95	797	66.47	0.1481	0.1395	0.0606	0.0023
KS	2.76	173	41.32	0.1323	0.1410	0.0235	0.0022
NE	7.21	951	52.84	0.1344	0.1274	0.0581	0.0021
NM	3.67	946	35.91	0.1096	0.1079	0.0477	0.0017
ID	3.47	170	31.67	0.0941	0.0930	0.0257	0.0016
OR	4.92	104	31.02	0.0855	0.0835	0.0373	0.0014
Average	4.43	1820	49.43	0.1258	0.1229	0.0434	0.0020

The average percentage of missing genotypes per individual, number of SNPs unique (private) to each population, percentage of polymorphic SNP loci, expected (H_E) and observed (H_O) heterozygosity, inbreeding coefficient (F_{IS}), and average nucleotide diversity (π). *All statistics, with the exception of π, use the final 48,060 SNP dataset. π was calculated with the block-filtered dataset containing 566,852 variant and 37,832,754 invariant sites.

Table 3: Pairwise F_{ST} and d_{xy} across all painted turtle sampling locations.

Location	IL	MN	KS	NE	NM	ID	OR
IL	–	0.0026	0.0026	0.0026	0.0026	0.0025	0.0025
MN	0.0403	–	0.0024	0.0024	0.0024	0.0022	0.0022
KS	0.0572	0.0514	–	0.0023	0.0024	0.0022	0.0022
NE	0.0890	0.0713	0.0745	–	0.0023	0.0022	0.0021
NM	0.1584	0.1644	0.1818	0.1875	–	0.0022	0.0022
ID	0.1562	0.1500	0.1941	0.1674	0.2892	–	0.0016
OR	0.1617	0.1616	0.2201	0.1828	0.3106	0.0914	–

Pairwise F_{ST} estimates among locations are below the diagonal, and interpopulation nucleotide diversity estimates (d_{xy}) are above the diagonal. Pairwise F_{ST} were calculated with the final filtered dataset of 48,060 SNPs; d_{xy} was calculated with the block-filtered dataset containing 566,852 variant and 37,832,754 invariant sites.

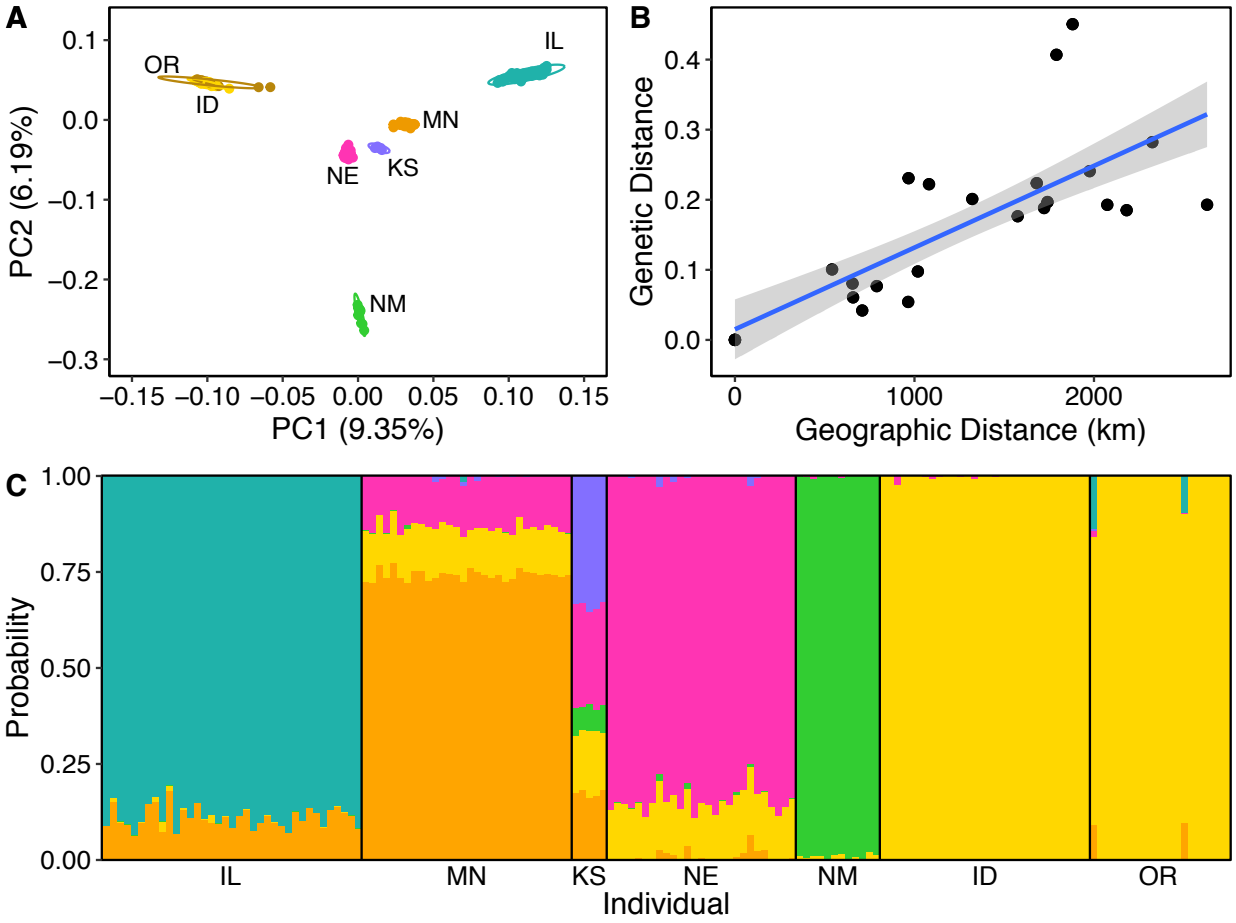

Figure 1: Population genomic structure among sampled painted turtle populations demonstrates distinct clustering consistent with isolation by distance. A) Principal components analysis (PCA) of genetic variation, depicted with 95% confidence ellipses. B) Relationship between straight-line geographic distance in kilometers and genetic distance, $F_{ST}/(1-F_{ST})$ for each pairwise population comparison, with 95% confidence interval shown in grey. C) STRUCTURE results for individual assignments of K=6 groupings.

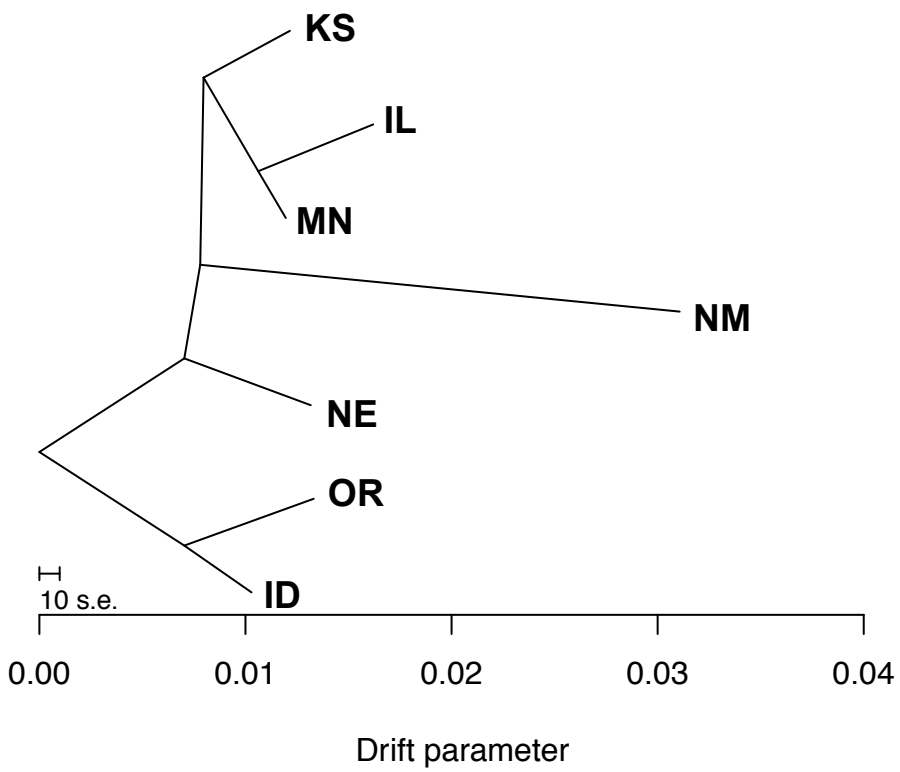

Figure 2: Genetic variation among painted turtle populations is explained at least in part by genetic drift. TreeMix results of the tree that best explains allelic covariance among individuals with no migration; s.e. is standard error.

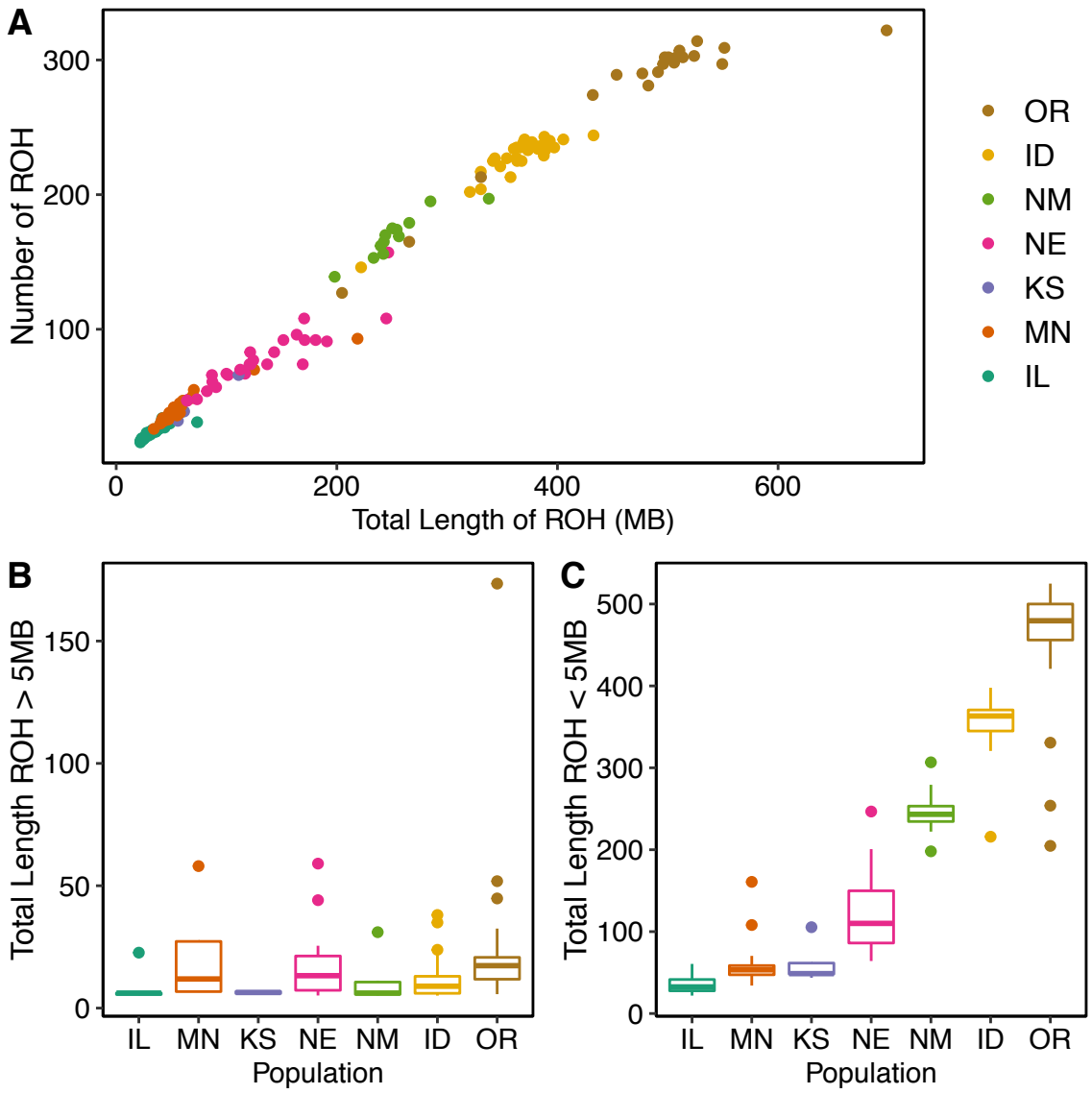

Figure 3: Patterns of runs of homozygosity (ROH) vary across populations of painted turtles consistent with founder effects. A) Relationship between the total length of all ROH in megabases (MB) and number of ROH in each individual, colored by population. B) Boxplot of total ROH length in MB including only ROH greater than 5 MB for each population. C) Boxplot of total ROH length in MB including only ROH less than 5 MB for each population.

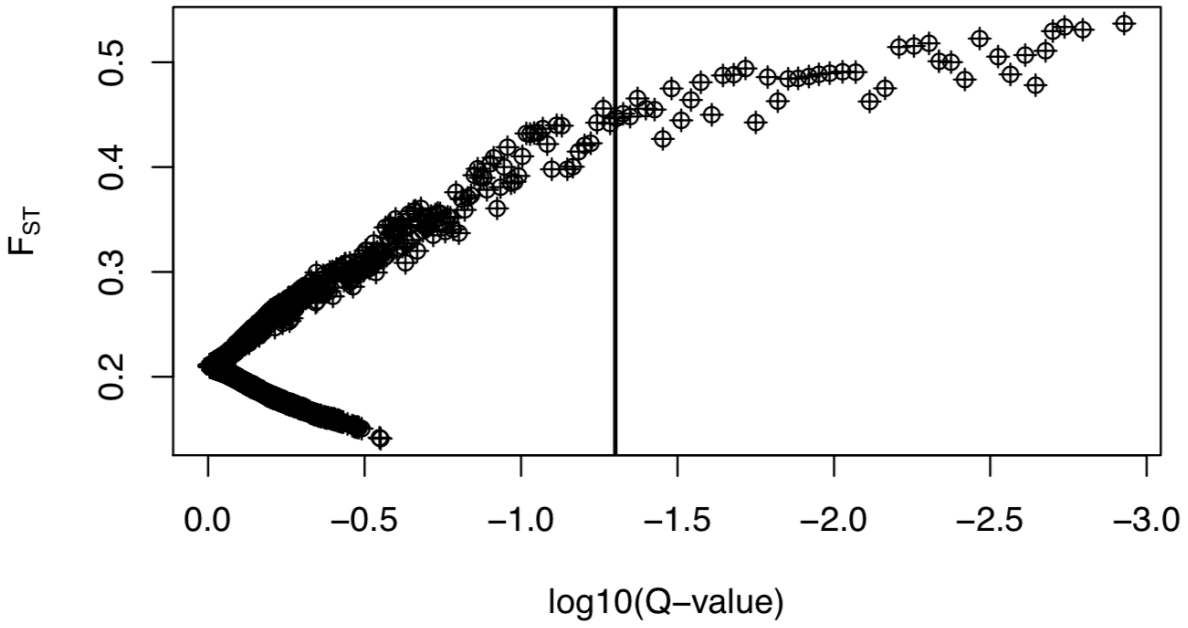

Figure 4: 43 F_{ST} outlier loci were identified across painted turtle individuals at the 0.05 false discovery rate (FDR), denoted by the grey vertical line. $\log_{10}$(Q-value) is a logarithmic decision factor to determine selection in BayeScan.

Supplemental Material

Supplementary Table 1: Filtering steps and their results on the number of SNPs and individuals included in the dataset.

Filtering Step	Number of SNPs Retained	Number of Monomorphic Sites Retained	Number of Individuals Retained
Joint Genotyping	3542834	607318979	164
SNPs Only	3527082	—	164
GATK Variant Filtration	2477216	—	164
Depth > 2X	—	—	161
Mean GQ > 20.0	824960	—	161
Biallelic Sites	809741	—	161
Remove Indels	794654	605549873	161
HWE	703974	—	161
Fixed for Non-Ref Allele	701364	—	161
Missingness < 25%	614281	40932105	161
Depth Filter & Block Filter	566852	37832754	161
SNP Missingness < 10%	253365	—	161
MAF > 1/(2*n)	212670	—	161
One SNP per block	48060	—	161

Supplementary Table 2: F_{ST} outliers identified with a false discovery rate of 0.05 in BayeScan.

prob	log10.PO.	qval	alpha	fst	Chromosome/ Scaffold	Position	Gene	In CDS?
0.95321	1.309	0.016301	1.5628	0.48586	NC_024219.1	19224187	UBE2E2	N
0.91531	1.0337	0.024584	1.3679	0.44993	NC_024219.1	33070667	CRTAP	N
0.99882	2.9276	0.00118	1.8408	0.53687	NC_024220.1	25457941	LCLAT1	N
0.99225	2.1073	0.0038109	1.5536	0.48348	NC_024224.1	6076538	LOC101952333	N
0.99531	2.3268	0.002725	1.5802	0.48842	NC_024224.1	6076727	LOC101952333	N
0.98411	1.7919	0.0062019	1.7198	0.5145	NC_024225.1	24993581	TNR	N
0.96416	1.4298	0.013027	1.5574	0.48463	NW_007281338.1	11729335	-	
0.99798	2.6938	0.0016	1.8098	0.53107	NW_007281344.1	10569480	-	
0.96921	1.498	0.012035	1.5673	0.48639	NW_007281363.1	319850	-	
0.97088	1.523	0.011182	1.5787	0.48849	NW_007281363.1	426599	MARCH1	N
0.96219	1.4056	0.014018	1.5551	0.48423	NW_007281363.1	427308	MARCH1	N
0.88078	0.86851	0.03745	1.3906	0.45484	NW_007281363.1	427637	MARCH1	N
0.97417	1.5765	0.0093936	1.5917	0.4909	NW_007281394.1	3393798	TMEM68	N
0.9765	1.6186	0.0085285	1.5903	0.49059	NW_007281394.1	3393806	TMEM68	N
0.99751	2.6027	0.001995	1.8022	0.52966	NW_007281451.1	398299	LRRC7	N
0.89668	0.93845	0.030786	1.3375	0.44457	NW_007281481.1	1723112	SCAP	N
0.99028	2.0081	0.0049722	1.7394	0.51807	NW_007281500.1	2117699	-	
0.94188	1.2097	0.019178	1.6065	0.49405	NW_007281500.1	2170929	-	
0.98627	1.8563	0.0055561	1.7252	0.51549	NW_007281543.1	887784	-	
0.99071	2.0279	0.004607	1.6466	0.50092	NW_007281613.1	318103	-	
0.85354	0.7655	0.049486	1.344	0.44659	NW_007281615.1	773628	-	
0.85986	0.78786	0.044837	1.3528	0.44814	NW_007281615.1	773761	-	
0.90542	0.98105	0.028653	1.4418	0.464	NW_007281633.1	763107	-	
0.88629	0.89177	0.03524	1.2428	0.42688	NW_007281645.1	690474	LRP1	N
0.99771	2.6392	0.00183	1.8236	0.53369	NW_007281680.1	425400	-	
0.94209	1.2113	0.017787	1.3316	0.44257	NW_007281756.1	175648	ZNF436 - like	N
0.99494	2.2936	0.0029845	1.6706	0.50533	NW_007282845.1	22035	RDH-E2 - like	N
0.92851	1.1135	0.020922	1.5737	0.48814	NW_007359844.1	1257506	ZNF521	N
0.92564	1.0951	0.022645	1.5697	0.48745	NW_007359844.1	1257525	ZNF521	N
0.85992	0.78808	0.042454	1.4462	0.46549	NW_007359849.1	1806459	PPM1D	N
0.99648	2.4519	0.0024443	1.6785	0.50683	NW_007359852.1	1233571	-	
0.98243	1.7475	0.0068707	1.5083	0.47513	NW_007359859.1	9669370	SORCS2	N
0.99746	2.5941	0.002104	1.7004	0.51092	NW_007359868.1	7610047	-	
0.90708	0.98953	0.026655	1.5326	0.48086	NW_007359868.1	8719663	MBOAT2	N
0.99693	2.5115	0.002265	1.5256	0.47812	NW_007359883.1	6525921	-	
0.865	0.80668	0.039951	1.3934	0.45567	NW_007359884.1	12929080	-	
0.99269	2.1329	0.003417	1.7637	0.52258	NW_007359899.1	14551614	CASKIN1	N
0.97826	1.6532	0.0076967	1.4412	0.46253	NW_007359899.1	15610177	RBBP6	Y
0.88737	0.89645	0.03306	1.4993	0.47495	NW_007359903.1	2265693	SIM2	N
0.97098	1.5245	0.010328	1.5844	0.48958	NW_007359904.1	4918299	-	
0.95712	1.3487	0.015128	1.4407	0.46286	NW_007359905.1	1859521	-	
0.99132	2.0577	0.0042167	1.6424	0.50007	NW_007359906.1	3611486	NTRK3	N
0.85686	0.77714	0.047177	1.3673	0.45092	NW_007359909.1	1746941	PPM1K	N

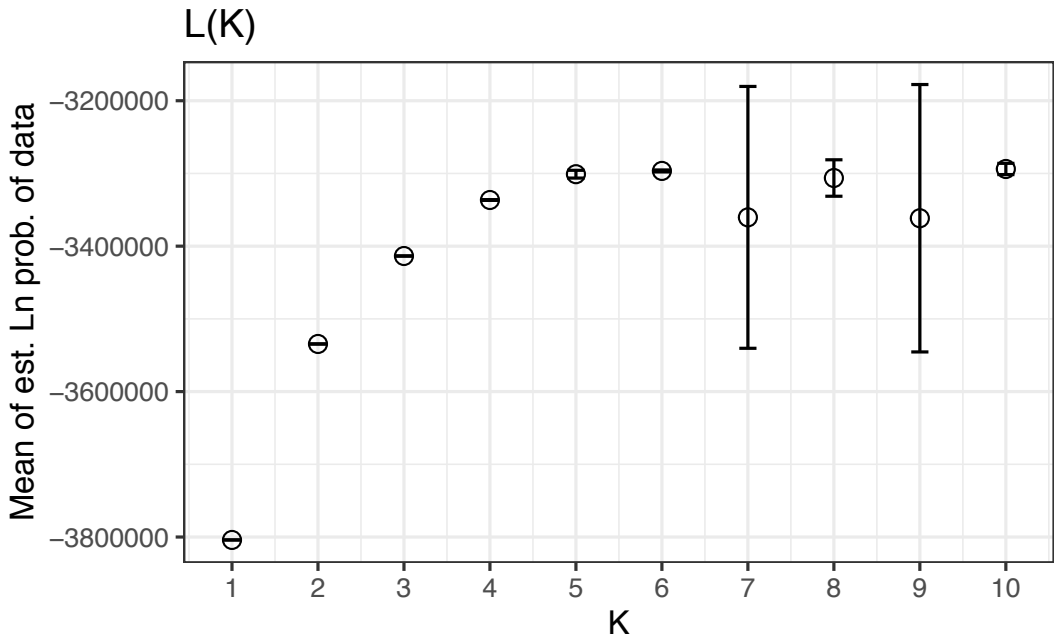

Figure S1: Plot of mean likelihoods for each value of K, with bars indicating standard deviation. This analysis suggests the best K of the genetic data is K=5 or K=6.

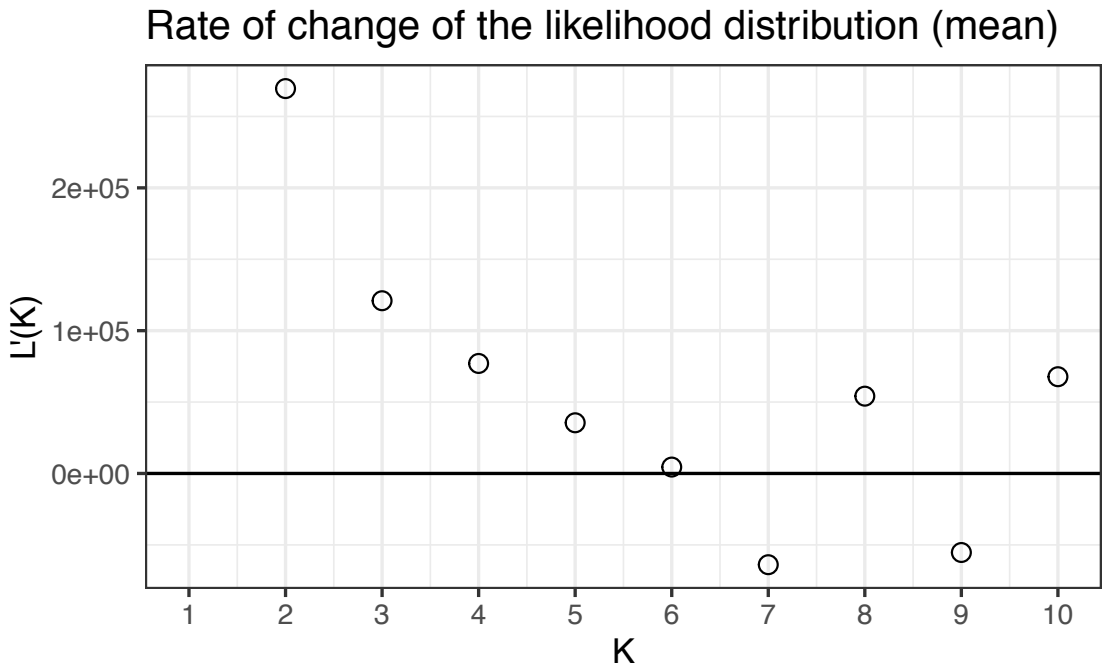

Figure S2: Plot of the mean rate of change of the likelihood distribution across replicates for each run of K.

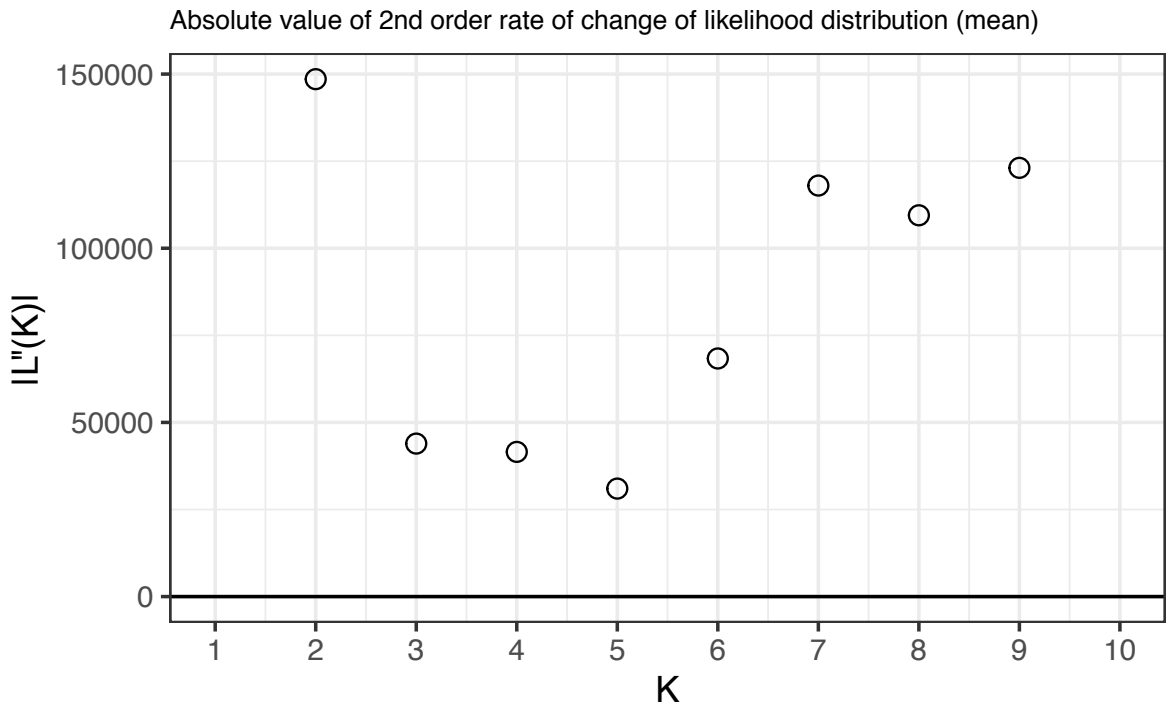

Figure S3: Plot of the absolute value of the second order mean rate of change of the likelihood distribution across replicates for each run of K.

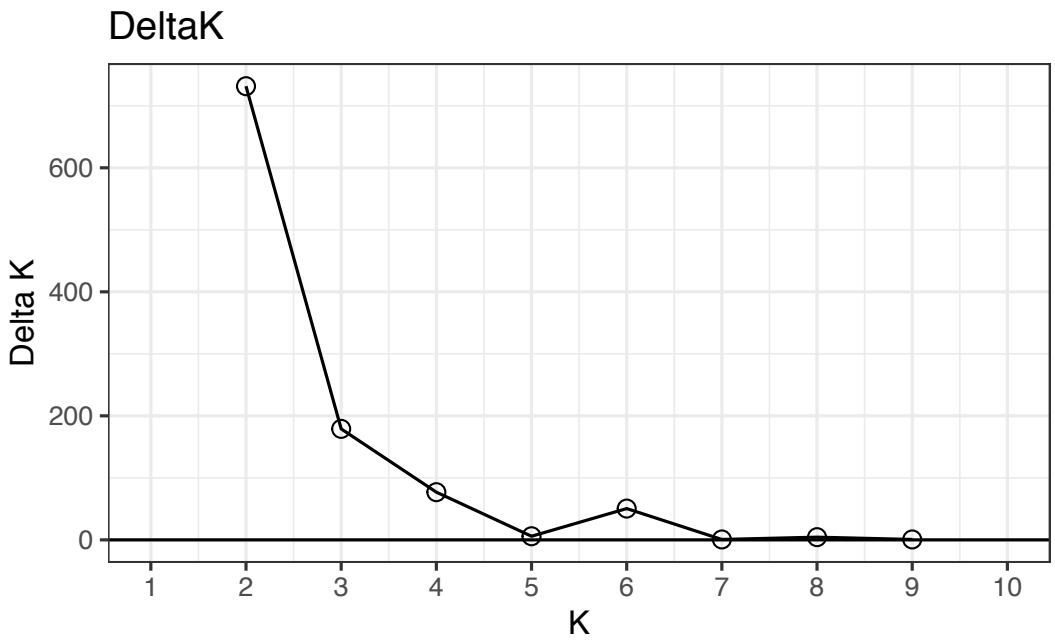

Figure S4: Plot of ΔK. The highest ΔK value suggests two genetic groups in the sampled individuals (Evanno et al. 2005).

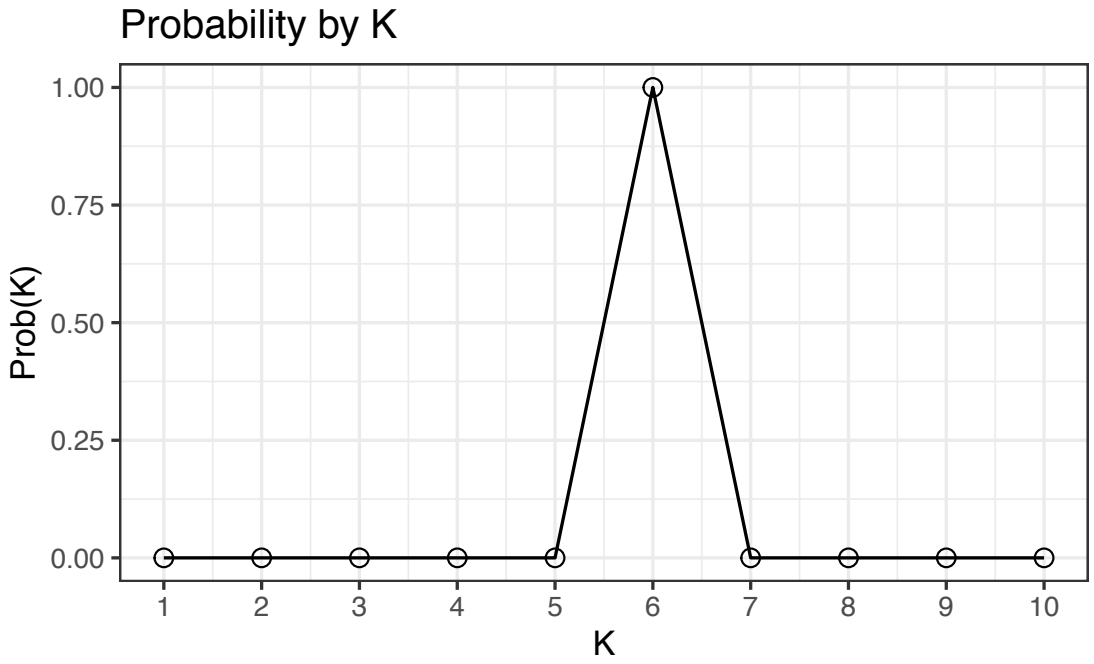

Figure S5: Plot of probability for each K (Pritchard et al. 2000) suggests that the best number of groups in the genetic data is K=6.

CHAPTER 5. GENOMIC ARCHITECTURE UNDERLIES TWO DISTINCT LIFE-HISTORY STRATEGIES IN THE WESTERN TERRESTRIAL GARTER SNAKE (*THAMNOPHIS ELEGANS*)

Jessica M. Judson and Anne M. Bronikowski

Department of Ecology, Evolution, and Organismal Biology, Iowa State University, Ames, Iowa, USA

Modified from a manuscript to be submitted to *Molecular Ecology*

Abstract

Selection has shaped the evolution of life-history traits across organisms, and some species demonstrate distinct life-history strategies among populations consistent with extrinsic mortality imposed by their environments. Though life-history variation has been well documented for many decades, the genomic underpinnings of this variation are only now open to investigation in organisms with few genomic resources. New questions regarding the patterns of genomic variation associated with life-history divergence, the impact of gene flow on maintenance of these life-history traits, and the influence of genes of large or small effect can now be investigated in these non-model organisms. Western terrestrial garter snakes (*Thamnophis elegans*) in California have been the subject of >40 years of long-term monitoring, and populations exhibit one of two life-history strategies: a slow-paced strategy with longer lifespan and older age at maturity (M-slow), and a fast-paced strategy with faster growth and maturation with shorter lifespan (L-fast). This study investigated the genomic differences between the two life-history strategies and across 11 populations using genome resequencing of 121 snakes. Gene flow was abundant across populations, and levels of divergence across the

genome were low on average. However, localized regions of the genome were highly differentiated among M-slow and L-fast populations, and these regions showed genomic patterns consistent with inversions containing genes related to metabolic function, DNA damage repair pathways, and color, which all vary among life-history strategies. These results are consistent with strong selection in the face of gene flow and the reduction of recombination in regions important to producing the distinct phenotypes observed in each life-history strategy. Further, the large divergence within putative inversions across the genome suggest strong selection on these genes of large effect, or "supergenes", which allow suites of genes important for differences in life-history strategy to be inherited together as large genomic blocks. This study provides the first evidence of the role of inversions in the evolution of life-history traits in a reptile and adds to the increasing evidence that inversions are a widespread mechanism reducing recombination at ecologically relevant genes across the genome.

Introduction

The genetic underpinnings of life-history evolution have been the subject of decades of research, particularly in model organisms, as the genetic contributions to life-history variation provide insight into evolutionary responses to natural selection (Stearns, 1992; Charlesworth, 1994). Discrete life-history strategies among populations are often consistent with divergence in selection induced by environmental conditions experienced by each population. For example, predation pressure is strongly associated with divergent life-history strategies of Trinidadian guppy populations (Reznick, 1982), such that populations with higher predation pressure exhibit shorter lifespans and faster development than populations with low predation pressure. Additionally, this predation pressure has contributed to parallel evolution of life-history traits even when the predators are different species across drainages (Reznick et al., 1996). Thus, local

adaptation to environmental variation can include adaptation through the evolution of life-history traits, including lifespan, age and size at maturity, and reproductive output. With rapidly expanding genomic resources, we can now more deeply assess the relationships among population genomic variation and life-history divergence across the tree of life. Thus, genomic data from populations with discrete life-history strategies can address whether adaptation occurs through standing genetic variation, whether variants of large or small effect contribute to life-history evolution, and how life-history variation is maintained in populations with migration.

Metapopulation dynamics can shape life-history evolution, as migration and subsequent gene flow can hinder local adaptation and homogenize variation among populations. Contemporary gene flow from invasive to native populations can alter the life-history traits of these populations when the variation has a genetic basis (Bolstad et al., 2017), and gene flow among populations of the same species can hinder adaptive responses to local environments (Bisschop et al., 2019). Despite the theoretical expectations that gene flow hinders local adaptation (Kawecki and Ebert, 2004), a growing body of evidence demonstrates that gene flow can be overcome or even prevented by strong selection and changes in genomic architecture, including inversions and reduced recombination in regions of the genome important to adaptive variation (reviewed in Tigano and Friesen, 2016). Reduced recombination between genomic regions important to locally adapted phenotypes allows the inheritance of suites of linked genes, even in offspring that result from gene flow among populations. The transfer of these ‘supergenes’ to migrant offspring can facilitate rapid adaptation to these distinct environments (e.g., Joron et al., 2011).

Reptiles exhibit multiple traits that make them particularly informative for understanding life-history evolution. Reptiles continue growth after initial reproductive bouts, unlike avian

reptiles and mammals, and often exhibit increasing reproductive output with advancing age (reviewed in Hoekstra et al., 2020). However, genomic resources for reptiles still lag behind those of other vertebrate groups, and longitudinal studies of reptiles to understand life-history traits are often logistically difficult (McDiarmid et al., 2012; Reinke et al., 2019). New genomic resources offer the opportunity to identify the genomic underpinnings of life-history variation among populations of reptiles that have been the subject of long-term monitoring. Populations of western terrestrial garter snakes (*Thamnophis elegans*) surrounding Eagle Lake in California, USA have been monitored for multiple decades, exhibit growth after initial reproductive bouts, and increased reproductive output with size. Additionally, populations display one of two distinct life-history strategies, which are associated with divergent environmental conditions including elevation, predation pressure, and prey availability (Bronikowski and Arnold, 1999; Sparkman et al., 2013). This study assessed genomic differentiation among populations of western terrestrial garter snakes, with particular focus on divergence between the two life-history strategies, to understand the genomic determinants of life history and how this variation is maintained in this metapopulation of reptiles.

Methods

Study Organism

Western terrestrial garter snakes from the vicinity of Eagle Lake (Lassen County) in California, USA have been the subject of over four decades of research on the evolution and ecology of behavior and life-histories (Arnold, 1981; Kephart and Arnold, 1982). These populations are characterized by two distinct life-history strategies: “slow-pace-of-life” meadow populations and “fast-pace-of-life” lakeshore populations (“M-slow” and “L-fast” hereafter). M-slow individuals exhibit slower growth and maturation, longer lifespans, smaller adult body size,

and smaller litters than L-fast individuals (reviewed in Schwartz et al., 2015). M-slow and L-fast populations also differ in additional phenotypes, including color and stripe patterns (Manier et al., 2007), metabolic physiology (e.g., Bronikowski and Vleck, 2010; Schwartz and Bronikowski, 2013; Gangloff et al., 2020), stress physiology (Palacios et al., 2012), and immune function (reviewed in Palacios et al., 2020). Life-history divergence in these snakes is consistent with both selection on L-fast populations to mature early due to higher extrinsic mortality through predation (Miller et al., 2011) and selective pressure on M-slow populations to delay maturation due to highly variable and unpredictable prey availability (Robert and Bronikowski, 2010). Laboratory common-garden and reciprocal transplant experiments found that both significant genetic and environmental variation contribute to this life-history phenotypic variation (Bronikowski, 2000; Gangloff et al., 2015). Further supporting a role of genetic divergence in maintaining life-history traits, mitochondrial genome sequences revealed two variants that segregate between the life-history strategies, including a nonsynonymous variant in the Cytochrome B gene (Schwartz et al., 2015). These mitochondrial haplotypes were indeed associated with variation in whole-organism metabolic rate (Gangloff et al., 2020). However, low neutral divergence measured with microsatellite loci (Manier and Arnold, 2005; Manier et al., 2007; Gangloff et al. In revision) and a large degree of plasticity across all life-history traits within populations (Miller et al., 2014) suggest life-history divergence may have complex genetic and environmental components. Low divergence among microsatellite loci suggests gene flow among populations, yet strong selection on certain genes and genomic architecture (e.g., inversions) may contribute to genetic divergence among life-history strategies despite gene flow. Whole genome sequencing thus can provide insight into the processes of selection that drive differentiation among life-history strategies in the face of gene flow.

Sample Collection and Genome Sequencing

We hand-captured 121 female garter snakes from 11 populations in the vicinity of Eagle Lake in Lassen Co., California from 2005 to 2019 (Table 1; Fig. 1). We drew a 150-350μL blood sample from the caudal vein of each individual with a heparin-rinsed syringe and centrifuged samples to isolate red blood cells. We snap-froze blood cells in liquid nitrogen before long-term storage at –80°C. We extracted DNA from blood cells using either a Qiagen DNeasy Blood and Tissue Kit (Qiagen, Germantown, MD) or a phenol-chloroform DNA extraction protocol (Sambrook et al., 1989; Judson et al. in prep). Prior to sequencing, we quantified DNA using a NanoDropTM 2000 Spectrophotometer and performed gel electrophoresis using a 1% agarose gel to assess DNA quality. For library preparation of DNA for whole genome re-sequencing, we prepared libraries of 250bp insert size and sequenced libraries on a DNBSEQ-G400 with 100bp paired-end reads.

Read Processing and Variant Calling

Following sequencing, we trimmed raw reads that contained adapter sequences, contained more than 10% unknown bases, or had more than 50% low quality bases ($Q \leq 12$) with cutadapt v2.5 (Martin, 2011). We downloaded the *Thamnophis elegans* reference genome from NCBI (Annotation Release 100, Bronikowski, 2020), which was sequenced and assembled from a female M-slow individual, and aligned reads to the reference genome using BWA-mem (Li, 2013) in bwa v0.7.17 (Li and Durbin, 2009; Li and Durbin, 2010). To assess sequence quality, we generated post-alignment statistics using FastQC v0.11.7 (Andrews, 2010), the stats algorithm in SAMtools v1.9 (Li et al., 2009), and calculated genome coverage statistics using BEDTools2 v.2.27.1 (Quinlan and Hall, 2010; Quinlan, 2014).

We used SAMtools v1.9 (Li et al., 2009) to remove unmapped reads, reads not in primary alignment, improperly paired reads, and reads with mapping quality (MAPQ) < 30 before merging all reads for each individual. We used a modified Sentieon DNAseq workflow (v 201808.01; https://support.sentieon.com/manual/DNAseq_usage/dnaseq/) to call variants across all sequenced garter snakes (Kendig et al., 2019). Using the Sentieon tools on each individual's merged reads, we first marked duplicate reads with –LocusCollector and removed these reads from downstream analyses with –Dedup. We then used the Realigner tool to realign reads around insertions and deletions (indels). Finally, we created genomic variant call format files (GVCFs) for each individual using the Haplotyper algorithm. We joint-called variants across all GVCFs using GVCFtyper with a minimum base quality > 20. As confident monomorphic site calls are also important for understanding population demographic structure (Pfeifer et al., 2018), we used the '–emit_mode confident' option of GVCFtyper to create a variant call format (VCF) file which includes both variant and invariant sites with a genotype quality of ≥ 30.

We used GATK v4.0.4.0 (McKenna et al., 2010; DePristo et al., 2011) to apply hard filtering to the VCF of variant and invariant sites. We first created VCFs containing only single nucleotide polymorphisms (SNPs), only indels and mixed sites, and only monomorphic sites, and then applied filters to these VCFs separately (Table S1). As all individuals had average depth greater than 18X across all unfiltered SNPs, we kept all *T. elegans* individuals in genomic analysis. We used VCFtools v0.1.14 (Danecek et al., 2011) and GATK v4.0.4.0 to further filter VCFs on the following criteria. We removed variants that were not biallelic and variants that were fixed for the non-reference allele, which would be indicative of errors in the reference genome. To avoid calling errors due to indels, we removed indels ± 3 base pairs upstream and downstream from the variant and invariant VCFs using a custom R script (R Core Team, 2020).

We then removed both variant and invariant sites with greater than 25% missing genotypes across individuals and removed variant sites with excess heterozygosity (ExcessHet > 20). We further filtered the SNP VCF by site sequencing depth to include only sites with mean depth across genotypes greater than 10X and less than 60X to exclude sites potentially in paralogous regions. We assigned genotypes with depth less than 4 or greater than 100 as missing data, and removed heterozygote genotypes using an allele balance threshold (depth of allele 1 / depth of allele 2) of less than 0.2 or greater than 4 using BCFtools v1.10 (Li et al., 2009) to prevent heterozygote calls based on biased allele depths, which may be technical errors. Then we removed sites with greater than 10% missing data. Finally, for ADMIXTURE, principal components analysis, and population genomic statistics, we filtered based on minor allele frequency (MAF) to remove singletons and retained one SNP in each non-overlapping window of 10KB to reduce linkage among SNPs. To account for different evolutionary rates of sex chromosomes, we limited our analyses to the defined autosomes in the reference genome, and thus filtered out undefined scaffolds and the Z chromosome from variant and invariant VCFs.

Population Genomic Analysis

We utilized the linkage-filtered autosomal dataset to calculate population genomic statistics and assess groupings among individuals. To evaluate population structure among the sampled individuals, we first assessed cluster membership using ADMIXTURE v1.3.0 (Alexander et al., 2009; Alexander and Lange, 2011) with 10 runs of each number of groupings (K) from K=1 to K=11 with cross validation to assess the best number of groupings. We further assessed genomic structuring among individuals by performing a principal components analysis (PCA) in PLINK v1.9 (Purcell and Chang; Purcell et al., 2007). From these analyses, we identified one individual from L4 (Table 1) that appeared to be a potentially mislabeled

individual and removed this individual from the following population genomic statistics, though we included this individual as an M-slow individual for later selection analyses. We used VCFtools v0.1.14 to assess average percent of missing genotypes and polymorphism across populations, the R package "vcfR" v1.12.0 (Knaus and Grünwald, 2017) to process VCFs in R, and "poppr" v2.8.7 (Kamvar et al., 2014) to calculate private alleles for each population. The R package "adegenet" v2.1.3 (Jombart and Ahmed, 2011) was used to calculate observed and expected heterozygosity, and "hierfstat" v0.5.7 (Goudet and Jombart, 2020) was used to calculate F_{IS}. To calculate F_{ST} and pairwise F_{ST}, we used "SNPRelate" v1.22.0 (Zheng et al., 2012), which uses Weir and Cockerham's F_{ST} estimate (Weir and Cockerham, 1984). We used the allele balance-filtered autosome variant dataset of 19,181,591 SNPs to calculate average nucleotide diversity (π) by site within each population in VCFtools v0.1.14, and then weight-averaged these values by the total number of variant and filtered invariant sites on the autosomes (1,271,159,831; Martin et al., 2018).

Detecting Candidate Regions of Selection on Life-History Strategies

To understand the regions of the genome likely under selection between the two life-history strategies, we first used genetic groupings identified from the first principal component of the PCA and the ADMIXTURE analysis to regroup populations into an "M-slow" genetic group and an "L-fast" genetic group. We removed four individuals that were intermediate between the two genetic groups (PC1 scores close to zero). Using these groupings, we analyzed the allele balance-filtered SNP VCF to calculate average pairwise F_{ST} between the two genetic groups across non-overlapping sliding windows of 20KB across autosomes using VCFtools v0.1.14. This size of sliding windows was an appropriate balance between revealing finer scale patterns across the chromosomes without obscuring larger scale patterns with extraneous points during

plotting. We excluded MAF and linkage filters to increase coverage of the genome, decrease bias from removing singletons, and assess linkage among regions with high F_{ST}. We identified windows with pairwise F_{ST} values in the top 1% of the distribution of pairwise F_{ST} and queried those windows against the reference genome to identify genes within those regions using BEDTools v2.27.1 (Quinlan and Hall, 2010; Quinlan, 2014). We assessed genotypic patterns of the highest outlier region, which motivated further study of genomic architecture between the life-history strategies.

In addition to this sliding window F_{ST} analysis, we used this same SNP set in the R package "lostruct" to identify regions of the genome with differential population structure without assigning individuals to pre-defined groupings (Li and Ralph, 2019). This method performs PCA of sliding windows across the genome and constructs a distance matrix based on these PCs. We used windows of 1000 SNPs for PCA and mapped distances using multidimensional scaling (MDS) in 1-dimensional space (Sparkman et al., 2009; Huang et al., 2020). To define outlier genomic windows, we used the same method of Huang et al. (2020) by assigning windows as outliers if the absolute value of the window is greater than four standard deviations from the mean for the first dimension. We clustered outlier regions that were adjacent to each other, forming clusters of outlier windows that had fewer than 4 windows between them. All clusters we used for further investigation contained at least 4 outlier windows (4,000 SNPs). This method of PCA in sliding windows is ideal for detecting inversions across the genome, but can also detect linked selection across regions. To distinguish between these alternatives, we used "SNPRelate" v1.22.0 to perform and plot a PCA of the SNPs within clusters identified from "lostruct". If the outlier windows correspond to inversions in the genome, there should be three distinct clusters along the first PC, corresponding with the two homozygote groups and the

heterozygotes intermediate between them (Huang et al., 2020). We clustered the genotypes of putative inversions using "kmeans" in R (Hartigan and Wong, 1979) on the first PC. Initial cluster centers were the maximum PC1 score, minimum PC1 score, and median PC1 score. As in Huang et al. (2020), we evaluated discreteness of the three clusters by comparing the proportion of between-cluster sum of squares over the total sum of squares. Finally, if the central cluster indeed corresponds to heterozygotes at an inversion, individuals within the middle cluster should have higher heterozygosity across SNPs in the inversion than either homozygote cluster. Thus, we plotted heterozygosity, the proportion of heterozygote genotypes across the putative inversion, of the three clusters to confirm higher heterozygosity of the middle cluster.

Results

121 female *T. elegans* were sequenced for this study (Table 1), with an average of > 464 million reads mapped per individual. These reads covered an average of 86% of the *T. elegans* reference autosomal genome at a depth of at least 15X. The final numbers of confident variant and invariant sites after filtering were 139,441 and 1,251,978,240, respectively (Table 2). This final variant set had only 0.9% missing sites on average across populations (Table 3).

Both ADMIXTURE and PCA indicate the major genetic groupings among individuals are largely consistent with life-history strategy. The first principal component (PC), accounting for 14% of the genetic variation, separated M-slow populations from L-fast populations with few exceptions (Fig. 2, Fig. 3). Individuals from two L-fast populations (L7 and L8) grouped with either M-slow or L-fast populations, with a few intermediate individuals, suggesting that these populations result from gene flow from M-slow populations nearby. Additionally, a few individuals from L6 also had intermediate positions on PC1, suggesting gene flow from an M-slow population(s). These L-fast populations are close to the mouth of creeks that flow through

meadows which were also sampled in this study (M6 and M8; Fig. 1). The position of these admixed individuals in the PCA is consistent with admixture between the M-slow and L-fast populations along these creeks. The second PC suggested genetic variation within the groupings of life-history strategy found from PC1, which is consistent with isolation by distance among M-slow populations and among L-fast populations, respectively. The ADMIXTURE cross-validation approach suggested the best number of groupings in the variant data was K=2 (Fig. 3, Fig. S1), which again was largely consistent with the division among populations in life-history strategy. Summary statistics for population private alleles, polymorphism, and heterozygosity are summarized in Table 3; M-slow populations had higher numbers of private alleles than L-fast populations, and two populations (M1 and M3) had the highest levels of polymorphism, even when including a population that seems to be the result of a zone of interbreeding between M-slow and L-fast populations (L8). Overall weighted F_{ST} and mean F_{ST} of the linkage-filtered dataset were 0.06 and 0.05, respectively. Pairwise F_{ST} results from this linkage-filtered dataset were largely similar to PCA and ADMIXTURE analyses; the largest divergence was between M-slow and L-fast populations, with other patterns of divergence consistent with distance among populations (Table 4). Similar to the PCA results, pairwise F_{ST} found the same two populations (L7 and L8) did not follow expectations according to their original assignment of life-history strategy as L-fast. Specifically, L8 showed low pairwise F_{ST} across all pairwise comparisons, while L7 exhibited lower pairwise F_{ST} with M-slow populations than with other L-fast populations, despite its classification as an L-fast population.

The sliding window F_{ST} analysis comparing individuals in the M-slow and L-fast genetic clusters from Figure 3 using 19,181,591 SNPs revealed that the overall mean Weir and Cockerham's F_{ST} across the genome was 0.02 between the genetic clusters. Plotting pairwise F_{ST}

across the genome between the M-slow and L-fast genetic groups, however, showed many regions with high divergence between the life-history strategies (Fig. 4). The 733 windows in the top 1% of pairwise F_{ST} values overlapped with 287 known unique genes (Table S2). We assessed functional categories of these genes using PANTHER v.16.0 (Mi et al., 2020) using the *Anolis carolinensis* database, and we found that of the 249 genes in our set found in the *A. carolinensis* database, most genes belong to the cellular (143) and metabolic process (77) functional categories (Table S3).

The lostruct analysis, which analyzes population structure in sliding windows across the genome and can find structural changes like inversions, found 17 clusters of outliers across the first dimension from MDS (Table S4). Putative inversions spanned large regions of the chromosome in some cases, up to 5,000kb for a single putative inversion on the first chromosome. Most putative inversions from the first MDS dimension were from the first chromosome, with the remaining clusters on the second, third, fourth, and tenth chromosome. These chromosomes also show high F_{ST} between genetic clusters in the sliding window analysis (Fig. 4). PCA and heterozygosity of the putative inversions support that these regions are likely outliers due to inversions, rather than linked selection (Fig. S2). Further, these putative inversions contained over 150 genes. We investigated function of these genes with STRING v11.0 (Szklarczyk et al., 2019) using *Homo sapiens* as the reference organism. According to STRING, the network of genes from these inversions had significantly more interactions than expected ($P < 0.001$), which would suggest that these proteins are more functionally related through similar pathways and cellular functions than expected. There were 14 genes associated with KEGG metabolic pathways, 5 with carbon metabolism, 4 with cancer pathways, 3 with cellular senescence, and 9 genes associated with pigmentation in mammals. We chose the

putative inversion with the highest pairwise F_{ST} between life-history strategies for further investigation, located on the first chromosome. We plotted the heterozygosity across individuals and found that consistent with an inversion, individuals were either homozygous for the reference from a M-slow individual, homozygous for the alternate alleles, or heterozygous at every site along that region. Further, aligning this region of the *T. elegans* reference with the draft genome of *Thamnophis sirtalis* (GCF_001077635.1), the most closely related species for which genome information is available, confirmed that the M-slow haplotype closely matches the *T. sirtalis* haplotype. Thus, consistent with earlier phylogeographic analyses (Bronikowski and Arnold, 2001) the M-slow haplotype is likely the ancestral orientation of this region, and L-fast individuals have the derived, inverted haplotype. This putative inversion contains a gene, RPAP1, that is differentially expressed between L-fast and M-slow individuals (T. Schwartz, unpublished data). L-fast individuals have lower expression of RPAP1 than M-slow.

Discussion

In this study, we investigated the genomic underpinnings of the life-history variation found in populations of western terrestrial garter snakes in Lassen Co., California. We found that gene flow among populations is frequent, with evidence of multiple creeks serving as corridors for migration from the high elevation meadows to the lower elevation lakeshore habitat. Despite gene flow, there are strongly diverged regions of the genome between populations of the two life-history strategies. These regions show signatures of inversions, which would allow these regions to be inherited as supergenes and prevent recombination from breaking up adaptive haplotypes, even with high gene flow among populations. Population genomic structure and putative inversions collectively suggest strong selection against individuals that are mismatched

for their habitat, and the genomes provide evidence that genes of large effect contribute to phenotypic and life-history divergence in this system of snakes.

We found evidence across analyses that the largest genomic divergence among populations of *T. elegans* was consistent with the life-history strategy. However, when averaging divergence across the genome between the genetic groups based on life-history strategy, average F_{ST} was very low (0.02). This result is consistent with past genetic studies using microsatellites, which found low genetic divergence among populations regardless of life-history strategy and thus concluded gene flow was abundant between geographically proximate populations (Manier and Arnold, 2005; Manes et al. unpublished data). The microsatellite allele frequencies also generally matched a pattern of isolation by distance, and Manier and Arnold (2005) concluded gene flow followed patterns of source-sink dynamics with M1 serving as a source of migrants for other populations. Our study also found evidence of genetic variation consistent with isolation by distance, reflected most clearly by the second PC in the PCA. However, this divergence accounted for less variation than the first PC, which aligned with expectations based on divergence in life-history strategy. As microsatellites only sample a small portion of the genome, and much of the divergence among individuals in this study was localized to specific regions of the genome (Fig. 4), it is not surprising that previous studies did not detect strong divergence associated with the influence of selection on population divergence.

Based on previous mark/recapture field efforts, coupled with analyses of microsatellite loci, one-directional movement from meadows to lakeshores has been documented (Bronikowski and Arnold, 1999; Bronikowski and Arnold, 2001; Manier and Arnold, 2005). However, using this genomic sampling, we were able to localize ongoing and recent gene flow among populations. First, the lakeshore population that genetically grouped more closely to other

meadow populations (L7) is at the mouth of a creek that flows directly from a meadow above it (Fig. 1), yet L7 physiologically groups with other L-fast populations with respect to hormonal profiles, immune function, and stress biology (Sparkman and Palacios, 2009; Sparkman et al., 2009; Schwartz and Bronikowski, 2013) Second, the L-fast populations with individuals intermediate on the first PC, L6 and L8, are populations that are close to creeks that empty into Eagle Lake from upper elevation meadows. Pine Creek flows through M6 emptying to the south of L6, and Merrill Creek empties into L7, which is just southeast of L8 (Fig. 1). Another creek (Papoose Creek) flows from M1 to L1; however, L1 was not sampled in the present study. Similar to L7, all of these lakeshore populations that receive meadow gene flow (L1, L6, and L8) group physiologically and morphologically with other L-fast populations (Manier et al., 2007; Bronikowski, 2008; Bronikowski and Vleck, 2010; Palacios et al., 2013; Addis et al., 2017).

Despite the migration among populations of snakes, and resulting low divergence on average across the genome between M-slow and L-fast genetic groups (F_{ST}=0.02), there are many regions of the genome that exhibit strong divergence between the two genetic groups, which are largely consistent with life-history strategy. These divergent regions also overlap with putative inversions across multiple chromosomes and contain many genes, which supports a role of strong selection in the maintenance of differences between populations. Further, these putative inversions contain genes associated with processes that diverge between the two life-history strategies, including color, metabolic physiology, and immune function (Manier et al., 2007; Gangloff et al., 2020; Palacios et al., 2020). For inversions with high fitness alleles to be favored in a population, as is suggested by these results, selection must be exceedingly strong compared to migration (Kirkpatrick and Barton, 2006). Selection would favor inversions if the alleles within these inversions are beneficial to fitness when they are inherited together, or prevent the

deleterious influence of alleles from separate selective backgrounds being inherited together, as inversions reduce recombination that would separate favorable allelic combinations (Kirkpatrick and Barton, 2006). In this system of garter snakes, multiple habitat characteristics between the two life-history strategies likely impose strong selection on individuals that are mismatched for their environment. Coloration of lakeshore snakes is grey with black patterning and a tan dorsal stripe, while meadow snakes are darker with a yellow dorsal stripe, and these colors blend well into the rocky lakeshore and grassy meadow habitats, respectively (Manier et al., 2007). Avian predators, with highly visual prey detection, are known predators of these snakes, and these avian predators are more abundant in lakeshore habitats (Sparkman et al., 2013). Thus, selection on individuals of mismatched coloration are likely under strong selection in lakeshore habitats, which is also supported by the higher mean mortality in L-fast populations (Miller et al., 2011). Another habitat difference is food availability: meadow habitats are highly variable in anuran abundance, which serves as the primary food source for M-slow animals, while lakeshore habitats are relatively consistent in availability of fish and leech prey (Kephart and Arnold, 1982). The lack of consistently available food in meadow habitats likely imposes strong selective pressures on fast-growing individuals in these meadow environments (Robert and Bronikowski, 2010), and L-fast snakes have higher mass-specific resting metabolic rates than M-slow snakes (Bronikowski and Vleck, 2010). This strong selective environment on individual phenotypes would support the presence of inversions that allow inheritance of many genes important for matching phenotype to habitat.

In addition to finding many putative inversions, the presence of many regions with high F_{ST} are consistent with the prediction that in systems with gene flow, alleles or genes of large effect on phenotype in local adaptation are more abundant due to their resistance to swamping

effects of migration (Yeaman and Otto, 2011). Inversions with large effects on phenotype have been found increasingly across species, specifically species that demonstrate large, canalized changes in phenotype in different environments, both biotic and abiotic. In *Heliconius* butterflies, mimicry wing pattern phenotypes are associated with an inversion containing at least 18 genes, which serves as a supergene controlling wing phenotype despite gene flow among morphs in sympatry (Joron et al., 2011). Japanese grenadier anchovies display freshwater and anadromous forms, which are distinguished by two large chromosomal inversions with many genes related to metabolism and osmoregulation (Zong et al., 2020). These inversions were concluded to be the potential driver of rapid parallel adaptive divergence in response to freshwater environments. With next-generation sequencing, a new appreciation of the role in inversions and other structural genomic changes has emerged (Schwander et al., 2014; Wellenreuther and Bernatchez, 2018; Wellenreuther et al., 2019; Mérot et al., 2020). However, this study represents the first evidence that genomic architecture plays a role in the divergence of two distinct-life history strategies in a reptile.

While this study provides strong evidence of inversions, future genomic resources could confirm the breakpoints of these inversions and compare recombination rates across populations. These include optical mapping and a reference genome of an L-fast individual. Evidence of gene flow between populations of different life-history strategies suggest that testcross mapping approaches may be possible even in this long-lived reptile, which could provide insight into recombination patterns at these regions including putative inversions. Future studies should focus on connecting genotypes at putative inversions in this study with gene expression and phenotypic information, including lifespan, reproductive output, physiology measures, and color, all of which are likely under strong selection given genomic patterns in this system.

Acknowledgements

This work was supported by grants from the National Science Foundation (IOS-1558071, IOS-0922528, DEB-0323379). We thank the people who participated in blood collection of the snakes from the Bronikowski, D. Miller, A. Sparkman, and S. Arnold lab groups. We also thank F. Janzen for comments on drafts of this manuscript and L. Hoekstra and S. McGaugh for feedback on approaches and analyses in this manuscript.

References

Addis, E. A., Gangloff, E. J., Palacios, M. G., Carr, K. E. and Bronikowski, A. M. (2017). Merging the "Morphology–Performance–Fitness" paradigm and life-history theory in the Eagle Lake garter snake research project. Integr. Comp. Biol. 57(2): 423-435.

Alexander, D. H. and Lange, K. (2011). Enhancements to the ADMIXTURE algorithm for individual ancestry estimation. BMC Bioinformatics 12(1): 1-6.

Alexander, D. H., Novembre, J. and Lange, K. (2009). Fast model-based estimation of ancestry in unrelated individuals. Genome Res. 19(9): 1655-1664.

Andrews, S. (2010). FastQC: a quality control tool for high throughput sequence data. v0.11.7. https://www.bioinformatics.babraham.ac.uk/projects/fastqc/.

Arnold, S. J. (1981). Behavioral variation in natural populations. I. Phenotypic, genetic and environmental correlations between chemoreceptive responses to prey in the garter snake, *Thamnophis elegans*. Evolution 35(3): 489-509.

Bisschop, K., Mortier, F., Etienne, R. S. and Bonte, D. (2019). Transient local adaptation and source-sink dynamics in experimental populations experiencing spatially heterogeneous environments. Proc. R. Soc. B. 286(1905): 20190738.

Bolstad, G. H. et al. (2017). Gene flow from domesticated escapes alters the life history of wild Atlantic salmon. Nat. Ecol. Evol. 1(5): 1-5.

Bronikowski, A. (2020). *Thamnophis elegans* (Western terrestrial garter snake). Accession GCA_009769535.1. https://www.ncbi.nlm.nih.gov/assembly/GCF_009769535.1.

Bronikowski, A. and Vleck, D. (2010). Metabolism, body size and life span: A case study in evolutionarily divergent populations of the garter snake (*Thamnophis elegans*). Integr. Comp. Biol. 50(5): 880-887.

Bronikowski, A. M. (2000). Experimental evidence for the adaptive evolution of growth rate in the garter snake *Thamnophis elegans*. Evolution 54(5): 1760-1767.

Bronikowski, A. M. (2008). The evolution of aging phenotypes in snakes: a review and synthesis with new data. Age 30(2-3): 169-176.

Bronikowski, A. M. and Arnold, S. J. (1999). The evolutionary ecology of life history variation in the garter snake *Thamnophis elegans*. Ecology 80(7): 2314-2325.

Bronikowski, A. M. and Arnold, S. J. (2001). Cytochrome b phylogeny does not match subspecific classification in the western terrestrial garter snake, *Thamnophis elegans*. Copeia 2001(2): 508-513.

Charlesworth, B. (1994). Evolution in age-structured populations: Cambridge University Press Cambridge.

Danecek, P. et al. (2011). The variant call format and VCFtools. Bioinformatics 27(15): 2156-2158.

DePristo, M. A. et al. (2011). A framework for variation discovery and genotyping using next-generation DNA sequencing data. Nat. Genet. 43(5): 491-498.

Gangloff, E. J., Vleck, D. and Bronikowski, A. M. (2015). Developmental and immediate thermal environments shape energetic trade-offs, growth efficiency, and metabolic rate in divergent life-history ecotypes of the garter snake *Thamnophis elegans*. Physiol. Biochem. Zool. 88(5): 550-563.

Gangloff, E. J., Schwartz, T. S., Klabacka, R., Huebschman, N., Liu, A.-Y. and Bronikowski, A. M. (2020). Mitochondria as central characters in a complex narrative: Linking genomics, energetics, and pace-of-life in natural populations of garter snakes. Exp. Gerontol. 137: 110967.

Goudet, J. and Jombart, T. (2020). hierfstat: Estimation and tests of hierarchical F-statistics. https://CRAN.R-project.org/package=hierfstat

Hartigan, J. A. and Wong, M. A. (1979). A K-means clustering algorithm. J. Roy. Stat. Soc. Ser. C. (Appl. Stat.) 28(1): 100-108.

Hoekstra, L. A., Schwartz, T. S., Sparkman, A. M., Miller, D. A. and Bronikowski, A. M. (2020). The untapped potential of reptile biodiversity for understanding how and why animals age. Funct. Ecol. 34: 38-54.

Huang, K., Andrew, R. L., Owens, G. L., Ostevik, K. L. and Rieseberg, L. H. (2020). Multiple chromosomal inversions contribute to adaptive divergence of a dune sunflower ecotype. Mol. Ecol. 29(14): 2535-2549.

Jombart, T. and Ahmed, I. (2011). adegenet 1.3-1: new tools for the analysis of genome-wide SNP data. Bioinformatics 27(21): 3070-3071.

Joron, M. et al. (2011). Chromosomal rearrangements maintain a polymorphic supergene controlling butterfly mimicry. Nature 477(7363): 203-206.

Kamvar, Z. N., Tabima, J. F. and Grünwald, N. J. (2014). Poppr: an R package for genetic analysis of populations with clonal, partially clonal, and/or sexual reproduction. PeerJ 2: e281.

Kawecki, T. J. and Ebert, D. (2004). Conceptual issues in local adaptation. Ecol. Lett. 7(12): 1225-1241.

Kendig, K. I., et al. (2019). Sentieon DNASeq variant calling workflow demonstrates strong computational performance and accuracy. Front. Genet. 10: 736.

Kephart, D. G. and Arnold, S. J. (1982). Garter Snake Diets in a Fluctuating Environment: A Seven-Year Study. Ecology 63(5): 1232-1236.

Kirkpatrick, M. and Barton, N. (2006). Chromosome Inversions, Local Adaptation and Speciation. Genetics 173(1): 419-434.

Knaus, B. J. and Grünwald, N. J. (2017). vcfr: a package to manipulate and visualize variant call format data in R. Mol. Ecol. Resour. 17(1): 44-53.

Li, H. (2013). Aligning sequence reads, clone sequences and assembly contigs with BWA-MEM. ArXiv 1303.3997v1 [q-bio.GN].

Li, H. and Durbin, R. (2009). Fast and accurate short read alignment with Burrows-Wheeler transform. Bioinformatics 25(14): 1754-1760.

Li, H. and Durbin, R. (2010). Fast and accurate long-read alignment with Burrows-Wheeler transform. Bioinformatics 26(5): 589-595.

Li, H. and Ralph, P. (2019). Local PCA shows how the effect of population structure differs along the genome. Genetics 211(1): 289-304.

Li, H. et al. (2009). The Sequence Alignment/Map format and SAMtools. Bioinformatics 25(16): 2078-2079.

Manier, M. K. and Arnold, S. J. (2005). Population genetic analysis identifies source-sink dynamics for two sympatric garter snake species (*Thamnophis elegans* and *Thamnophis sirtalis*). Mol. Ecol. 14(13): 3965-3976.

Manier, M. K., Seyler, C. M. and Arnold, S. J. (2007). Adaptive divergence within and between ecotypes of the terrestrial garter snake, *Thamnophis elegans*, assessed with FST-QST comparisons. J. Evol. Biol. 20(5): 1705-1719.

Martin, H. C. et al. (2018). Insights into Platypus Population Structure and History from Whole-Genome Sequencing. Mol. Biol. Evol. 35(5): 1238-1252.

Martin, M. (2011). Cutadapt removes adapter sequences from high-throughput sequencing reads. EMBnet J. 17(1): 10-12.

McDiarmid, R. W., Foster, M. S., Guyer, C., Chernoff, N. and Gibbons, J. W. (2012). Reptile biodiversity: standard methods for inventory and monitoring. Univ of California Press.

McKenna, A. et al. (2010). The Genome Analysis Toolkit: a MapReduce framework for analyzing next-generation DNA sequencing data. Genome Res. 20(9): 1297-1303.

Mérot, C., Oomen, R. A., Tigano, A. and Wellenreuther, M. (2020). A roadmap for understanding the evolutionary significance of structural genomic variation. Trends Ecol. Evol. 35(7): 561-572.

Mi, H., Ebert, D., Muruganujan, A., Mills, C., Albou, L.-P., Mushayamaha, T. and Thomas, P. D. (2020). PANTHER version 16: a revised family classification, tree-based classification tool, enhancer regions and extensive API. Nucleic Acids Res. 49(D1): D394-D403.

Miller, D. A., Clark, W. R., Arnold, S. J. and Bronikowski, A. M. (2011). Stochastic population dynamics in populations of western terrestrial garter snakes with divergent life histories. Ecology 92(8): 1658-1671.

Miller, D. A., Janzen, F. J., Fellers, G. M., Kleeman, P. M. and Bronikowski, A. M. (2014). Biodemography of ectothermic tetrapods provides insights into the evolution and plasticity of mortality patterns. In Sociality, Hierarchy, Health: Comparative Biodemography: A Collection of Papers. Weinstein, M. and Lane, M. A., eds. Washington, D.C.: The National Academies Press.

Palacios, M. G., Sparkman, A. M. and Bronikowski, A. M. (2012). Corticosterone and pace of life in two life-history ecotypes of the garter snake *Thamnophis elegans*. Gen. Comp. Endocrinol. 175(3): 443-448.

Palacios, M. G., Cunnick, J. E. and Bronikowski, A. M. (2013). Complex interplay of body condition, life history, and prevailing environment shapes immune defenses of garter snakes in the wild. Physiol. Biochem. Zool. 86(5): 547-558.

Palacios, M. G., Gangloff, E. J., Reding, D. M. and Bronikowski, A. M. (2020). Genetic background and thermal environment differentially influence the ontogeny of immune components during early life in an ectothermic vertebrate. J. Anim. Ecol. 89: 1883-1894.

Pfeifer, S. P. et al. (2018). The evolutionary history of Nebraska deer mice: Local adaptation in the face of strong gene flow. Mol. Biol. Evol. 35(4): 792-806.

Purcell, S. and Chang, C. PLINK v1.9. www.cog-genomics.org/plink/1.9/

Purcell, S. et al. (2007). PLINK: a tool set for whole-genome association and population-based linkage analyses. Am. J. Hum. Genet. 81(3): 559-575.

Quinlan, A. R. (2014). BEDTools: The swiss-army tool for genome feature analysis. Curr. Protoc. Bioinformatics 47(1): 11-34.

Quinlan, A. R. and Hall, I. M. (2010). BEDTools: a flexible suite of utilities for comparing genomic features. Bioinformatics 26(6): 841-842.

R Core Team (2020). R: A language and environment for statistical computing. R Foundation for Statistical Computing.

Reinke, B. A., Miller, D. A. W. and Janzen, F. J. (2019). What Have Long-Term Field Studies Taught Us About Population Dynamics? Annu. Rev. Ecol. Evol. Syst. 50(1): 261-278.

Reznick, D. (1982). The impact of predation on life history evolution in Trinidadian guppies: genetic basis of observed life history patterns. Evolution 36(6): 1236-1250.

Reznick, D. N., Rodd, F. H. and Cardenas, M. (1996). Life-History Evolution in Guppies (*Poecilia reticulata*: Poeciliidae). IV. Parallelism in Life-History Phenotypes. Am. Nat. 147(3): 319-338.

Robert, K. A. and Bronikowski, A. M. (2010). Evolution of senescence in nature: physiological evolution in populations of garter snake with divergent life histories. Am. Nat. 175(2): 147-159.

Sambrook, J., Fritsch, E. and Maniatis, T. (1989). Molecular Cloning: a Laboratory Manual, 2nd edn. New York: Cold Spring Harbor Laboratory Press.

Schwander, T., Libbrecht, R. and Keller, L. (2014). Supergenes and complex phenotypes. Curr. Biol. 24(7): R288-R294.

Schwartz, T. S. and Bronikowski, A. M. (2013). Dissecting molecular stress networks: identifying nodes of divergence between life-history phenotypes. Mol. Ecol. 22(3): 739-756.

Schwartz, T. S., Arendsee, Z. W. and Bronikowski, A. M. (2015). Mitochondrial divergence between slow-and fast-aging garter snakes. Exp. Gerontol. 71: 135-146.

Sparkman, A., Bronikowski, A., Billings, J., Von Borstel, D. and Arnold, S. (2013). Avian predation and the evolution of life histories in the garter snake *Thamnophis elegans*. Am. Mid. Nat. 170(1): 66-85.

Sparkman, A. M. and Palacios, M. G. (2009). A test of life-history theories of immune defence in two ecotypes of the garter snake, *Thamnophis elegans*. J. Anim. Ecol. 78(6): 1242-1248.

Sparkman, A. M., Vleck, C. and Bronikowski, A. (2009). Evolutionary ecology of endocrine-mediated life-history variation in the garter snake *Thamnophis elegans*. Ecology 90: 720-728.

Stearns, S. C. (1992). The evolution of life histories. Oxford: Oxford University Press.

Szklarczyk, D. et al. (2019). STRING v11: protein–protein association networks with increased coverage, supporting functional discovery in genome-wide experimental datasets. Nucleic Acids Res. 47(D1): D607-D613.

Tigano, A. and Friesen, V. L. (2016). Genomics of local adaptation with gene flow. Mol. Ecol. 25(10): 2144-2164.

Weir, B. S. and Cockerham, C. C. (1984). Estimating F-statistics for the analysis of population structure. Evolution 38(6): 1358-1370.

Wellenreuther, M. and Bernatchez, L. (2018). Eco-evolutionary genomics of chromosomal inversions. Trends Ecol. Evol. 33(6): 427-440.

Wellenreuther, M., Mérot, C., Berdan, E. and Bernatchez, L. (2019). Going beyond SNPs: The role of structural genomic variants in adaptive evolution and species diversification. Mol. Ecol. 28(6): 1203-1209.

Yeaman, S. and Otto, S. P. (2011). Establishment and maintenance of adaptive genetic divergence under migration, selection, and drift. Evolution 65(7): 2123-2129.

Zheng, X., Levine, D., Shen, J., Gogarten, S. M., Laurie, C. and Weir, B. S. (2012). A high-performance computing toolset for relatedness and principal component analysis of SNP data. Bioinformatics 28(24): 3326-3328.

Zong, S.-B., Li, Y.-L. and Liu, J.-X. (2020). Genomic architecture of rapid parallel adaptation to fresh water in a wild fish. Mol. Biol. Evol. 38(4): 1317-1329.

Tables and Figures

Table 1: Sampling information for western terrestrial garter snake (*Thamnophis elegans*) females in this study. Three-letter population codes from Manier and Arnold (2005), population numbers from Bronikowski and Arnold (1999).

Population	Population #	N	Life-history Strategy	Latitude	Longitude	Elevation (m)
Christie Beach (CHR)	L8	10	L-fast	40.560	−120.827	1554
Eagle Lake Field Station (ELF)	L4	15	L-fast	40.618	−120.731	1556
Eagle Lake Pikes and Marina (PIK)	L2	15	L-fast	40.560	−120.783	1576
Merrill Creek (MER)	L7	7	L-fast	40.550	−120.807	1556
Rocky Point (RKY)	L6	11	L-fast	40.684	−120.757	1556
Stones Beach (STO)	L5	9	L-fast	40.718	−120.721	1556
Mahogany Lake (MAH)	M3	15	M-slow	40.534	−120.732	2065
Papoose Meadow (PAP)	M1	15	M-slow	40.528	−120.757	1645
Pine Valley Meadow (PVM)	M6	5	M-slow	40.619	−120.969	1730
Roney Corral (RON)	M8	9	M-slow	40.511	−120.857	1825
Summit Lake (SUM)	M5	10	M-slow	40.766	−120.839	1890
Total		121				

N is sample size of sequencing, life-history strategy is according to field records.

Table 2: Filtering steps for single nucleotide polymorphisms and monomorphic sites from the 121 genotyped *T. elegans* females.

Filtering Step	Number of SNPs Retained	Number of Monomorphic Sites Retained
Joint Genotyping	31197568	1515486984
GATK Variant Filtration	24180841	—
Biallelic Sites	23397828	—
Fixed for Non-Ref Allele	23319518	—
Remove Indels	22338317	1488559680
Missingness < 25%	21925727	1390994679
Excess Heterozygosity	21018514	—
Mean Site Depth	20539500	—
Genotype Depth	20539500	—
Allele Balance	20539500	—
SNP Missingness < 10%	19484787	—
Minor Allele Frequency	17149600	—
Linkage Disequilibrium	154911	—
Autosome Only	139441	1251978240

Table 3: Summary genomic statistics for western terrestrial garter snake populations.

Pop ID	% Missing	Private Alleles	% Poly	H_E	H_O	F_{IS}	π*
L8	0.7	282	67.00	0.1810	0.1841	0.0214	0.0029
L4	0.9	805	64.11	0.1773	0.1821	0.0077	0.0028
L2	0.8	750	64.99	0.1768	0.1749	0.0348	0.0027
L7	1.0	313	57.80	0.1660	0.1817	-0.0196	0.0027
L6	0.8	503	64.86	0.1792	0.1797	0.0324	0.0029
L5	1.5	436	60.76	0.1791	0.1937	-0.0179	0.0029
M3	0.8	1016	69.54	0.1731	0.1755	0.0178	0.0027
M1	0.8	799	71.95	0.1750	0.1769	0.0185	0.0027
M6	0.8	205	52.43	0.1573	0.1713	0.0041	0.0027
M8	0.8	806	61.01	0.1611	0.1651	0.0231	0.0026
M5	0.8	1251	66.52	0.1774	0.1843	0.0078	0.0029
Avg.	0.9	651	63.72	0.1730	0.1790	0.0118	0.0028

The average percentage of missing genotypes per individual within populations, number of SNPs unique (private) to each population, percentage of polymorphic SNP loci, expected (H_E) and observed (H_O) heterozygosity, inbreeding coefficient (F_{IS}), and average nucleotide diversity (π). *All statistics, with the exception of π, use the final 139,441 SNP dataset. π was calculated with the allele balance-filtered autosome dataset containing 19,181,591 variant and 1,251,978,240 invariant sites. We removed one individual from L4 that appeared to be a mislabeled sample for these analyses.

Table 4: Pairwise F_{ST} across all sampled garter snake populations.

Population	L8	L4	L2	L7	L6	L5	M3	M1	M6	M8	M5
L8	–										
L4	0.0327	–									
L2	0.0253	0.0401	–								
L7	0.0154	0.0591	0.0508	–							
L6	0.0212	0.0297	0.0392	0.0415	–						
L5	0.0293	0.0316	0.0442	0.0548	0.0221	–					
M3	0.0266	0.0550	0.0497	0.0298	0.0451	0.0592	–				
M1	0.0197	0.0480	0.0443	0.0238	0.0381	0.0511	0.0043	–			
M6	0.0165	0.0639	0.0607	0.0214	0.0404	0.0599	0.0314	0.0249	–		
M8	0.0297	0.0700	0.0669	0.0248	0.0531	0.0723	0.0314	0.0263	0.0217	–	
M5	0.0207	0.0570	0.0552	0.0251	0.0360	0.0503	0.0338	0.0279	0.0107	0.0282	–

Pairwise F_{ST} values were calculated with the final filtered dataset of 139,441 SNPs excluding one individual from L4 that appeared to be a mislabeled sample. L-fast comparisons are in the top left quadrant, M-slow comparisons are in the bottom right quadrant, and comparisons across life-history strategies are in the bottom left quadrant.

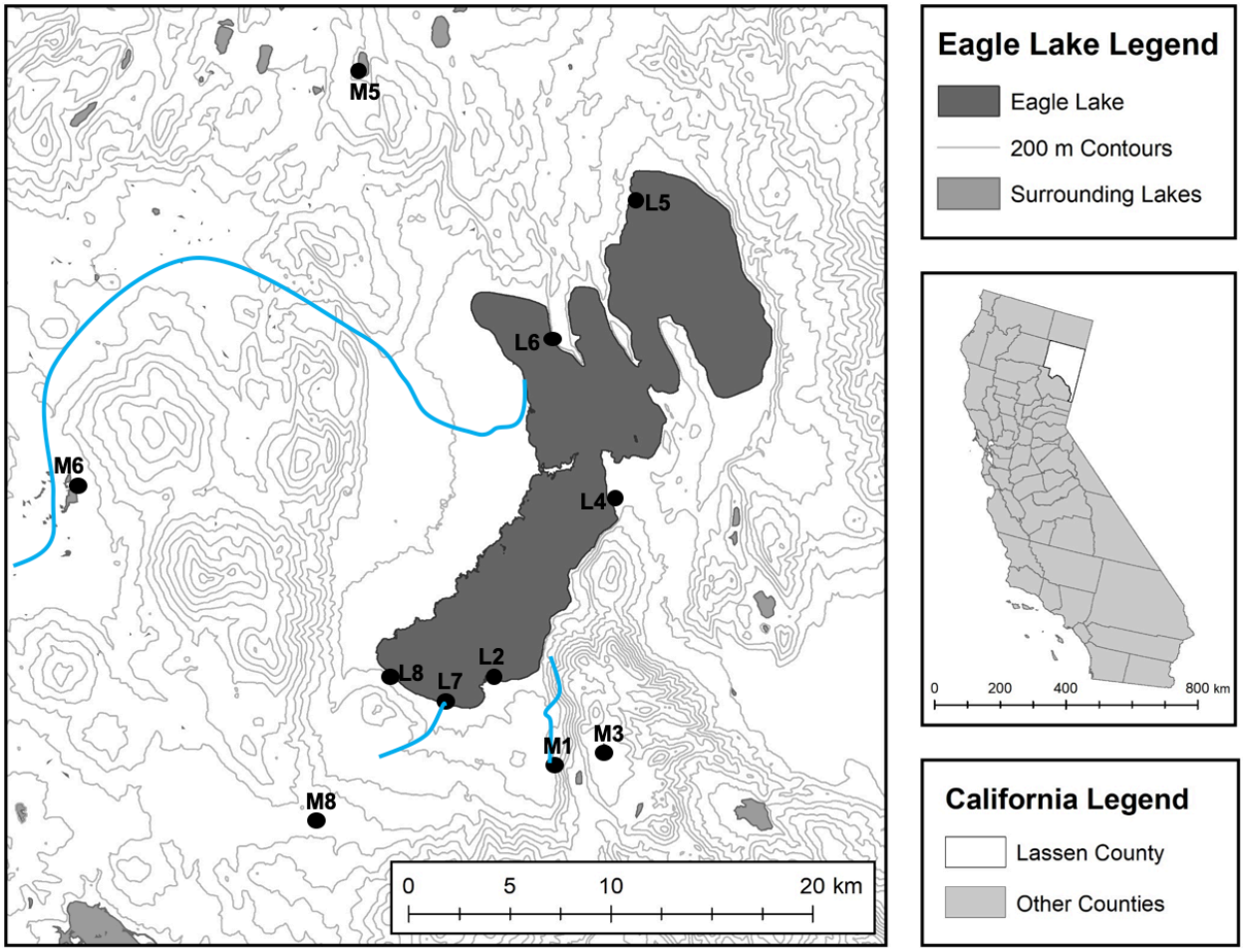

Figure 1: Map of populations of western terrestrial garter snakes sampled for this study. Populations are colored by their life-history strategy from mark-recapture study; M-slow populations are labeled with "M", L-fast populations are labeled with "L" (Table 1). Creeks are labeled in blue.

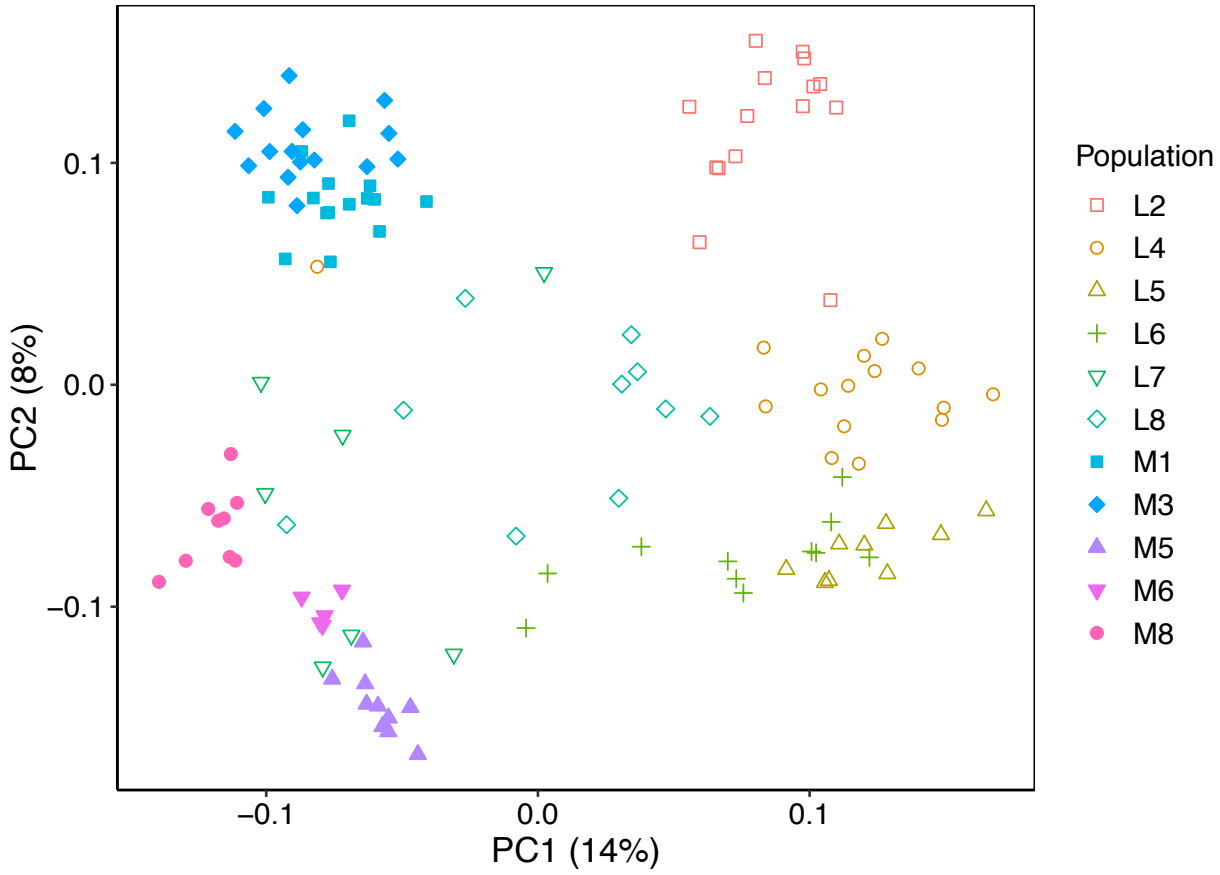

Figure 2: Principal components analysis of single nucleotide polymorphisms from all sampled western terrestrial garter snake populations surrounding Eagle Lake in Lassen County, California, USA separated populations by life-history strategy (PC1) and geographic distance (PC2). Populations associated with the "M-slow" life-history strategy based on phenotypes are specified by filled points, while "L-fast" populations are shown with unfilled points (Table 1).

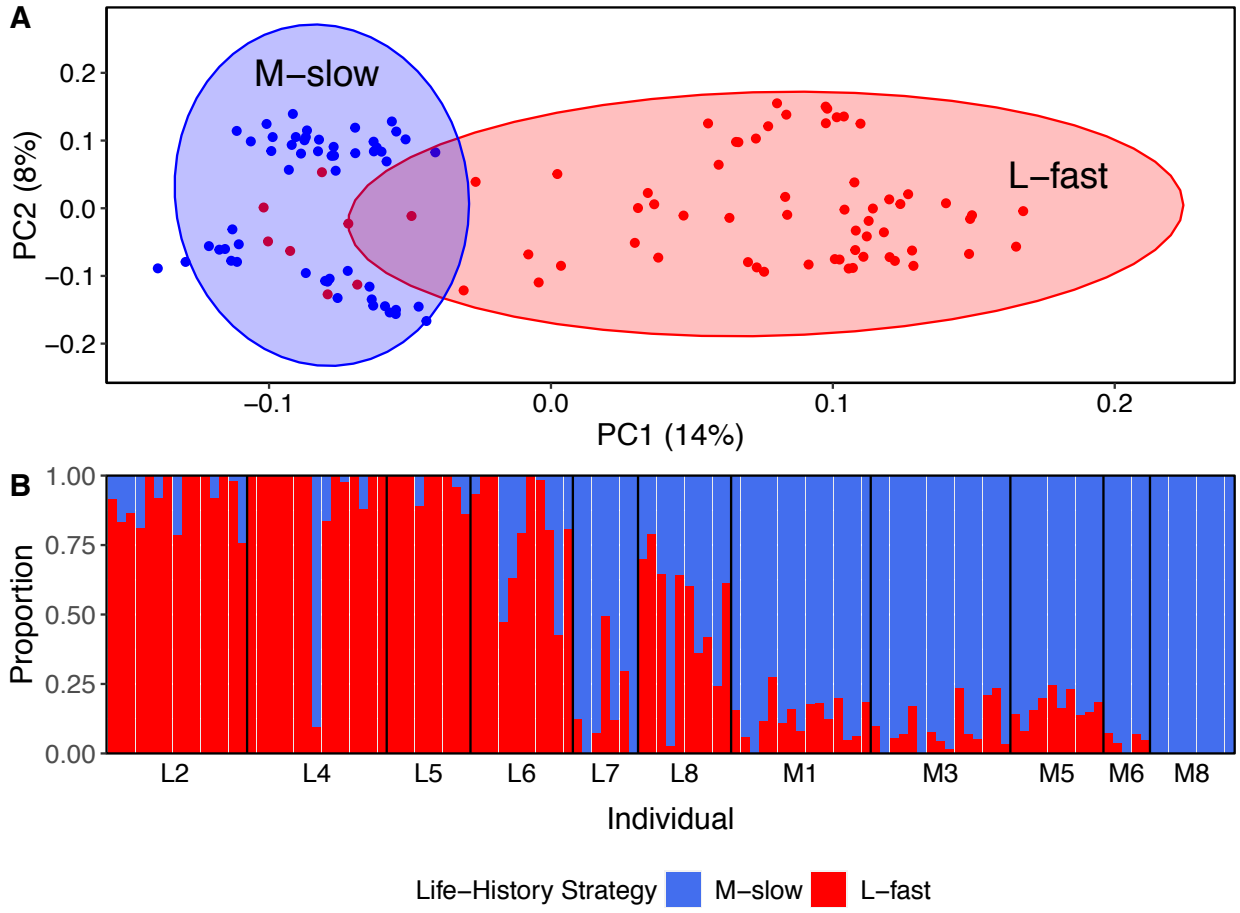

Figure 3: Groupings of western terrestrial garter snake populations were largely consistent with life-history strategy, though some populations exhibited mixed ancestry. A: First two principal components, with individuals colored by their life-history strategy depicted with 95% confidence ellipses. B: ADMIXTURE analysis results of the best number of groupings (K=2), with individuals grouped by population on the x-axis.

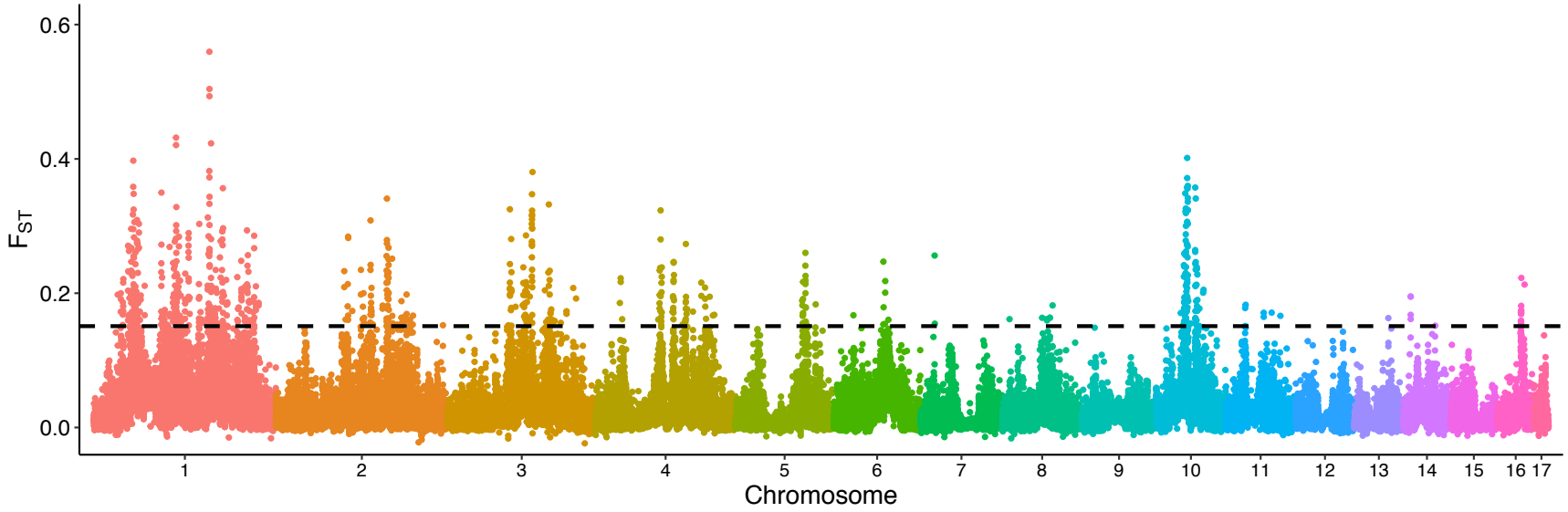

Figure 4: Sliding window pairwise F_{ST} between genetic groups, defined by the first principal component. The dashed line indicates the 99^{th} percentile of average F_{ST} values across sliding windows.

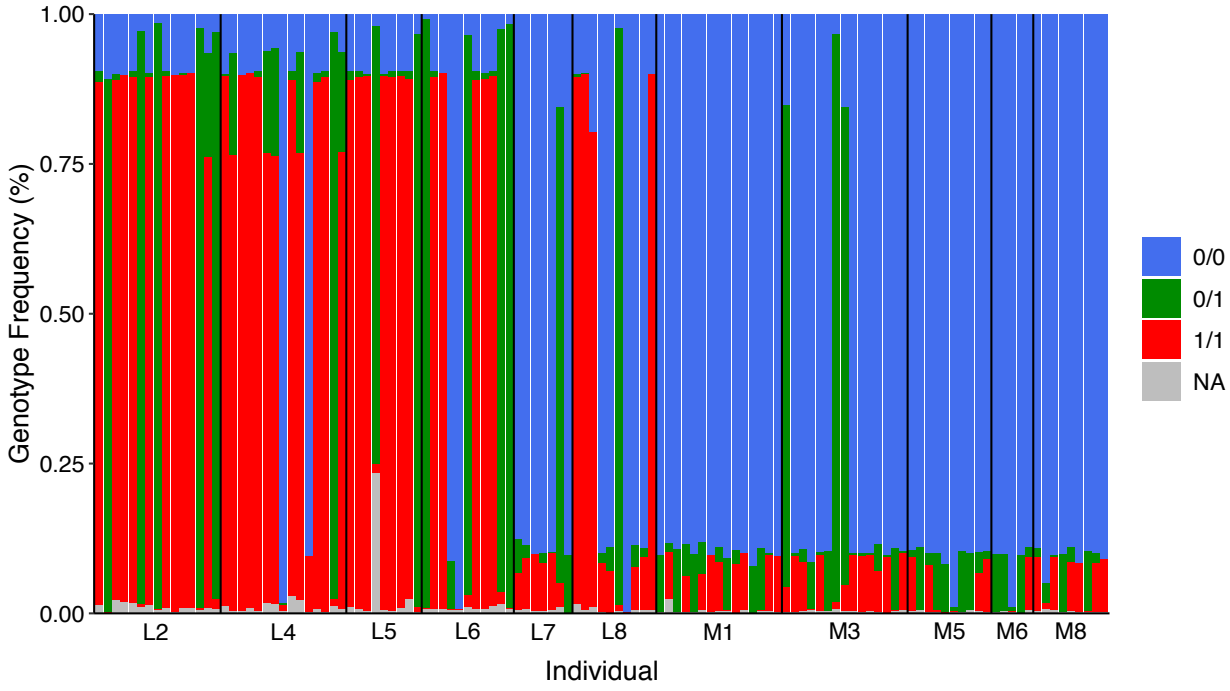

Figure 5: Genotype frequency across individuals within the putative inversion on the first chromosome, with each column representing an individual. Individuals are grouped by population on the x-axis.

Supplemental Material

Table S1: Hard filtering parameters of GATK v4.0.4.0 for removal of SNPs and for Indels/mixed sites

Filter Name	SNP Filter	Indel/Mixed Site Filter
Quality by Depth (QD)	< 2.0	< 2.0
Fisher Strand Bias (FS)	> 60.0	> 200.0
Strand Odds Ratio (SOR)	> 3.0	–
Mapping Quality Rank Sum Test (MQRankSum)	< -12.5	–
Read Position Rank Sum Test (ReadPosRankSum)	< -8.0	< -20.0
RMS Mapping Quality (MQ)	< 40.0	–

Table S2: List of genes in 20KB windows with F_{ST} values in top 1% of F_{ST} values across genome between the two genetic groupings.

Gene ID	Gene ID	Gene ID
TSPAN18	GPHB5	LOC116515752: RAB3IL1-like
CREB3L1	RHOJ	CPT1A
DDB2	LOC116506336: KCNK16-like	TSPAN4
PACSIN3	KIAA0586	TSPAN32
MYBPC3	TIMM9	CD81
PTGR2	ARID4A	TRPM5
UBR1	TOMM20L	KCNQ1
TTBK2	KTN1	OSBPL5
LOC116521796: NAIF1-like	TMEM260	IGSF22
STARD9	LOC116519422: SLC35F4-like	TSG101
CAPN3	ARMH4	GTF2H1
GANC	ANO8	HPS5
LOC116512719: PLA2G4E-like	LOC116508186: MAP3K20-like	SERGEF
LOC116505955: PLA2G4E-like	STK39	KCNC1
LOC116505973: TMEM151B-like	COBLL1	OTOG
RPAP1	GRB14	SOX6
LTK	GALNT13	PDE3B
ITPKA	FMNL2	PSMA1
LOC116505984: CHST14-like	PRPF40A	COPB1
RHOV	MMADHC	DENND2B
DISP2	LYPD6	LOC116503227: uncharacterized
CCDC9B	LYPD6B	DENND5A
PLCB2	MBD5	SWAP70
PAK6	ORC4	MICAL2
BUB1B	ACVR2A	BTBD10
BMF	ZEB2	MPPED2
AQR	GTDC1	SLC17A6
SEC23A	VWDE	ANO5
MIA2	THSD7B	NELL1
FAM161B	CXCR4	ATP2B2
ZNF410	GPR39	FGD3
COQ6	ITGB5	BICD2
ALDH6A1	LOC116514818: MPEG1-like	TKT
BBOF1	LOC116520281: FAM111A-like	DCP1A
LIN52	LOC116516020: FAM111A-like	CACNA1D
ABCD4	LOC116516010: FAM111A-like	CHDH
VRTN	DTX4	IL17RB
SYNDIG1L	MPEG1	CACNA2D3
ISCA2	LOC116503193: Struthiocalcin-2-like	ERC2
NPC2	PATL1	PLXNA1
FCF1	LOC116510113: MS4A15-like	SRGAP3
YLPM1	LOC116510164: MS4A8-like	MITF
GPATCH2L	LOC116510149: MS4A15-like	MAGI1
LOC116506152: NRXN3-like	BAAT	PTPRG
DIO2	ZP1	LOC116503347: A1M-like
CEP128	SLC15A3	CCNG1
STON2	LOC116510365: CYB561A3-like	NUDCD2
HHIPL1	TMEM138	LOC116504856: DLC1-like
WARS1	TMEM216	SLIT3

Table S2: Continued

Gene ID	Gene ID	Gene ID
BEGAIN	SYT7	ERGIC1
WDR89	LOC116510602: FADS1-like	SPOCK1
RASGEF1C	KTI12	EPHB1
ADAMTS2	VASH2	KY
EBF1	RCOR3	CEP63
RNF145	SYT14	ANAPC13
LOC116504575: Ovomucoid-like	LOC116507529: NPAS4-like	COL4A3
LOC116523973: Spink10-like	EIF2S2	COL4A4
MACIR	RALY	SLC19A3
PPIP5K2	MAP1LC3A	DAW1
SLCO4C1	PIGU	SPHKAP
LOC116506398: uncharacterized	LOC116508760: ADRB3-like	PID1
RFESD	PTPRT	DNER
SPATA9	TSHZ2	GRK7
FAM172A	HUNK	ATR
CRHBP	CFAP298	PLS1
PDE4D	EVA1C	SLC9A9
ADAMTS12	SETD4	AGTR1
SH3GL2	TMPRSS3	LOC116514268: ywrD-like
KCNV2	SDR16C5	VEPH1
DMRT2	LACTB2	MAP3K15
TJP2	TRAM1	PDHA1
LOC116505957: TRPM3-like	XKR9	RASA3
TMC1	CNGB3	ABCC4
LOC116505329: CYP1A1-like	ARMH3	OGDH
PCSK5	HS6ST1	SMG1
PRUNE2	MYO7B	IQGAP1
FANCC	DGKD	MAP1A
PTCH1	SAG	PPIP5K1
ERCC6L2	ATG16L1	CKMT1A
SLC35D2	INPP5D	FURIN
HABP4	NGEF	FES
ZNF367	GIGYF2	MAN2A2
CDC14B	KCNJ13	UNC45A
SLC25A46	EFHD1	LOC116518909: HDHD3-like
TMEM232	ERFE	MYMK
EFNA5	ILKAP	NEK6
PINX1	PCCB	PSMB7
INTS9	SLC35G2	ANGEL2
LOC116508181: PRKG2-like	VPS8	DZIP1L
CCT6A	C10H3orf70	UBE2G2
FAM120B	EHHADH	TSPEAR
PDCD2	MAP3K13	LOC116514283: TRPM2-like
TBP	DGKG	PFKL
GNPAT	PTTG1IP	DNAJB11
C4H1orf131	LOC116514061: SUMO3-like	LOC116513992: EPCR-like
PGBD5	RPS6KC1	TBCCD1
NTPCR	ZFAND3	DNAH8
PCNX2	MDGA1	

Table S3: Results of PANTHER Gene List Analysis for the genes with high pairwise FST between genetic groups.

Category Name (Accession)	# Genes	% Genes[1]	% Process[2]
cellular process (GO:0009987)	143	57.4%	30.0%
reproductive process (GO:0022414)	2	0.8%	0.4%
localization (GO:0051179)	46	18.5%	9.6%
interspecies interaction between organisms (GO:0044419)	3	1.2%	0.6%
reproduction (GO:0000003)	2	0.8%	0.4%
biological regulation (GO:0065007)	76	30.5%	15.9%
response to stimulus (GO:0050896)	44	17.7%	9.2%
signaling (GO:0023052)	34	13.7%	7.1%
developmental process (GO:0032502)	17	6.8%	3.6%
multicellular organismal process (GO:0032501)	16	6.4%	3.4%
biological adhesion (GO:0022610)	5	2.0%	1.0%
locomotion (GO:0040011)	10	4.0%	2.1%
metabolic process (GO:0008152)	77	30.9%	16.1%
immune system process (GO:0002376)	2	0.8%	0.4%

[1]Percent of gene hit against total # genes; [2]Percent of gene hit against total # Process hits

Table S4: Results of lostruct analysis from first dimension of multidimensional scaling. B_{SS}/T_{SS} is the sum of squares between genotype clusters divided by the total sum of squares.

Cluster ID	Chromosome	Positions	# SNPs	B_{SS}/T_{SS}	# Genes
1	NC_045541.1	38129743-43017350	37001	0.938	14
2	NC_045541.1	44271498-47436891	21001	0.940	25
3	NC_045541.1	83683687-85202738	11001	0.963	12
4	NC_045541.1	96258066-97547507	11001	0.929	4
5	NC_045541.1	106890538-107330608	3001	0.962	6
6*	NC_045541.1	117357736-117713021	3001	0.950	8
7	NC_045541.1	123870900-125146145	9001	0.944	3
8	NC_045541.1	130362524-131177882	9001	0.923	17
9	NC_045542.1	95995875-96393871	3001	0.985	1
10	NC_045543.1	59923556-63336953	24001	0.966	11
11	NC_045543.1	84950849-85284737	3001	0.956	3
12	NC_045543.1	102301913-103052318	5001	0.970	3
13	NC_045544.1	78321618-79244390	7001	0.924	2
14	NC_045550.1	28772659-29836462	8001	0.922	19
15	NC_045550.1	30565596-31669528	11001	0.958	4
16	NC_045550.1	38861630-39592977	6001	0.946	8
17	NC_045550.1	40234157-40899104	4001	0.985	15

*Includes putative inversion plotted in Figure 5 of main text.

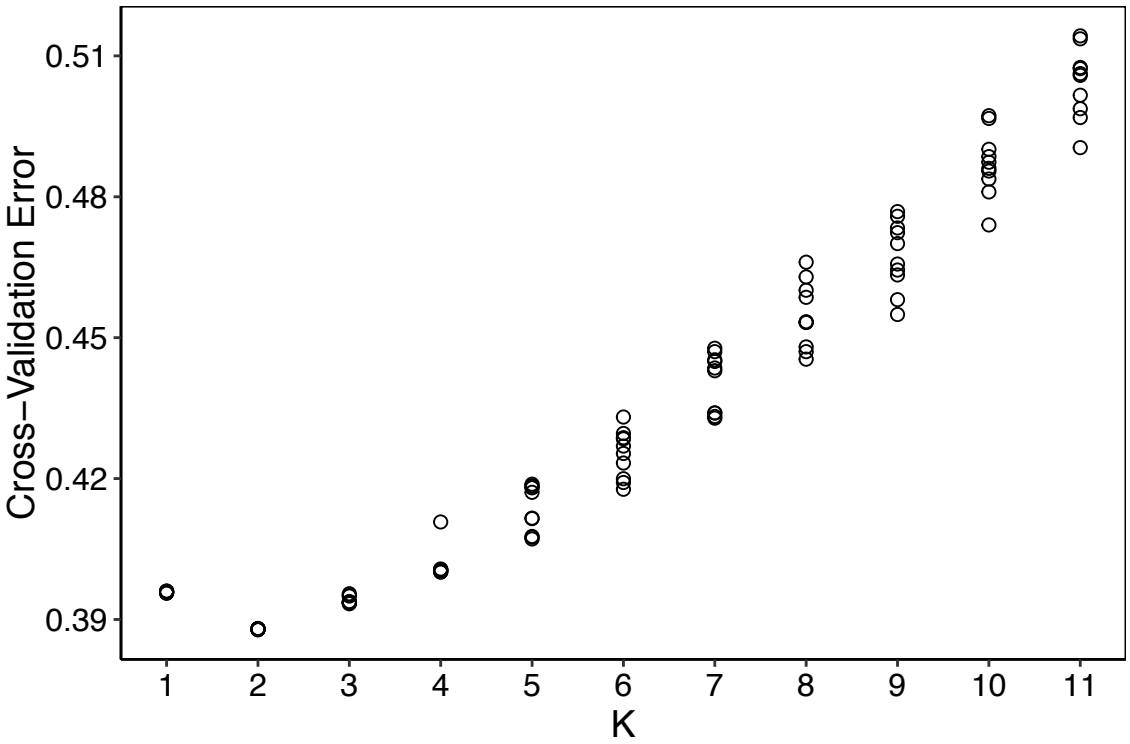

Figure S1: Cross-validation error for each run of ADMIXTURE with K groupings. Each value of K was run 10 times.

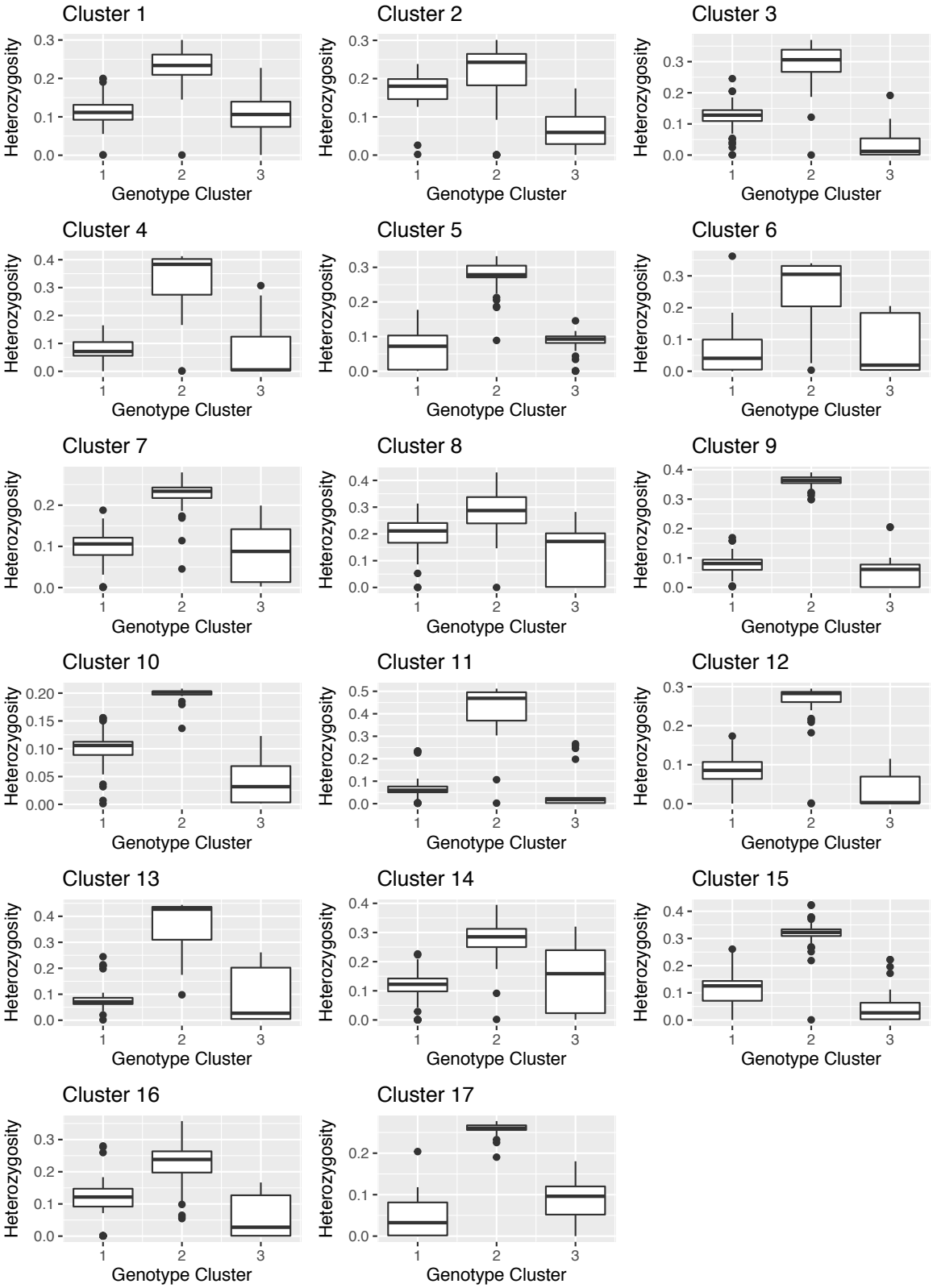

Figure S2: Results of individual heterozygosity for each genotype within putative inversions.

CHAPTER 6. CONCLUSION

Genomic analyses offer insight into the selective forces that shape the evolution of phenotypes across landscapes and through millions of years of evolutionary time. For my dissertation, I was interested in understanding the relationships of different environmental conditions, population dynamics, and selection in shaping the evolution of two long-lived reptile species that have been monitored for decades (Fig. 1). Despite the relatively long-lived life histories of these reptiles, the patterns I found across populations were in stark contrast to one another. Painted turtles showed little evidence of local adaptation in response to the diverse environments the species inhabits across the western United States, a scale of thousands of kilometers. Populations of western terrestrial garter snakes, however, were strongly differentiated at many regions across the genome in a pattern consistent with the different habitats (lakeshore and meadow) and life-history strategies exhibited (fast-paced and slow-paced) by populations surrounding Eagle Lake in California. This is despite the much smaller geographic scale (tens of kilometers) and the presence of gene flow among populations. These differences between species provoke several questions regarding the pace of evolution in turtles and snakes. Specifically, how do rates of molecular evolution impact divergence, how do other phenotypes and life history influence the evolution of local adaptation or phenotypic plasticity, and is the presence of gene flow between different

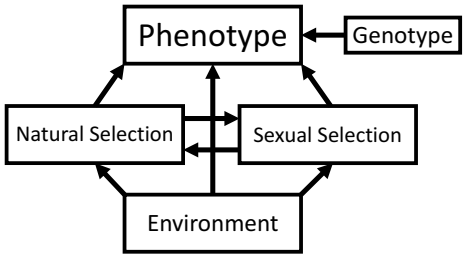

Fig. 1: Diagram of the forces shaping phenotypes, and the translation of changes in phenotype to potential changes in genotypes at the population level. Environmental contexts, including both abiotic factors and biotic factors (e.g., population demography), influence selective pressures, which in turn are the result of interactions between sexual selection and natural selection. These selective pressures shape phenotypes through evolutionary time.

habitats important for the process of local adaptation? Turtles, particularly the painted turtle, have slower molecular substitution rates compared to other model organisms. These reptiles also have a protective shell, which may change the predation pressure on adults in a way that is not present in garter snakes. Further, painted turtles have longer lifespans than western terrestrial garter snakes, and may be under stronger selection for phenotypic plasticity to accommodate for the environmental pressures experienced during an individual's lifespan. The garter snake system also introduces the opportunity for gene flow to interact with selection, which likely contributes to the evolution of strongly diverged regions of the genome.

While much of my dissertation focused on the interactions of natural selection and population dynamics shaping the evolution of these reptiles, sexual selection can also influence phenotypic evolution. I was interested in understanding whether sexually dimorphic phenotypes and population demographics, like adult sex ratios, may predict reproductive success in painted turtles and thus be shaped by sexual selection. Alternatively, sexually dimorphic phenotypes may be the result of different responses to natural selection between the sexes, including selection favoring larger female body size to produce more offspring. These questions are particularly interesting to study in a species with temperature-dependent sex determination (TSD), as there are no sex chromosomes harboring genes that produce sex-specific phenotypes. Further, shifting adult sex ratios may be expected in populations that experience different temperatures from year to year, which may change the selective pressures on the sexes through mate choice and competition both within and across populations.

In summary, I used genomic tools to understand the role of sexual and natural selection and population demography in shaping phenotypes across populations of painted turtles and western terrestrial garter snakes. Broadly, I found that phenotypic variation can be explained by

sexual selection and phenotypic plasticity in painted turtles, and strong selection in western terrestrial garter snakes of Eagle Lake. I found that mate choice in painted turtles may be a complex process involving male choice of females, which may change through ontogeny. I also found that adult sex ratio at least weakly influenced male reproductive success, which may have implications for the future reproductive patterns of this species with TSD. Painted turtle populations display phenotypic variation across the western range of the species, but genomic analysis found that while past demography, particularly founder effects, has shaped population genomic structure, there was no evidence of local adaptation driving these differences in phenotypes. The methods used for identifying regions of the genome under selection in this manner, however, are underpowered for detecting loci of small effect. While I may not have found patterns of local adaptation for this reason, phenotypic plasticity may also explain the variation in phenotypes across populations of this widespread reptile. Finally, my final study found that genes of large effect appear to greatly contribute to local adaptation among populations of western terrestrial garter snakes, even with abundant gene flow. This may be facilitated by multiple inversions across the genome, which reduce recombination and allow suites of genes (i.e., "supergenes") important for matching phenotype and habitat to be inherited together.

While these studies have some limitations given the difficulty of finding loci of small effect using these approaches, future work can approach these questions in new ways to understand the effects of these loci. Specifically, quantitative genetic approaches can find loci important to phenotype, which while difficult in many systems is possible in these long-term studies. Future work in the painted turtle system should include investigating the role of phenotypic plasticity versus loci of small effect in phenotypic divergence across populations. In

the garter snake system, genotyping the inversions in more individuals and associating those genotypes directly with individual phenotypes will further elucidate the role of these inversions in the evolution of adaptive phenotypes of the two life-history strategies. Photographic color analyses, in particular, could be used to investigate the role of coloration in adaptation and how genotype and phenotype are associated. Finally, there are epigenetic mechanisms that may also be at play between the two aging strategies. Investigating the genomic and epigenetic underpinnings of these life-history strategies could have implications not only for understanding reptile evolution, but also understanding the aging process itself. I hope to continue investigating these questions and others related to the forces shaping the evolution of populations over time and space.